

Supplementary Information

Nanoscale and Chiral Metal–Organic Framework for Asymmetric Reaction in Water: Bridging Lewis Acid Catalysis to Biological Systems

Watchara Srimontree, Taku Kitanosono,* Yasuhiro Yamashita, Shū Kobayashi*

Department of Chemistry, School of Science, The University of Tokyo, Bunkyo-ku, Tokyo 113-0033, Japan

1. General experimental	S2
2. Initial discovery through the design of chiral H ₂ BPVB linker 5	S3
3. Synthesis of the chiral H ₂ BPVB linker 5	S9
4. Synthesis of BPVB-NMOF-Sc-DS	S17
5. Control experiments for epoxide ring-opening reactions	S22
6. Typical procedure for epoxide ring-opening reactions in water	S24
7. Spectroscopic data of the products	S26
8. Typical procedure for biocompatible epoxide ring-opening reactions	S30
9. General procedure for recovery and reuse experiments	S32
10. TG analysis	S33
11. SEM analysis	S34
12. PXRD analysis	S36
13. Water stability test of BPVB-NMOF and BPVB-NMOF-Sc-DS	S37
14. STEM/EDS analysis	S39
15. N ₂ adsorption/desorption isotherms	S52
16. XPS study	S54
17. Computational details	S55
18. References	S59
19. ¹ H & ¹³ C NMR spectra and HPLC chromatograms	S61

1. General experimental

Nuclear magnetic resonance (NMR) spectra were recorded on JEOL ECX-600 spectrometers, operating at 600 MHz for ^1H and 151 MHz for ^{13}C NMR in CDCl_3 and are reported relative to the solvent residual ^1H -signal (CHCl_3 , $\delta(\text{H}) = 7.26$) for ^1H -NMR and CDCl_3 ($\delta = 77.0$) for ^{13}C -NMR. Infrared (IR) spectra were obtained using a SHIMADZU IRSpirit spectrometer, data are represented as frequency of absorption (cm^{-1}). High-performance liquid chromatography was carried out using the following apparatuses: SHIMADZU LC-10ATvp (liquid chromatograph), SHIMADZU SPD-10A (UV detector), and SHIMADZU C-R8A (Chromatopac) using Daicel Chiralpak[®] or Chiralcel[®] columns. Preparative thin-layer chromatography (PTLC) was carried out using Wakogel B-5F from Wako Pure Chemical Industries, Ltd. High-resolution mass spectra (HRMS) were recorded using a JEOL JMS T100TD (DART) or T100LC (ESI) spectrometer. Optical rotations were measured on a JASCO P2100 polarimeter using a 2 mL cell with 1 dm path length. Data are reported as follows: $[\alpha]_{\text{D}}^{\text{T}}$ (c in g/100 mL, solvent). All melting points were determined on a YAZAWA micro melting point BY-1 apparatus and are uncorrected. Inductively Coupled Plasma (ICP) analysis was performed on Shimadzu ICPS-7510 equipment. Centrifugation was performed by using KOKUSAN H-36 centrifuge with 3500 rpm for 10 minutes, unless otherwise noted. TG analysis was performed on Rigaku Thermoplus TG 8120. XPS analysis was performed on JPS-9010MC with a Mg Ka X-ray source. The Au $4f^{7/2}$ line at 84.0 eV was used as a reference to correct the binding energy of C 1s. The corrected C 1s (283.4 eV) was used as reference to correct the binding energy of other samples. PXRD analysis was performed on MiniFlex 600 from Rigaku. STEM/EDS images were obtained using a JEOL JEM-2100F instrument operated at 200 kV. All STEM specimens were prepared by placing a drop of the solution on carbon-coated grids and allowed to dry in air (without staining). SEM analysis was measured by a JEOL JSM-6700F. Nitrogen absorption/desorption isotherms were recorded on a BELSORP-mini Microtrac Bell. Calculation study to estimate the length of linkers was performed using the functional B3LYP together with 6-31G+(d,p) basis set for C, H, N, O, and LanL2DZ for Sc. Deionized water from a MILLIPORE MilliQ machine (Integral 3) was used as a solvent without further treatment. All organic solvents used were commercially available dry solvents. Commercially available reagents (in liquid form) for the ring-opening reactions of epoxides were distilled before use.

2. Initial discovery through the design of chiral H₂BPVB linker 5

In our initial exploration, the chiral H₂BPV linker **3** was synthesized from 2,6-dibromopyridine in 9 steps (Figure S1).

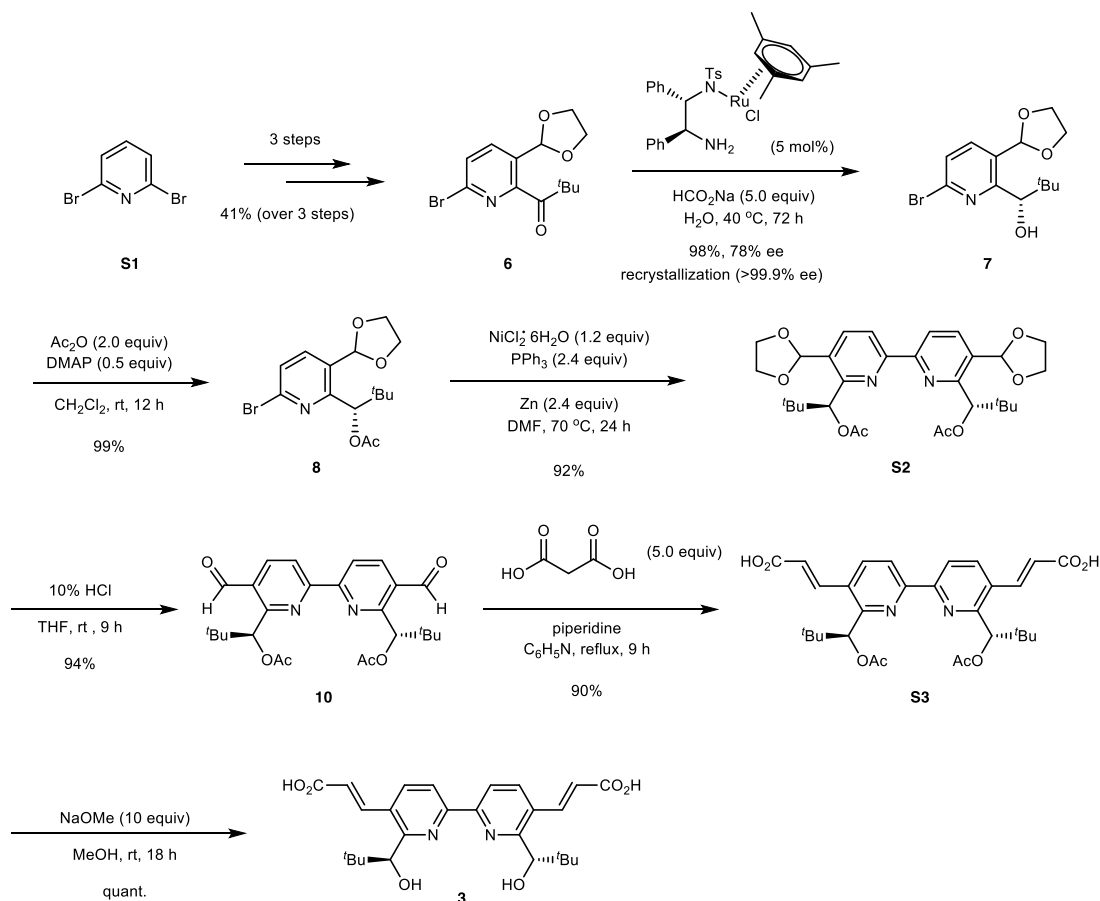


Figure S1. Synthesis of chiral H₂BPV **3**.

Following the successful synthesis of chiral linker **3**, the subsequent phase of our investigation entailed the preparation of the corresponding BPV-MOF through a solvothermal process.¹ The reaction conditions for MOF construction were systematically explored and refined, as outlined in Table S1. After the completion of the reactions, the resulting precipitates underwent thorough ¹H-NMR analysis to assess the degree of linker occupancy. Unexpectedly, our analysis uncovered the presence of undesired linkers **B** and **C**, originating from intramolecular 1,4-addition, during the self-assembly process (Figure S2).

Table S1. Optimization in the preparation of chiral BPV-MOF via solvothermal process.

Reaction conditions: ZrCl_4 (1.3 equiv), AcOH (x equiv), H_2O (10 equiv), DMF (5.0 mL), temp, time.

Starting material: **3** (0.03 mmol)

Process flow: ZrCl_4 (1.3 equiv), 5 mL DMF, H_2O (10 equiv) → sonication (10 min) at rt → modulator (x equiv) → sonication (5 min) at rt → **3** (0.03 mmol) → sonication (5 min) at rt → filtration (mesh 0.2 mm) → heater (temp, time) → centrifugation → filtration (washing w/ DMF, THF) → dry in vacuo.

Entry	Heater (temp, °C)	Modulator (x equiv)	Time (h)	Yield (mg)	A : B : C ^a
1	oven (120)	AcOH (30)	48	9.9	24 : 76 : 0
2	oven (120)	AcOH (30)	24	7.8	23 : 71 : 6
3	oven (110)	AcOH (30)	24	7.1	41 : 54 : 5
4	oven (100)	AcOH (30)	40	3.9	67 : 30 : 3
5	oven (90)	AcOH (30)	70	6.5	85 : 2.5 : 12.5
6	oven (80)	AcOH (30)	135	4.2	53 : 27 : 20
7	oven (90)	AcOH (10)	70	9.7	42 : 24 : 34
8	oven (90)	—	70	8.1	47 : 2 : 51
9 ^b	oven (90)	AcOH (30)	70	12.8	36 : 9 : 55
10 ^b	oil bath (90)	AcOH (30)	70	21.0	47 : 38.5 : 14.5
11 ^c	oil bath (90)	AcOH (30)	70	39.5	59 : 34 : 7
12	microwave (90)	AcOH (30)	8	n.d.	—
13	oil bath (90)	PhCO ₂ H (30)	70	n.d.	—
14	oil bath (90)	TFA (30)	70	n.d.	—
15	oil bath (90)	HCOOH (30)	70	10.0	29 : 65 : 6
16	oil bath (90)	HCl (30)	32	6.8	42 : 49 : 9
17	oil bath (90)	HCl (10)	35	4.9	42 : 17 : 41

^a Ratio of occupancy was determined by ¹H NMR analysis. ^b 0.09 mmol scale. ^cCombination of 4 portions.

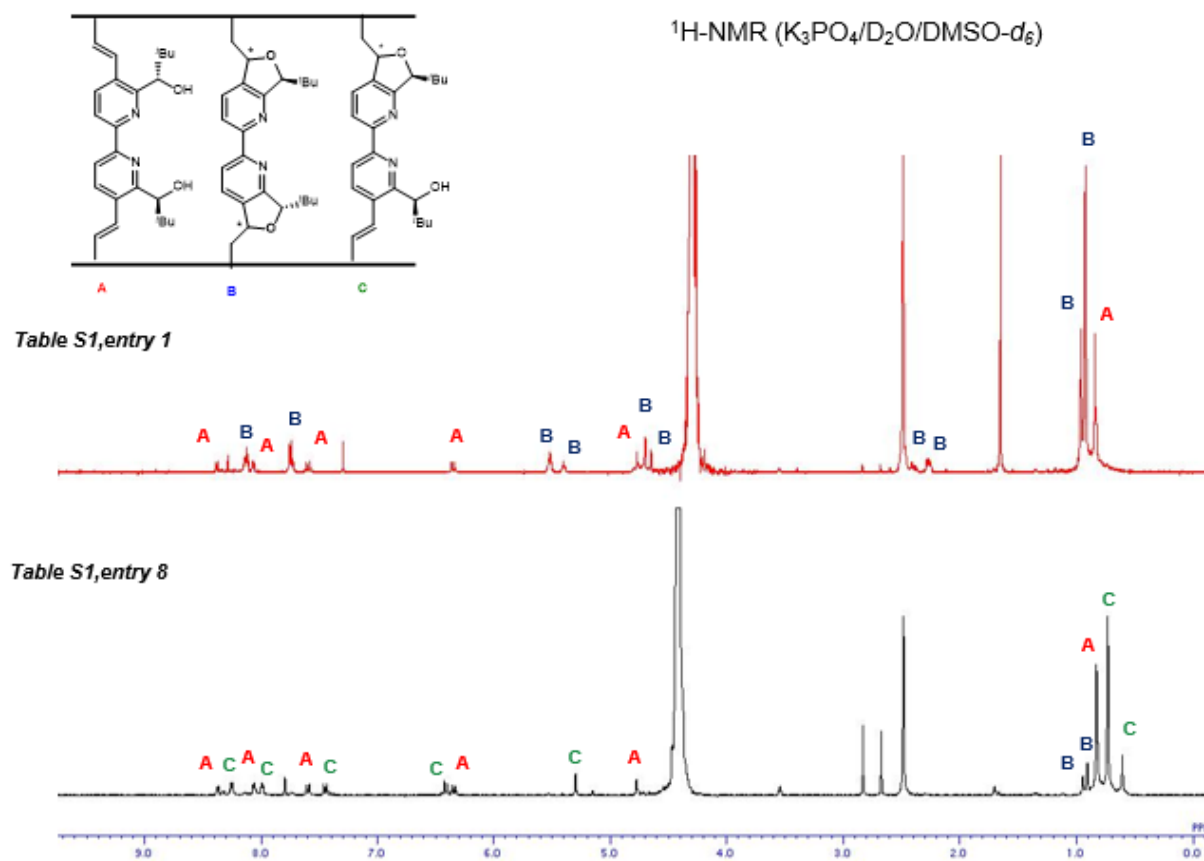
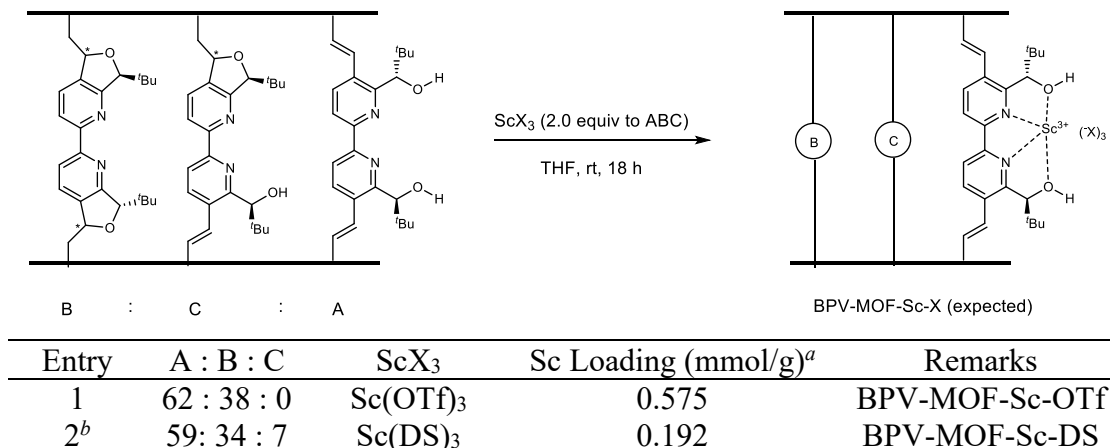
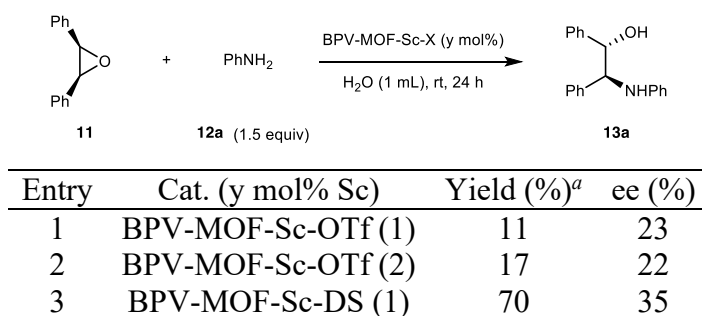


Figure S2. Assignment of linkers in BPV-MOF after solvothermal process.

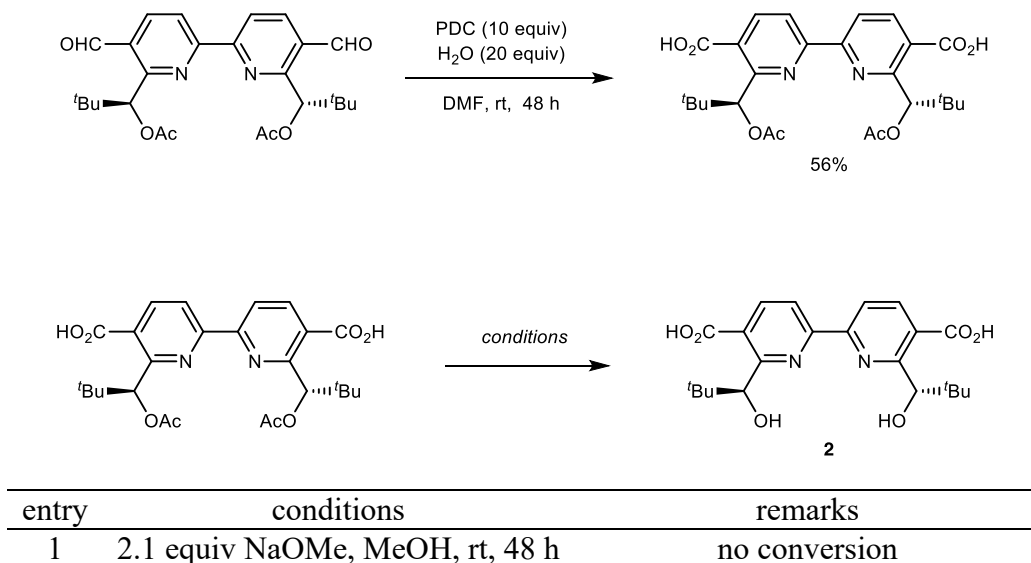
To investigate whether the decomposition of the chiral linker impacted the asymmetric reaction in water, we explored the post-synthetic metalation of the prepared Zr-MOFs using $\text{Sc}(\text{OTf})_3$ and $\text{Sc}(\text{DS})_3$, as detailed in Table S2. The successful incorporation of scandium was confirmed through ICP analysis. These catalysts were subsequently evaluated for their performance in the asymmetric ring-opening reaction of epoxide in water, as summarized in Table S3. When BPV-MOF-Sc-OTf was employed (entries 1 and 2), low yields and enantioselectivities were obtained. Notably, the substitution of the counter anion to dodecyl sulfate (DS^-) resulted in an improvement in reactivity and selectivity, with the desired product isolated in 70% yield with 35% ee. However, it is crucial to highlight that the observed low enantioselectivity was still evident, attributed to the deactivation of the chiral coordination site by Michael addition. Consequently, finding an alternative linker to suppress this issue is necessary.

Table S2. Preparation of chiral BPV-MOF-Sc catalysts.

^aBased on ICP analysis. ^bFew drops of H₂O was added.

Table S3. Evaluation of chiral BPV-MOF-Sc catalysts in asymmetric ring-opening reaction of epoxide.

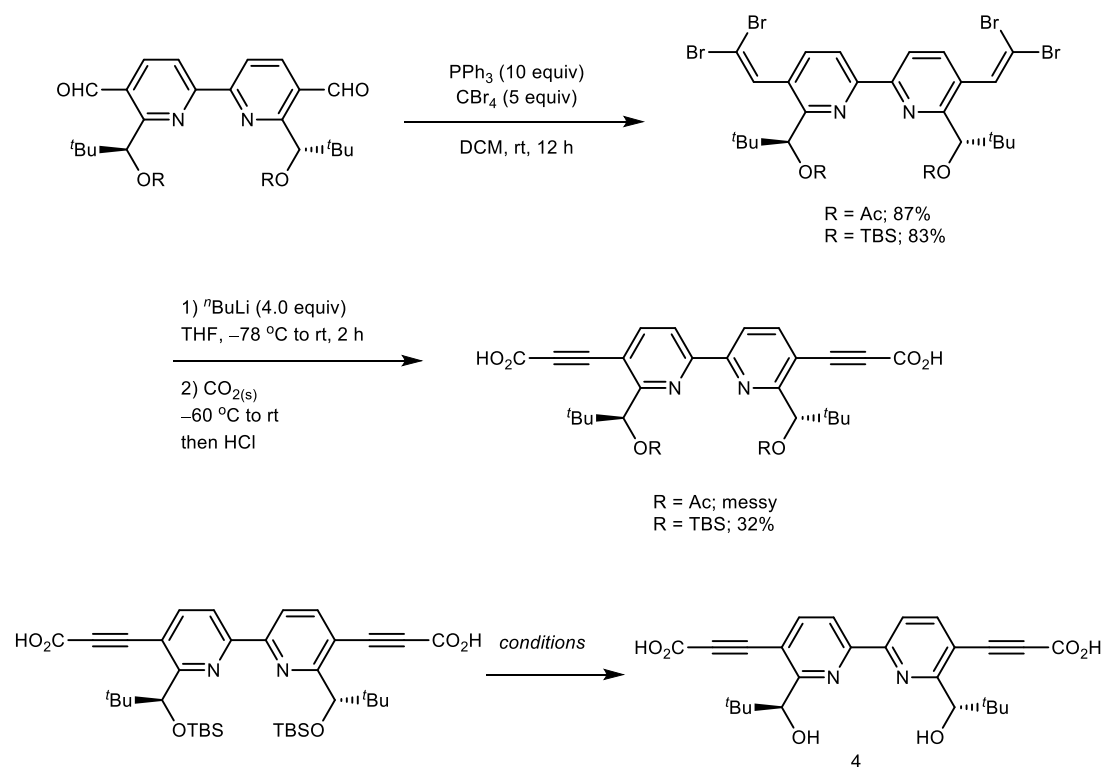
^a Isolated yield.

Table S4. Unsuccessful synthesis of chiral H₂BPDC linker **2**.

2	2.5 equiv NaOH, THF, rt, 18 h	messy
3 ^a	20 equiv NaOMe, MeOH, 40°C	full conversion, messy
4 ^a	2.5 equiv NaOMe, MeOH, 40°C	no conversion
5 ^a	5 equiv NaOMe, MeOH, 40°C	58% conv., complex mixture
6 ^a	10 equiv NaOMe, MeOH, 40°C	full conversion, under purification

^a stirred for 18 h.

Table S5. Unsuccessful synthesis of chiral H₂BPY linker **4**.



entry	conditions	remarks
1	TBAF (10 equiv), 40 °C, 20 h	decomposed
2	37% HCl, THF, 40 °C, 18 h	decomposed
3	4M HCl (in 1,4-dioxane)/MeOH, rt, 14 h	decomposed
4	AcOH/H ₂ O, THF, rt, 20 h	N.R. (decomposed at 60 °C)
5	TFA/H ₂ O, DCM, 12 h	N.R. (decomposed at 40 °C)
6	10% HCl, THF, rt, 24 h	N.R.
7	10% HCl, THF/MeOH, rt, 24 h	low conv. (decomposed at 40 °C)

Detected by-products:



In response to the challenges encountered with the chiral H₂BPV, H₂BPDC, and H₂BPY ligands, we have undertaken a modification of synthetic methods to design a new chiral linker by

introducing vinyl benzoate groups. We hypothesized that this modification not only addresses the linker decomposition or deprotection issues but also enhances hydrophobicity, rendering it a promising candidate for water-stable ligands. The proposed retrosynthesis of the chiral H₂BPVB linker **5** is illustrated in Figure S3, outlining three key synthetic steps: asymmetric transfer hydrogenation, Wittig olefination, and Ullmann-homocoupling reaction.

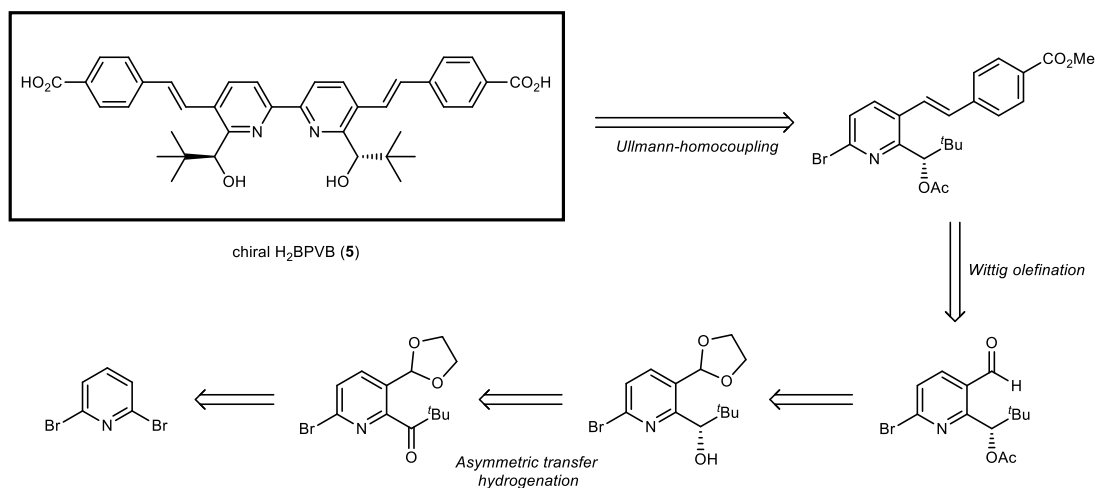


Figure S3. Retrosynthesis of chiral H₂BPVB linker **5**.

3. Synthesis of the chiral H₂BPVB linker 5

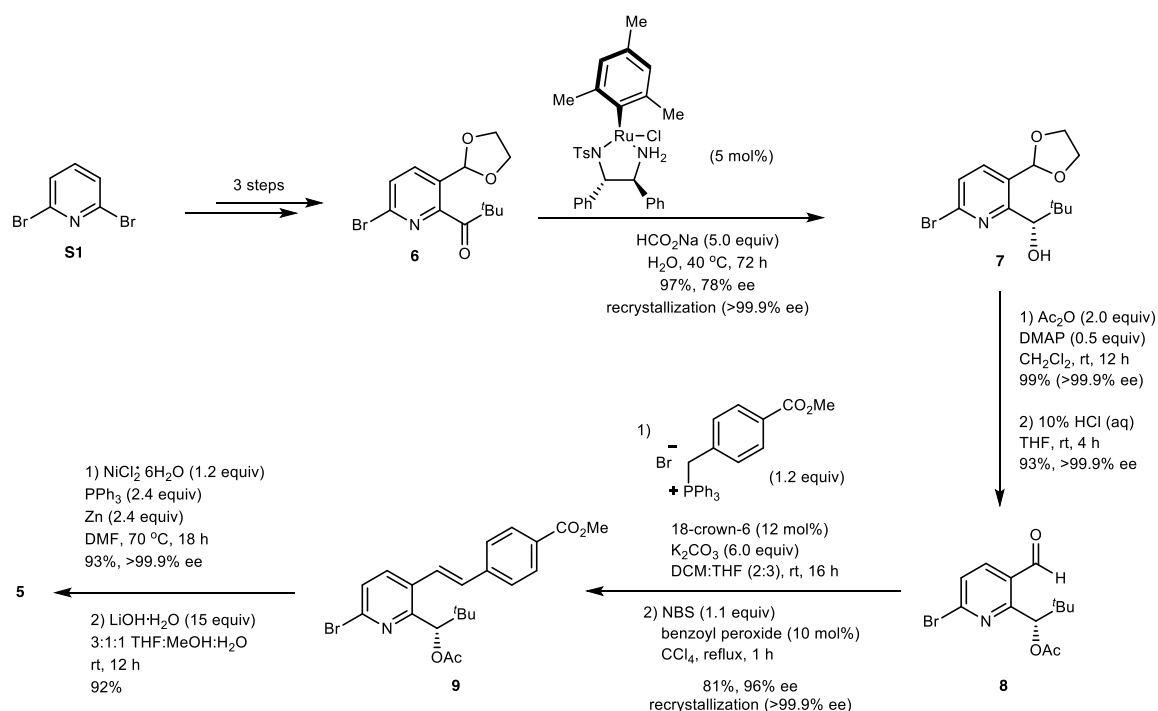
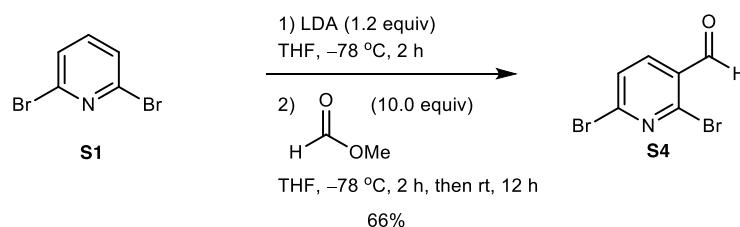


Figure S4. Overview synthetic pathways toward chiral H₂BPVB linker 5.

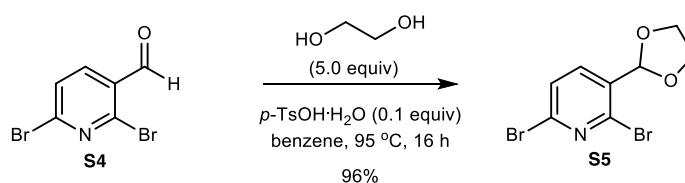
Synthesis of 2,6-Dibromonicotinaldehyde (S4)²



To an oven-dried 300 mL 3-necked round-bottom flask equipped with a stirring bar was charged diisopropylamine (16.9 mL, 120 mmol) under argon atmosphere, followed by the addition of 120 mL dry THF before setting at -78°C . A solution of *n*BuLi (1.56 M in *n*hexane, 76.9 mL, 120 mmol) was added dropwise into the reaction flask via a dropping funnel at -78°C . The mixture was stirred at -78°C for 1 hour to obtain lithium diisopropylamide (LDA). To an oven-dried 1 L 3-necked round-bottom flask containing a solution of 2,6-dibromopyridine (23.68 g, 100 mmol) in 200 mL dry THF at -78°C , was slowly transferred the prepared LDA solution via a Teflon cannula, the mixture solution was stirred at -78°C for 2 hours. Later, a solution of methyl formate (60.05 g, 1000 mmol) in 60 mL dry THF was added dropwise via a drooping funnel. The reaction mixture was then stirred at -78°C for 2 hours before gradually warming up to room

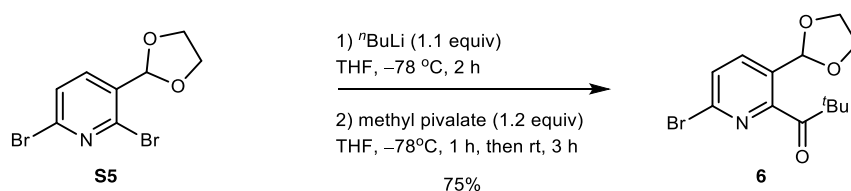
temperature and stirred at room temperature for 12 hours. Then, the reaction was quenched with saturated NH_4Cl (100 mL) and extracted with EtOAc (3×100 mL). Organic layers were combined and washed with brine, dried over anhydrous Na_2SO_4 , and evaporated. The crude product was purified by column chromatography (silica gel, $^n\text{hexane}/\text{EtOAc} = 20/1$) to give the title compound **S4** as a white solid. **Mp**: 125–126 °C; **IR** (neat): $\nu = 2884, 1665, 1552, 1424, 1385, 1004, 830$ cm^{-1} ; **^1H NMR** (600 MHz, CDCl_3): δ 10.28 (dd, $J = 1.8, 0.9$ Hz, 1H), 8.01 – 7.99 (m, 1H), 7.63 – 7.60 (m, 1H); **^{13}C NMR** (151 MHz, CDCl_3): δ 190.0, 146.4, 144.1, 139.3, 129.6, 128.2; **HRMS (DART)** for $\text{C}_6\text{H}_4\text{Br}_2\text{NO}$: calculated for $[\text{M}+\text{H}]^+$ 265.86392, found 265.86286.

Synthesis of 2,6-Dibromo-3-(1,3-dioxolan-2-yl)pyridine (**S5**)³



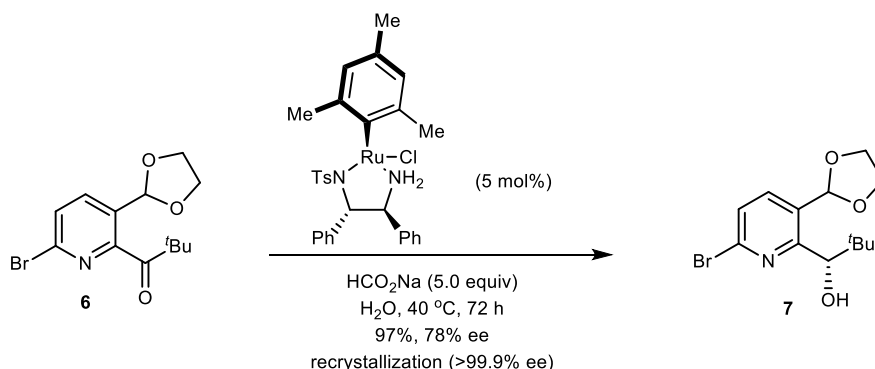
To a solution of 2,6-dibromonicotinaldehyde (**S4**, 12.4 g, 47 mmol) and $p\text{-TsOH}\cdot\text{H}_2\text{O}$ in 180 mL benzene, was added ethylene glycol (14.5 g, 234 mmol) via syringe. The reaction mixture was refluxed at 95 °C for 16 hours. After completion, the reaction was allowed to cool down to room temperature and quenched with H_2O (100 mL). It was extracted with EtOAc (3×50 mL) and the combined organic layer was washed with brine and dried over anhydrous Na_2SO_4 . After concentration under reduced pressure, the crude product was purified by column chromatography (silica gel, $^n\text{hexane}/\text{EtOAc} = 4/1$) to give the title compound **S5** as a white solid. **Mp**: = 75–77 °C; **IR** (neat): $\nu = 2898, 1564, 1538, 1414, 1374, 1108, 821$ cm^{-1} ; **^1H NMR** (600 MHz, CDCl_3): δ 7.72 (d, $J = 8.0$ Hz, 1H), 7.49 (d, $J = 8.0$ Hz, 1H), 5.97 (s, 1H), 4.15 – 4.11 (m, 2H), 4.11 – 4.07 (m, 2H); **^{13}C NMR** (151 MHz, CDCl_3): δ 141.0, 140.9, 138.3, 133.6, 127.2, 101.1, 65.6; **HRMS (DART)** for $\text{C}_8\text{H}_8\text{Br}_2\text{NO}_2$: calculated for $[\text{M}+\text{H}]^+$ 309.89013, found 309.89146.

Synthesis of 1-(6-Bromo-3-(1,3-dioxolan-2-yl)pyridin-2-yl)-2,2-dimethylpropan-1-one (**6**)⁴



To an oven-dried 100 mL 3-necked round-bottom flask equipped with a stirring bar was charged 2,6-dibromo-3-(1,3-dioxolan-2-yl)pyridine (**S5**, 6.2 g, 20 mmol), followed by addition of 60 mL dry THF under argon atmosphere. A solution of $^n\text{BuLi}$ (1.56 M in $^n\text{hexane}$, 14.2 mL, 22 mmol) was transferred to the reaction flask at -78°C via a dropping funnel. After the reaction mixture was allowed to stir at -78°C for 2 hours, a solution of methyl pivalate (4.7 g, 40 mmol) in 30 mL dry THF was transferred dropwise via a dropping funnel at -78°C and the mixture was continuously stirred at the same temperature for 1 hour. The reaction was gradually warmed up to room temperature and allowed to stir at room temperature for 3 hours. After completion, the solution was quenched with saturated NH_4Cl and extracted with EtOAc (3×30 mL). The organic phase was combined and washed with brine, dried over anhydrous Na_2SO_4 , and evaporated under reduced pressure. The crude product was purified by column chromatography (silica gel, $^n\text{hexane}/\text{EtOAc} = 4/1$) to give the title compound **6** as a colorless oil. **IR** (neat): $\nu = 2969, 2875, 1695, 1481, 1392, 1280, 1110, 978 \text{ cm}^{-1}$; **$^1\text{H NMR}$** (600 MHz, CDCl_3): δ 7.78 (d, $J = 8.2$ Hz, 1H), 7.50 (d, $J = 8.2$ Hz, 1H), 5.98 (s, 1H), 3.99 (s, 4H), 1.32 (s, 9H); **$^{13}\text{C NMR}$** (151 MHz, CDCl_3): δ 208.9, 156.6, 140.1, 137.5, 131.4, 128.3, 99.7, 65.2, 44.1, 27.3; **HRMS (DART)** for $\text{C}_{13}\text{H}_{17}\text{BrNO}_3$: calculated for $[\text{M}+\text{H}]^+$ 314.03918, found 314.03978.

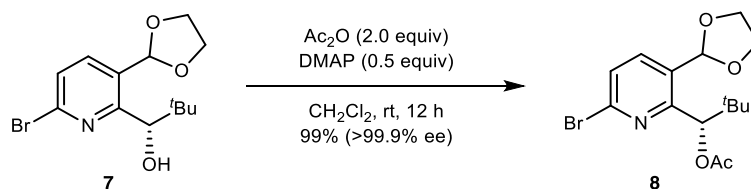
Synthesis of (*S*)-1-(6-Bromo-3-(1,3-dioxolan-2-yl)pyridin-2-yl)-2,2-dimethylpropan-1-ol (**7**)⁵



$\text{RuCl}_2[(S,S)\text{-Tsdpen}](\text{mesitylene})$ (395.1 mg, 0.6 mmol) was charged into 100 mL 2-necked round-bottom flask equipped with a stirring bar, then 30 mL degassed H_2O was added under argon atmosphere. After stirring the suspension at 40°C for 1 hour, a solution of sodium formate

in 30 mL degassed H₂O was added into the reaction flask followed by adding 1-(6-bromo-3-(1,3-dioxolan-2-yl)pyridin-2-yl)-2,2-dimethylpropan-1-one (**6**, 4.0 g, 13 mmol) via syringe. The reaction mixture was allowed to stir at 40 °C for 72 hours. After completion, the reaction was extracted with EtOAc (3 × 40 mL). The organic phase was combined and washed with brine, dried over anhydrous Na₂SO₄, and evaporated under reduced pressure. The crude product was purified by column chromatography (silica gel, ⁿhexane/EtOAc = 4/1). The resulting compound was recrystallized by using ⁿhexane to give the title compound **7** as a colorless crystal with single (*S*)-enantiomer (>99.9% ee). **Mp**: 73–74 °C; **IR** (neat): $\nu = 3523, 2884, 1574, 1445, 1362, 1173, 1044, 844 \text{ cm}^{-1}$; **¹H NMR** (600 MHz, CDCl₃): δ 7.74 (d, *J* = 8.2 Hz, 1H), 7.41 (d, *J* = 8.2 Hz, 1H), 6.00 (s, 1H), 4.71 (d, *J* = 9.9 Hz, 1H), 4.18 – 4.10 (m, 2H), 4.07 – 4.01 (m, 2H), 3.49 (d, *J* = 9.8 Hz, 1H), 0.95 (s, 9H); **¹³C NMR** (151 MHz, CDCl₃): δ 160.3, 141.4, 137.6, 130.7, 126.9, 99.5, 75.7, 65.7, 65.5, 36.9, 26.1; **HRMS (DART)** for C₁₃H₁₉BrNO₃: calculated for [M+H]⁺ 316.05483, found 316.05424; **HPLC** (Daicel Chiralpak[®] AD-3, ⁿhexane/ⁱPrOH = 9/1, flow rate 0.6 mL/min at a wavelength of 254 nm); *t*_R = 21.6 min (major, *S*), *t*_R = 36.5 (minor, *R*); [α]_D²⁶ = 13.6 (c = 1.00, CHCl₃, >99.9% ee [after recrystallization]).

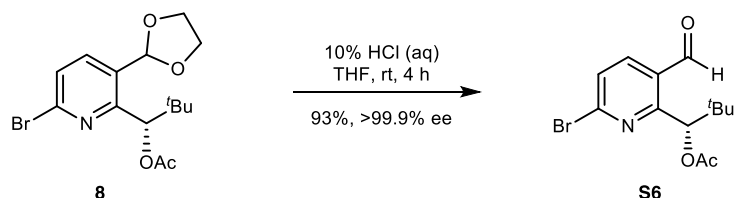
Synthesis of (*S*)-1-(6-Bromo-3-(1,3-dioxolan-2-yl)pyridin-2-yl)-2,2-dimethylpropyl acetate (**8**)⁶



To a solution of (*S*)-1-(6-bromo-3-(1,3-dioxolan-2-yl)pyridin-2-yl)-2,2-dimethylpropan-1-ol (**7**, 1.02 g, 3.2 mmol) and *N,N*-dimethylpyridin-4-amine (197 mg, 1.6 mmol) in 10 mL dry CH₂Cl₂, was added acetic anhydride (0.6 mL, 6.5 mmol) under argon atmosphere. The reaction mixture was stirred at room temperature for 12 hours. After completion, the solvent was removed under reduced pressure then the crude product was purified by column chromatography (silica gel, ⁿhexane/EtOAc = 4/1) to give the title product **8** as a white solid. **Mp**: = 101–103 °C; **IR** (neat): $\nu = 2966, 2878, 1731, 1571, 1558, 1437, 1364, 1098, 828 \text{ cm}^{-1}$; **¹H NMR** (600 MHz, CDCl₃): δ 7.77 (d, *J* = 8.2 Hz, 1H), 7.40 (d, *J* = 8.2 Hz, 1H), 6.26 (s, 1H), 5.70 (s, 1H), 4.16 – 4.02 (m, 4H), 2.08 (s, 3H), 1.02 (s, 9H); **¹³C NMR** (151 MHz, CDCl₃): δ 170.8, 156.8, 141.3, 137.3, 131.9, 127.2, 99.6, 78.2, 65.5, 65.4, 35.5, 26.6, 21.0; **HRMS (DART)** for C₁₅H₂₁BrNO₄: calculated for [M+H]⁺ 358.06540, found 358.06499; **HPLC** (Daicel Chiralpak[®] AD-H + AD-3,

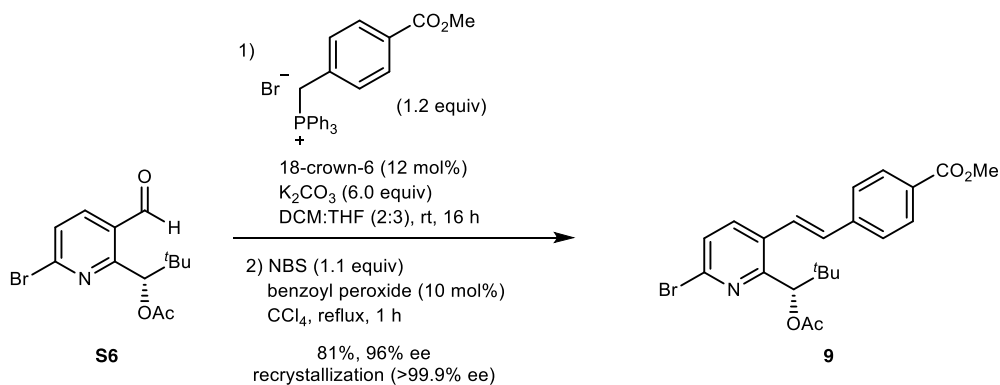
$n_{\text{hexane}}/i\text{PrOH} = 9/1$, flow rate 0.6 mL/min at a wavelength of 254 nm); $t_{\text{R}} = 15.8$ min (minor, *R*) $t_{\text{R}} = 19.7$ min (major, *S*); $[\alpha]_{\text{D}}^{26} = -7.3$ ($c = 1.01$, CHCl_3 , >99.9% ee).

Synthesis of (*S*)-1-(6-Bromo-3-formylpyridin-2-yl)-2,2-dimethylpropyl acetate (**S6**)⁷



To a solution of (*S*)-1-(6-bromo-3-(1,3-dioxolan-2-yl)pyridin-2-yl)-2,2-dimethylpropyl acetate (**8**, 1.41 g, 3.9 mmol) in 20 mL dry THF was added 10 mL of 10% HCl aqueous solution. The reaction mixture was stirred at room temperature for 3 hours. Another portion of 10% HCl (5 mL) was added, and the reaction mixture was continuously stirred at the same temperature for 1 hour. After completion, the solution was extracted with EtOAc (3×20 mL). The organic layers were combined and washed with brine, dried over anhydrous Na_2SO_4 , and evaporated under reduced pressure. The crude product was purified by column chromatography (silica gel, $n_{\text{hexane}}/\text{EtOAc} = 4/1$) to give the title compound **S6** as a colorless oil. **IR** (neat) $\nu = 2961, 2872, 1738, 1694, 1568, 1374, 1247, 821 \text{ cm}^{-1}$; **$^1\text{H NMR}$** (600 MHz, CDCl_3): δ 10.50 (d, $J = 1.1$ Hz, 1H), 7.98 (dd, $J = 8.2, 1.6$ Hz, 1H), 7.54 (dd, $J = 8.2, 1.2$ Hz, 1H), 6.05 (d, $J = 1.5$ Hz, 1H), 2.12 (d, $J = 1.6$ Hz, 3H), 1.01 (d, $J = 1.7$ Hz, 9H); **$^{13}\text{C NMR}$** (151 MHz, CDCl_3): δ 189.7, 170.7, 160.1, 145.8, 138.9, 129.8, 127.7, 78.7, 35.5, 26.3, 20.9; **HRMS (DART)** for $\text{C}_{13}\text{H}_{17}\text{BrNO}_3$: calculated for $[\text{M}+\text{H}]^+$ 314.03918, found 314.04009; **HPLC** (Daicel Chiralpak[®] AD-H + Daicel Chiralcel[®] OD-H, $n_{\text{hexane}}/i\text{PrOH} = 9/1$, flow rate 0.6 mL/min at a wavelength of 254 nm); $t_{\text{R}} = 18.7$ min (minor, *R*), $t_{\text{R}} = 20.8$ min (major, *S*); $[\alpha]_{\text{D}}^{23} = -23.8$ ($c = 0.51$, CHCl_3 , >99.9% ee).

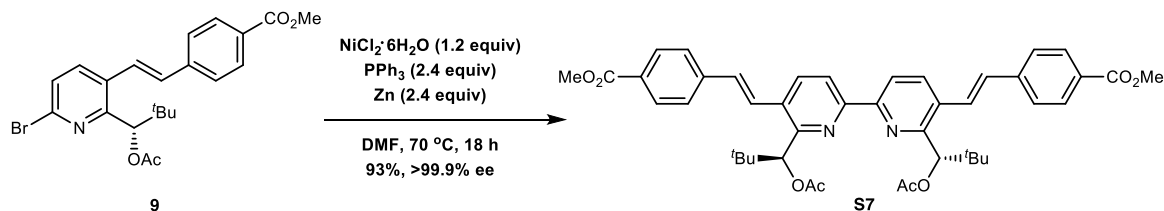
Synthesis of Methyl (*S,E*)-4-(2-(2-(1-acetoxy-2,2-dimethylpropyl)-6-bromopyridin-3-yl)vinyl)benzoate (**9**)^{8,9}



To an oven-dried 100 mL 2-necked round-bottom flask equipped with a stirring bar were charged (4-(methoxycarbonyl)benzyl)triphenylphosphonium bromide (1.60 g, 3.25 mmol), K₂CO₃ (2.25 g, 16.3 mmol), 18-crown-6 ether (87 mg, 0.3 mmol) under argon atmosphere. Subsequently, 10 mL dry THF and 14 mL dry CH₂Cl₂ were added, then the suspension was stirred at room temperature for 5 minutes. To the resulting suspension was slowly transferred a solution of (*S*)-1-(6-bromo-3-formylpyridin-2-yl)-2,2-dimethylpropyl acetate (**S6**, 852 mg, 2.7 mmol) in 11 mL dry THF. The reaction mixture was stirred at room temperature for 16 hours. After completion, the suspension was filtered through a celite pad, the filtrate was concentrated and then extracted with EtOAc (3 × 30 mL). The combined organic phase and washed with brine, dried over anhydrous Na₂SO₄, and evaporated under reduced pressure. The crude product was filtered through a short column (silica gel, ⁿhexane/EtOAc = 4/1) to obtain a mixture of (*E*)- and (*Z*)-isomers. To an oven-dried 50 mL round-bottom flask were charged the obtained crude product, 15 mL CCl₄, *N*-Bromosuccinimide (530 mg, 3.0 mmol), and benzoyl peroxide (65 mg, 0.3 mmol). The reaction mixture was refluxed at 80 °C for 1 hour. After completion, the reaction was extracted with CH₂Cl₂ (3 × 15 mL). The combined organic phase and washed with brine, dried over anhydrous Na₂SO₄, and evaporated under reduced pressure. The crude product was purified by column chromatography (silica gel, ⁿhexane/EtOAc/MeOH = 9/1/0.5). The resulting compound was recrystallized by using ⁿhexane to give the title compound **9** as a white crystal with single (*S*)-enantiomer (>99.9% ee). **Mp**: = 97–99 °C; **IR** (neat) ν = 2955, 1714, 1604, 1568, 1435, 1260, 1135, 767 cm⁻¹; **¹H NMR** (600 MHz, CDCl₃): δ 8.04 (d, *J* = 8.4 Hz, 2H), 7.67 (d, *J* = 8.2 Hz, 1H), 7.64 (d, *J* = 16.2 Hz, 1H), 7.57 (d, *J* = 8.3 Hz, 2H), 7.39 (d, *J* = 8.2 Hz, 1H), 6.93 (d, *J* = 16.1 Hz, 1H), 5.69 (s, 1H), 3.93 (s, 3H), 2.10 (s, 3H), 0.99 (s, 9H); **¹³C NMR** (151 MHz, CDCl₃): δ 171.0, 166.7, 155.9, 141.0, 140.0, 136.5, 132.0, 131.9, 130.1, 129.6, 127.2, 126.6, 126.5, 78.9, 52.1, 36.0, 26.4, 20.9; **HRMS (DART)** for C₂₂H₂₅BrNO₄: calculated for [M+H]⁺ 446.09670, found 446.09564; **HPLC** (Daicel Chiralpak[®] AD-H + Daicel Chiralcel[®] AD-3,

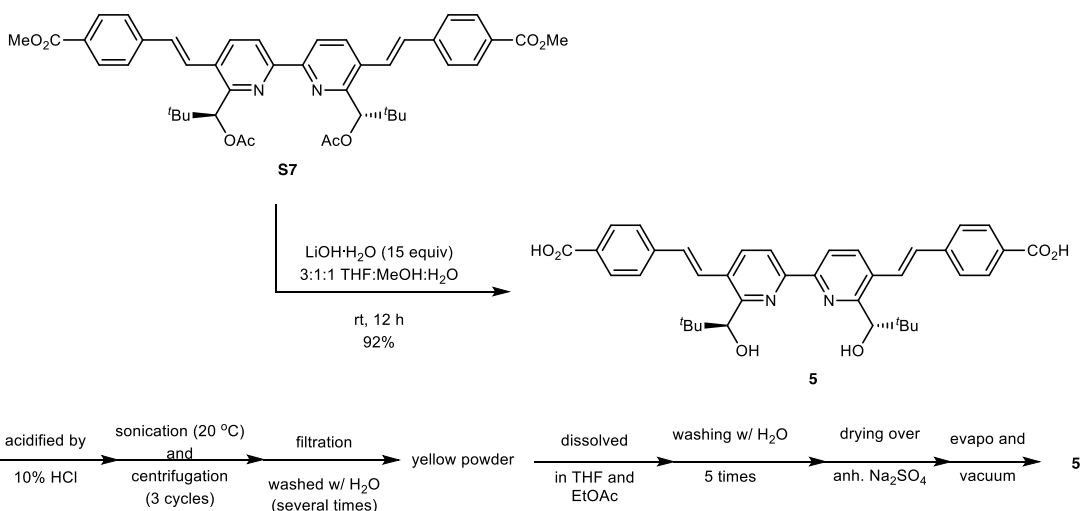
n hexane/ i PrOH = 9/1, flow rate 0.6 mL/min at a wavelength of 254 nm); t_R = 25.3 min (minor, *R*), t_R = 29.0 min (major, *S*); $[\alpha]_D^{25}$ = 139.2 (c = 0.52, CHCl₃, >99.9% ee [after recrystallization]).

Synthesis of Dimethyl 4,4'-((1*E*,1'*E*)-(6,6'-bis((*S*)-1-acetoxy-2,2-dimethylpropyl)-[2,2'-bipyridine]-5,5'-diyl)bis(ethene-2,1-diyl)dibenzoate (**S7**)¹⁰



To an oven-dried 15 mL sealed tube containing a stirring bar were charged Methyl (*S,E*)-4-(2-(2-(1-acetoxy-2,2-dimethylpropyl)-6-bromopyridin-3-yl)vinyl)benzoate (**9**, 500 mg, 1.12 mmol), PPh₃ (706 mg, 2.7 mmol), and NiCl₂ · 6H₂O (319 mg, 1.3 mmol). The tube was transferred into an argon-filled glovebox, Zn (176 mg, 2.7 mmol), and 10 mL dry DMF were added before closing with a screw cap and removing from the glovebox. The suspension was stirred at 70 °C for 18 hours. After completion, it was quenched with NH₃ solution in ethanol (3 mL) followed by filtration through a celite pad. The filtrate was extracted with Et₂O (3 × 15 mL) and the combined organic phase and washed with brine, dried over anhydrous Na₂SO₄, and evaporated under reduced pressure. The crude product was purified by column chromatography (silica gel, n hexane/EtOAc = 4/1) to give the title compound **S7** as a white solid with single (*S,S*)-enantiomer (>99.9% ee). **Mp**: = 249–250 °C; **IR** (neat) ν = 2955, 2872, 1717, 1604, 1432, 1365, 1275, 764 cm⁻¹; **¹H NMR** (600 MHz, CDCl₃): δ 8.41 (d, J = 8.2 Hz, 2H), 8.06 (d, J = 8.3 Hz, 4H), 7.98 (d, J = 8.2 Hz, 2H), 7.80 (d, J = 16.1 Hz, 2H), 7.61 (d, J = 8.3 Hz, 4H), 7.02 (d, J = 16.1 Hz, 2H), 5.85 (s, 2H), 3.94 (s, 6H), 2.09 (s, 6H), 1.08 (s, 18H); **¹³C NMR** (151 MHz, CDCl₃): δ 171.0, 166.8, 154.3, 153.9, 141.5, 134.8 (d, J = 16.6 Hz), 132.5 (d, J = 3.6 Hz), 131.4, 130.8, 130.0 (d, J = 1.3 Hz), 129.4, 126.6 (dd, J = 30.9, 2.4 Hz), 119.9, 79.7, 52.2, 35.9, 26.7 (q, J = 6.0 Hz), 21.0 (q, J = 12.2 Hz); **HRMS (ESI)** for C₄₄H₄₈N₂NaO₈: calculated for [M+Na]⁺ 755.3303, found 755.3285; **HPLC** (Daicel Chiralpak[®] AD-3, n hexane/ i PrOH = 9/1, flow rate 0.6 mL/min at a wavelength of 254 nm); t_R = 20.0 min (major, *S,S*), t_R = 23.8 min (minor, *R,R*); $[\alpha]_D^{24}$ = 99.7 (c = 0.25, CHCl₃, >99.9% ee).

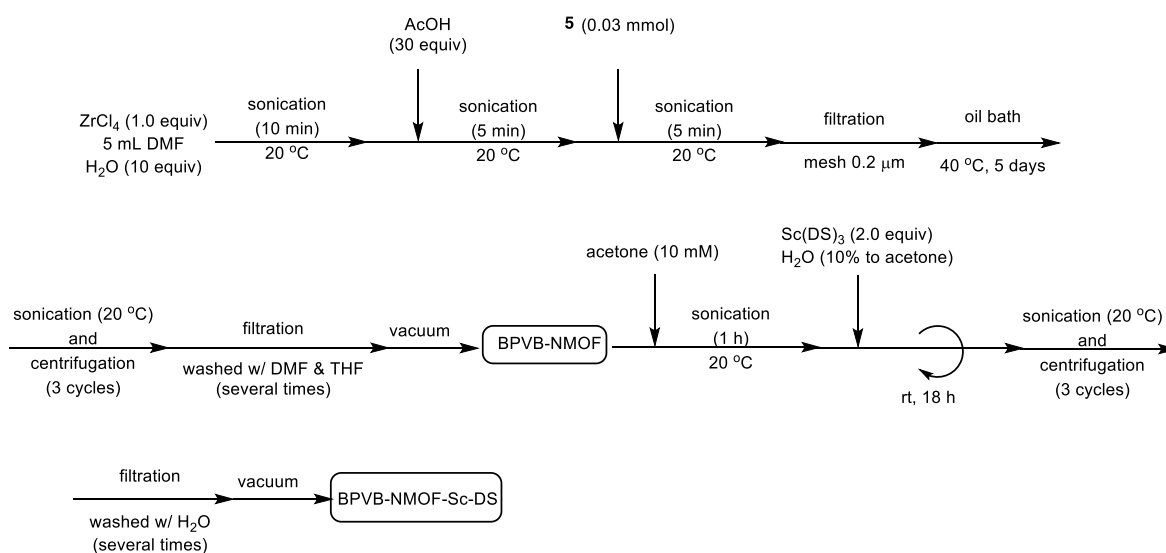
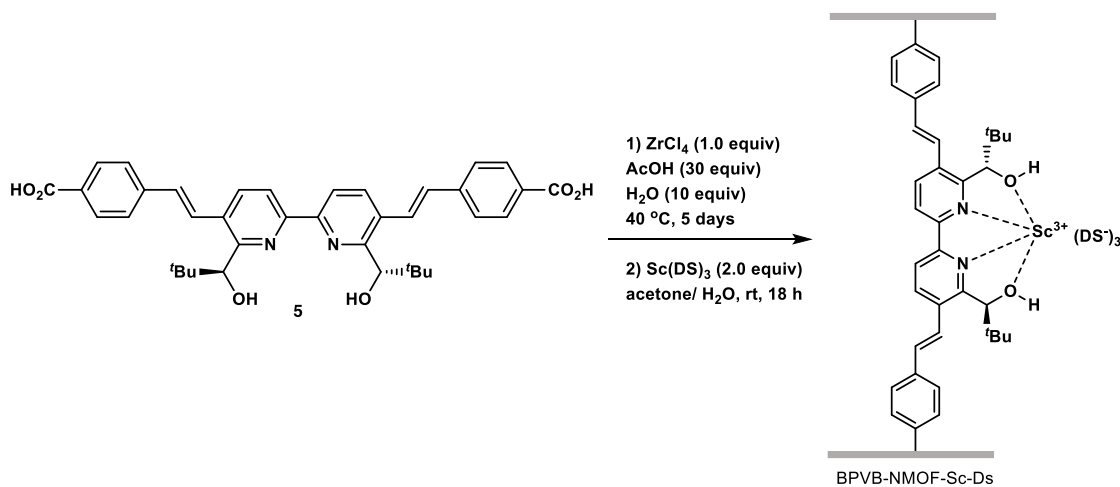
Synthesis of 4,4'-((1*E*,1'*E*)-(6,6'-bis((*S*)-1-hydroxy-2,2-dimethylpropyl)-[2,2'-bipyridine]-5,5'-diyl)bis(ethene-2,1-diyl)dibenzoic acid (**5**)¹¹



To a solution of dimethyl 4,4'-((1*E*,1'*E*)-(6,6'-bis((*S*)-1-acetoxy-2,2-dimethylpropyl)-[2,2'-bipyridine]-5,5'-diyl)bis(ethene-2,1-diyl)dibenzoate (**S7**, 420 mg, 0.6 mmol) in 7.5 mL THF and 2.5 mL MeOH, was slowly added a solution of LiOH · H₂O (359 mg, 8.6 mmol in 2.5 mL H₂O). The reaction mixture was stirred at room temperature for 12 hours. After completion, the solution was acidified by 10% HCl before sonication (at 20 °C, 1 hour) then centrifugation (3500 rpm, 10 minutes). The sonication and centrifugation were done repeatedly for 3 cycles (washing with H₂O), followed by filtration washed several times with H₂O. The filtered solid was dissolved in THF and EtOAc then washed with H₂O (5 times), dried over anhydrous Na₂SO₄, and concentrated under reduced pressure to give the title compound **5** as a pale yellow solid. **Mp**: >355 °C; **IR** (neat) $\nu = 2956, 2925, 2865, 1682, 1605, 1585, 1422, 1290, 1050, 843 \text{ cm}^{-1}$; **¹H NMR** (600 MHz, DMSO-*d*₆): δ 12.90 (s, 2H), 8.46 (d, *J* = 7.7 Hz, 2H), 8.29 (d, *J* = 7.8 Hz, 2H), 7.94 (d, *J* = 7.4 Hz, 4H), 7.89 (d, *J* = 16.1 Hz, 2H), 7.76 (d, *J* = 7.3 Hz, 4H), 7.31 (d, *J* = 16.0 Hz, 2H), 5.08 (d, *J* = 7.3 Hz, 2H), 4.92 (d, *J* = 7.0 Hz, 2H), 0.92 (s, 18H); **¹³C NMR** (151 MHz, DMSO-*d*₆): δ 167.6, 158.8, 153.0, 141.9, 135.1, 131.9, 130.8, 130.4, 127.7, 127.4, 119.8, 100.0, 77.4, 37.5, 27.0; **HRMS (ESI)** for C₃₈H₄₀N₂NaO₆: calculated for [M+Na]⁺ 643.2779, found 643.2764; $[\alpha]_{\text{D}}^{25} = 27.5$ (c = 0.26, DMSO).

4. Synthesis of BPVB-NMOF-Sc-DS

4.1 General procedure for the synthesis of BPVB-NMOF-Sc-DS



In a 20 mL vial, a solution of ZrCl_4 (7 mg, 0.03 mmol) in 5 mL dry DMF and H_2O (5.4 μL , 0.3 mmol) was sonicated at 20 °C for 10 minutes. AcOH (54.9 μL , 0.9 mmol) was added, and then sonicated at 20 °C for 5 minutes, followed by the addition of the chiral H_2BPVB (**5**, 18.6 mg, 0.03 mmol) and sonication at 20 °C for 5 minutes. The resulting solution was filtered by a PTFE membrane filter (mesh = 0.2 μm) into a 50 mL vial. Covered by a non-tight cap, the solution was put in an oil bath at 40 °C. After standing at 40 °C for 5 days, it was allowed to cool down to room temperature and sonicated (at 20 °C, 10 minutes) then centrifugation (3500 rpm, 10 minutes). The sonication and centrifugation were done repeatedly for 3 cycles (washing with DMF), followed by filtration washed several times with DMF and THF. The title BPVB-NMOF (10.3 mg, 47%) was obtained as a pale yellow solid after drying in *vacuo* at room temperature for 2 hours. To analyze linker occupancy in BPVB-NMOF, 10 mg of the resulting BPVB-NMOF

was digested in a 1:1 mixture of a saturated K_3PO_4/D_2O solution and $DMSO-d_6$ (0.6 : 0.6 mL). The suspension was sonicated at room temperature for 10 minutes, after which the organic layer was subjected to 1H -NMR analysis (Figure S5).

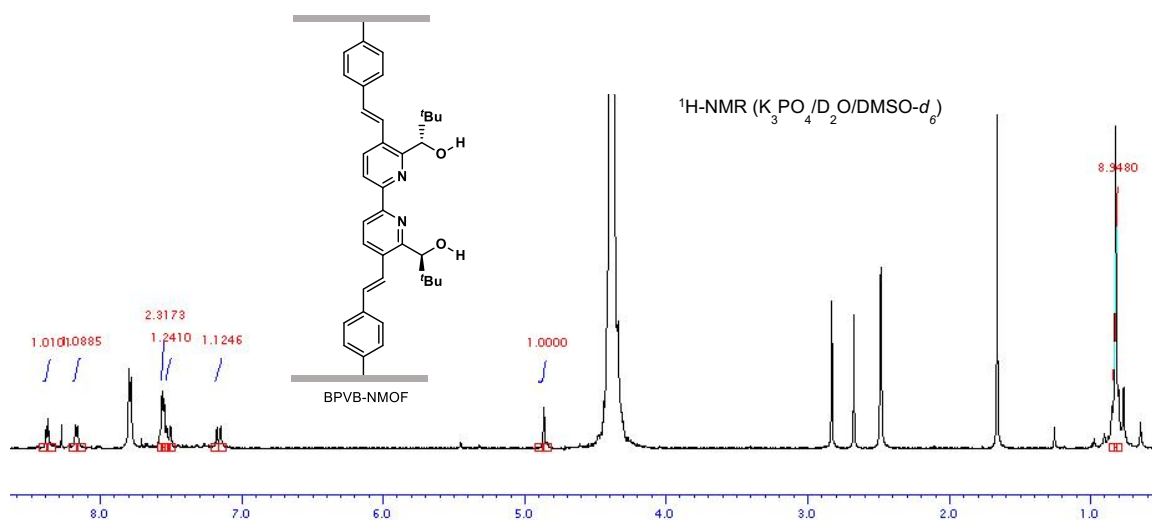
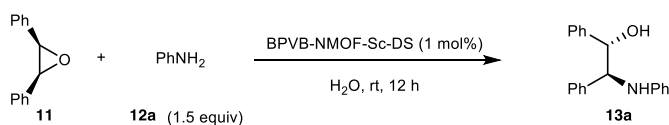
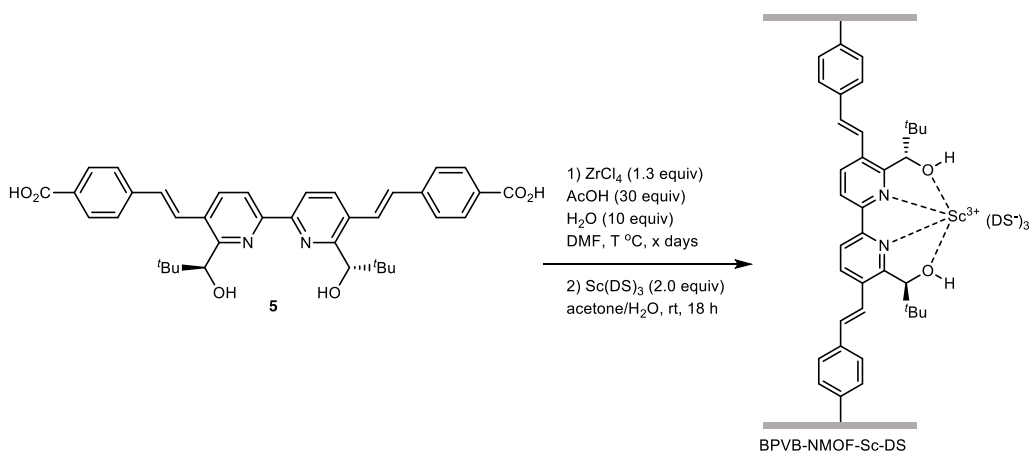


Figure S5. 1H -NMR Analysis of BPVB-NMOF.

BPVB-NMOF (24.7 mg, 0.0056 mmol, the weight of solvent-containing in MOF was omitted) was charged into a 2 mL vial, followed by the addition of acetone (0.6 mL, 10mM). The suspension was sonicated at 20 °C for 1 hour, $Sc(DS)_3$ (76.4 mg, 0.067 mmol, 2.0 equiv to bipyridine scaffold, assumed that no defect of the bipyridine linker during MOF construction) was added, followed by adding H_2O (60 μ L). The suspension was vigorously stirred at room temperature for 18 hours. After completion, it was sonicated (at 20 °C, 10 minutes) and then centrifugation (3500 rpm, 10 minutes). The sonication and centrifugation were done repeatedly for 3 cycles (washing with H_2O), followed by filtration washed several times with H_2O and acetone. The title BPVB-NMOF- Sc -DS (41.1 mg) was obtained as a yellow solid after drying in *vacuo* at room temperature for 12 hours. BPVB-NMOF- Sc -DS has Sc and Zr loadings of 0.451 and 0.818 mmol/g, respectively. Under the identical procedure, BPVB-NMOF- Sc -OTf has Sc and Zr loadings of 1.370 and 1.329 mmol/g, respectively.

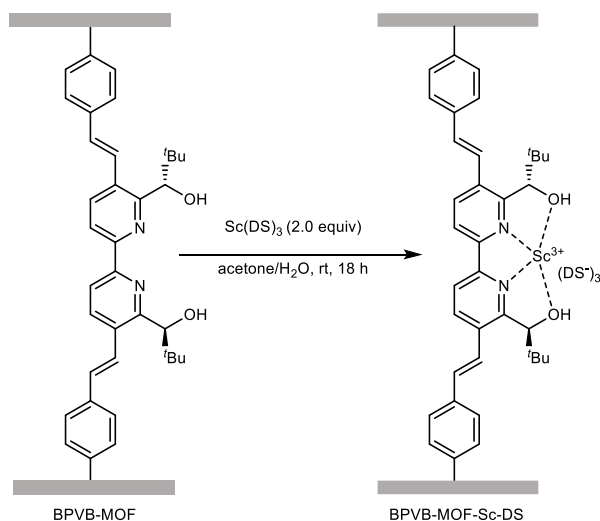
Table S6. Optimization in the preparation of BPVB-NMOF.



Entry	MOF Conditions	Results	ZrCl_4 Source
1	90 °C, 2 d	62% yield, 57% ee	Wako:LEG4496
2	90 °C, 2 d	82% yield, 70% ee	Wako:WTK0876
3	70 °C, 3 d	95% yield, 76% ee	Wako:WTK0876
4 ^a	70 °C, 3 d	88% yield, 79% ee	Wako:WTK0876
5 ^a	60 °C, 4 d	92% yield, 82% ee	Wako:WTK0876
6 ^a	60 °C, 3 d	94% yield, 82% ee	Aldrich ($\geq 99.9\%$)
7 ^a	50 °C, 5 d	91% yield, 84% ee	Aldrich ($\geq 99.9\%$)
8 ^a	40 °C, 7 d	93% yield, 84% ee	Aldrich ($\geq 99.9\%$)

^a1.0 equiv of ZrCl_4 was applied.

Table S7. Reproducibility of post-synthetic metalation step.



Trial	Sc Loading (mmol/g)	Zr Loading (mmol/g)	Sc/Zr ratio (%)
1 st	0.451	0.818	55
2 nd	0.499	0.972	51
3 rd	0.496	0.901	55

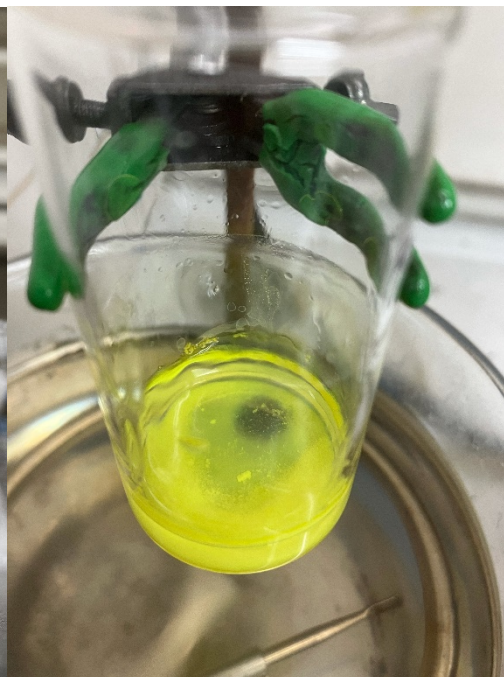
Table S8. Elemental analysis for nitrogen loading of the 3rd trial (in Table S7)

BPVB-MOF-Sc-DS (mg)	C (%)	H (%)	N (%)	N (mmol/g)	Sc/N ratio (%)
1.0839	45.52	6.97	1.36	0.971	102

a)



b)



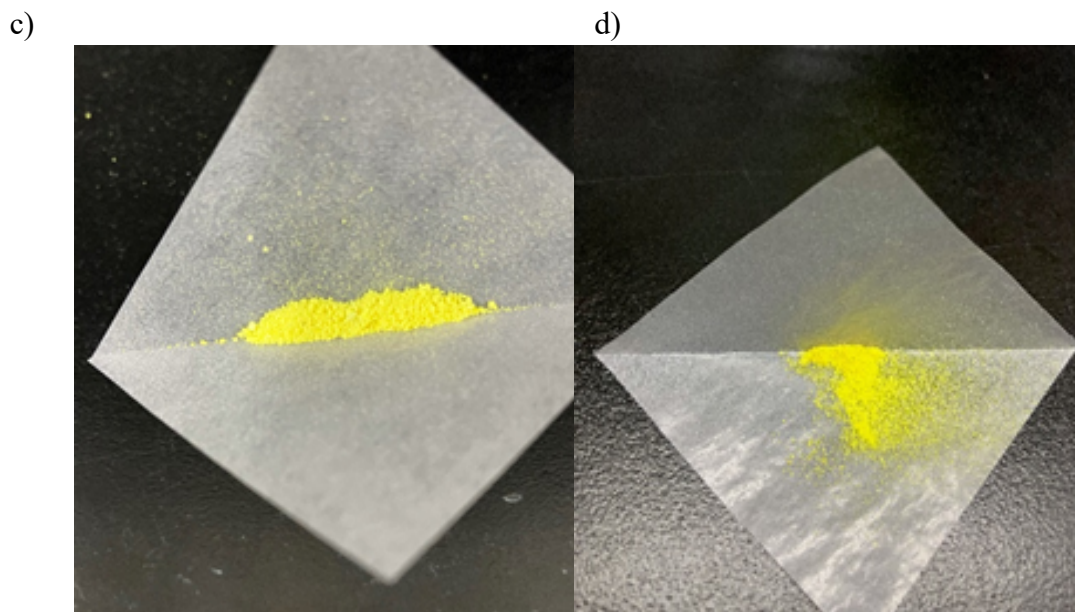
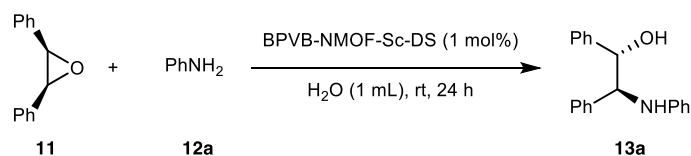


Figure S6. Preparation of chiral BPVB-NMOFs. **a**, A solution before solvothermal process. **b**, After precipitation at 40 °C. **c**, BPVB-NMOF after filtration and drying under vacuum. **d**, BPVB-NMOF-Sc-DS after filtration and drying under vacuum.

5. Control experiments for epoxide ring-opening reactions

Table S9. Control experiments in BPVB-NMOF-Sc-DS-catalyzed asymmetric ring-opening reaction of epoxide in water.



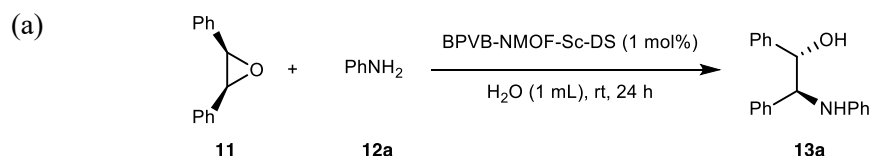
Entry	Deviation from standard conditions	Yield (%)	Ee (%)
1	none	>99	85
2	w/o catalyst	n.d.	-
3	Sc(DS) ₃ (1 mol%), 1 (1.2 mol%)	87	93
4	Sc(DS) ₃ (1 mol%), 5 (1.2 mol%)	61	49
5 ^a	BPVB-MOF (w/o Sc)	20	3
6	BPVB-MOF-OTf	22	61
7	0.5 mol%	82	76
8	0.25 mol%	77	70
9	12 h	93	84
10	6 h	80	83
11	THF	12	23
12	CH ₂ Cl ₂	32	49
13	MeCN	58	35
14	w/o solvent	89	31
15	MOPS buffer	74	70
16	entry 3 in MOPS buffer	27	86

Reaction conditions: **11** (0.2 mmol), BPVB-NMOF-Sc-DS (1 mol%, 0.002 mmol), **12a** (0.3 mmol), H₂O (1 mL), rt, 24 h, yield after isolation. ^aZr loading was controlled as same as the standard conditions (2.8 mol% Zr). MOPS buffer (0.2 M, pH = 7.5). DS = dodecyl sulfate. n.d.= not detected.

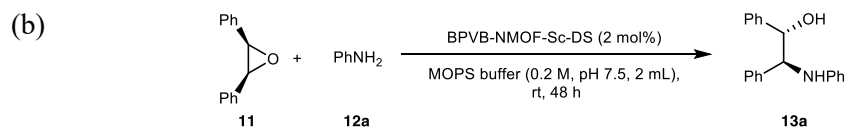
Table S10. Leaching issue of the standard reaction conditions.

Metal ion leaching	Aqueous phase (%)	Crude product (%)
Sc	UDL	UDL
Zr	UDL	UDL

Respective limit of detection for Sc and Zr is 0.65% and 0.44%, respectively.



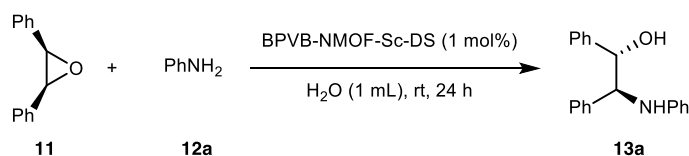
Sc loading of BPVB-NMOF-Sc-DS	Yield (%)	Ee (%)
0.350	>99	84
0.509	>99	85
0.705	98	84



Sc loading of BPVB-NMOF-Sc-DS	Yield (%)	Ee (%)
0.430	96	78
0.584	98	76

Table S11. Lot difference. (a) reaction in water; (b) reaction in MOPS buffer.

6. Typical procedure for epoxide ring-opening reactions in water

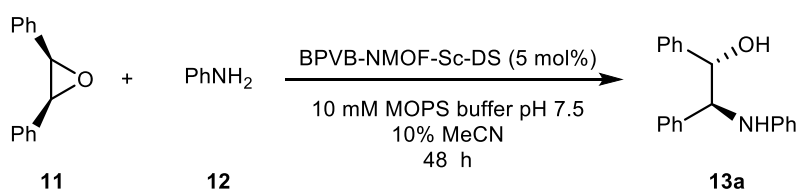


To a 2 mL vial equipped with a stirring bar were charged **11** (39.3 mg, 0.2 mmol) and BPVB-NMOF-Sc-DS (0.002 mmol, 1 mol% based on Sc³⁺), followed by adding degassed water (1 mL). It was flushed by argon before closing a cap to stir at room temperature for 1 hour. Aniline (27.4 μ L, 0.3 mmol) was loaded and again argon-flushed before stirring at room temperature. After 24 hours, the reaction mixture was filtered then the filtrate was extracted with EtOAc (3 x 15 mL). The combined organic phase was washed with brine, and dried over anhydrous Na₂SO₄. The crude product was obtained after filtration and concentration. It was then purified by preparative thin-layer chromatography (*n*-hexane/EtOAc = 3/1) to give the desired product **13a**.



Figure S7. Appearance of the reaction in water after completion.

<Conditions reported by Ueno *et al.*>



at rt; 18% conv., 76% ee
at 40 °C, dark; 49% conv., 76% ee
Ueno's conditions; 43% conv., -17% ee

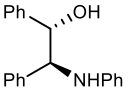
Figure S8. Comparison with Ueno's result.

To a 2 mL vial equipped with a stirring bar, BPVB-NMOF-Sc-DS (1.2×10^{-4} mmol, 5 mol% based on Sc^{3+}), 30 μL of acetonitrile (MeCN), and 540 μL of MOPS buffer (10 mM, pH 7.5) were added. This was followed by the addition of **11** (15 μL , 0.16 M in MeCN, 2.4×10^{-3} mmol) and **12** (15 μL , 0.16 M in MeCN, 2.4×10^{-3} mmol). The vial was flushed with argon before closing the cap and stirring at room temperature or 40 °C. After 48 hours, the reaction mixture was quenched by adding saturated NaHCO_3 (1 mL) and EtOAc (3 mL), then centrifuged at 3500 rpm for 10 minutes. This centrifugation step was repeated three times. The combined organic phase was washed with brine and dried over anhydrous Na_2SO_4 . The crude product was obtained after filtration and concentration. Conversion and enantioselectivity were determined by ^1H NMR analysis and HPLC, respectively.

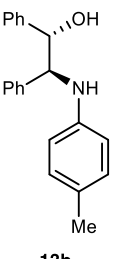
7. Spectroscopic data of the products

The obtained analytical data for literature-known compounds is in full agreement with reported data.

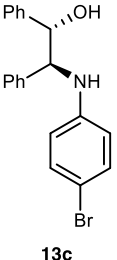
(1*S*,2*S*)-1,2-diphenyl-2-(phenylamino)ethan-1-ol (13a)¹²

**¹H NMR** (600 MHz, CDCl₃) δ 7.32 – 7.22 (m, 10H), 7.11 – 7.07 (m, 2H), 6.71 – 6.66 (m, 1H), 6.56 (dd, *J* = 8.6, 0.9 Hz, 2H), 4.87 (d, *J* = 5.9 Hz, 1H), 4.70 (br s, 1H), 4.55 (d, *J* = 5.9 Hz, 1H), 2.63 (br s, 1H); **¹³C NMR** (151 MHz, CDCl₃) δ 147.2, 140.5, 140.2, 129.0, 128.5, 128.2, 127.8, 127.5, 127.2, 126.5, 117.9, 114.1, 78.0, 64.7; **HPLC** (Daicel Chiralcel[®] OD-H, ⁿhexane/ⁱPrOH = 90/10, flow rate 1.0 mL/min at a wavelength of 254 nm, 35 °C); *t*_R = 13.0 min (minor), *t*_R = 17.2 min (major).

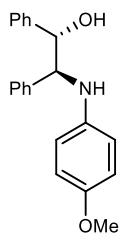
(1*S*,2*S*)-1,2-diphenyl-2-(*p*-tolylamino)ethan-1-ol (13b)¹³

**The crude mixture was purified by preparative TLC** (ⁿhexane/toluene/EtOAc = 3/1/1). **¹H NMR** (600 MHz, CDCl₃) δ 7.32 – 7.20 (m, 10H), 6.92 (d, *J* = 8.3 Hz, 2H), 6.51 (d, *J* = 8.4 Hz, 2H), 4.85 (d, *J* = 6.2 Hz, 1H), 4.51 (d, *J* = 6.2 Hz, 1H), 2.21 (s, 3H); **¹³C NMR** (151 MHz, CDCl₃) δ 144.9, 140.6, 140.2, 129.5, 128.4, 128.1, 127.8, 127.4, 127.3, 127.2, 126.6, 114.3, 78.0, 65.2, 20.3; **HPLC** (Daicel Chiralpak[®] AD-H, ⁿhexane/ⁱPrOH = 95/5, flow rate 1.0 mL/min at a wavelength of 254 nm); *t*_R = 25.9 min (major), *t*_R = 28.0 min (minor).

(1*S*,2*S*)-2-((4-Bromophenyl)amino)-1,2-diphenylethan-1-ol (13c)^{13,14}

**The crude mixture was purified by preparative TLC** (ⁿhexane/Et₂O = 3/2). **¹H NMR** (600 MHz, CDCl₃) δ 7.35 – 7.19 (m, 10H), 7.14 (d, *J* = 8.5 Hz, 2H), 6.40 (d, *J* = 8.5 Hz, 2H), 4.86 (d, *J* = 5.0 Hz, 1H), 4.78 (s, 1H), 4.49 (d, *J* = 5.3 Hz, 1H), 2.49 (s, 1H); **¹³C NMR** (151 MHz, CDCl₃) δ 146.2, 140.4, 139.7, 131.7, 128.6, 128.3, 128.0, 127.6, 127.2, 126.4, 115.6, 109.4, 77.9, 64.5; **HPLC** (Daicel Chiralcel[®] OD-H + Daicel Chiralpak[®] AD-H, ⁿhexane/ⁱPrOH = 95/5, flow rate 1.0 mL/min at a wavelength of 254 nm); *t*_R = 70.9 min (major), *t*_R = 82.4 min (minor).

(1*S*,2*S*)-2-((4-Methoxyphenyl)amino)-1,2-diphenylethan-1-ol (13d)¹³



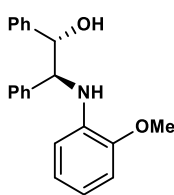
13d

The crude mixture was purified by twice preparative TLC (*n*-hexane/EtOAc = 4/1 then *n*-hexane/dichloromethane = 1/2).

¹H NMR (600 MHz, CDCl₃) δ 7.35 – 7.11 (m, 10H), 6.70 – 6.63 (m, 2H), 6.54 – 6.51 (m, 2H), 4.82 (d, *J* = 6.3 Hz, 1H), 4.50 – 4.23 (m, 2H), 3.68 (s, 3H), 2.85 (br s, 1H); **¹³C NMR** (151 MHz, CDCl₃) δ 152.5, 141.3, 140.6, 140.2, 128.4, 128.1, 127.8, 127.4, 127.3, 126.7, 115.7, 114.6, 78.1 (d, *J* = 3.1 Hz), 66.2, 55.6 (q, *J* = 3.1

Hz); **HPLC** (Daicel Chiralcel® OD-3, *n*-hexane/*i*-PrOH = 90/10, flow rate 1.0 mL/min at a wavelength of 254 nm); *t_R* = 24.7 min (major), *t_R* = 30.1 min (minor).

(1*S*,2*S*)-2-((2-Methoxyphenyl)amino)-1,2-diphenylethan-1-ol (13e)¹²



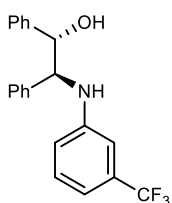
13e

The crude mixture was purified by preparative TLC (*n*-hexane/EtOAc = 9/1).

¹H NMR (600 MHz, CDCl₃) δ 7.37 – 7.11 (m, 10H), 6.78 (dd, *J* = 7.8, 1.4 Hz, 1H), 6.72 – 6.68 (m, 1H), 6.67 – 6.63 (m, 1H), 6.44 – 6.40 (m, 1H), 5.30 (br s, 1H), 4.89 (d, *J* = 6.4 Hz, 1H), 4.54 (d, *J* = 6.4 Hz, 1H), 3.89 (s, 3H), 2.80 (br s, 1H); **¹³C NMR** (151 MHz, CDCl₃) δ 147.4, 140.6, 140.1, 137.1, 128.4, 128.1,

127.7, 127.4, 127.3, 126.7, 121.0, 117.1, 111.7, 109.6, 78.3 (d, *J* = 3.3 Hz), 64.9, 55.6 (q, *J* = 3.2 Hz); **HPLC** (Daicel Chiralpak® AS-H, *n*-hexane/*i*-PrOH = 95/5, flow rate 0.8 mL/min at a wavelength of 254 nm); *t_R* = 15.1 min (major), *t_R* = 19.2 min (minor).

(1*S*,2*S*)-1,2-Diphenyl-2-((3-(trifluoromethyl)phenyl)amino)ethan-1-ol (13f)¹⁴



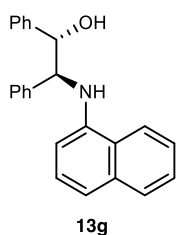
13f

The crude mixture was purified by preparative TLC (*n*-hexane/Et₂O = 3/2).

¹H NMR (600 MHz, CDCl₃) δ 7.35 – 7.23 (m, 10H), 7.12 (t, *J* = 7.9 Hz, 1H), 6.88 (d, *J* = 7.4 Hz, 1H), 6.77 (s, 1H), 6.61 (d, *J* = 8.2 Hz, 1H), 4.99 (br s, 1H), 4.90 (d, *J* = 5.5 Hz, 1H), 4.56 (d, *J* = 5.5 Hz, 1H), 2.49 (br s, 1H); **¹³C NMR** (151 MHz, CDCl₃) δ 147.4, 140.4, 139.6, 131.2 (q, *J* = 31.7 Hz), 129.4, 128.7, 128.3, 128.0,

127.7, 127.2, 126.4, 124.2 (q, *J* = 272.6 Hz), 116.5, 114.1 (q, *J* = 3.9 Hz), 110.5 (q, *J* = 4.0 Hz), 77.9, 64.3; **HPLC** (Daicel Chiralpak® AD-H, *n*-hexane/*i*-PrOH = 95/5, flow rate 1.0 mL/min at a wavelength of 254 nm); *t_R* = 15.2 min (major), *t_R* = 17.6 min (minor).

(1*S*,2*S*)-2-(Naphthalen-1-ylamino)-1,2-diphenylethan-1-ol (13g)¹²



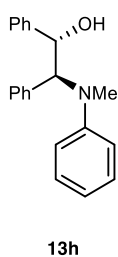
The crude mixture was purified by preparative TLC (*n*hexane/EtOAc = 4/1).

¹H NMR (600 MHz, CDCl₃) δ 8.07 – 8.02 (m, 1H), 7.84 – 7.79 (m, 1H), 7.58 – 7.47 (m, 2H), 7.40 – 7.27 (m, 10H), 7.24 – 7.13 (m, 2H), 6.40 – 6.32 (m, 1H), 5.58 (s, 1H), 5.04 (d, *J* = 5.4 Hz, 1H), 4.74 (d, *J* = 5.3 Hz, 1H), 2.56 (s, 1H); **¹³C**

NMR (151 MHz, CDCl₃) δ 142.1, 140.6, 139.9, 134.2, 128.6, 128.6, 128.3,

128.0, 127.5, 127.2, 126.5, 126.4, 125.6, 124.8, 123.9, 120.0, 117.7, 106.6, 78.2 (d, *J* = 3.4 Hz), 64.4 (d, *J* = 1.7 Hz); **HPLC** (Daicel Chiralcel® OD-3, *n*hexane/*i*PrOH = 95/5, flow rate 1.0 mL/min at a wavelength of 254 nm); *t*_R = 37.7 min (minor), *t*_R = 80.0 min (major).

(1*S*,2*S*)-2-(Methyl(phenyl)amino)-1,2-diphenylethan-1-ol (13h)¹²



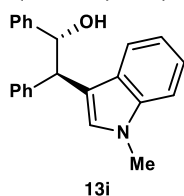
The crude mixture was purified by preparative TLC (*n*hexane/EtOAc = 4/1).

¹H NMR (600 MHz, CDCl₃) δ 7.43 (d, *J* = 7.8 Hz, 2H), 7.31 (t, *J* = 7.6 Hz, 2H), 7.26 (t, *J* = 7.5 Hz, 2H), 7.22 – 7.15 (m, 4H), 7.04 (d, *J* = 8.6 Hz, 2H), 7.03 – 6.99 (m, 2H), 6.96 – 6.93 (m, 1H), 5.32 (d, *J* = 10.0 Hz, 1H), 4.91 (d, *J* = 10.0 Hz, 1H), 4.01

(br s, 1H), 2.73 (s, 3H); **¹³C NMR** (151 MHz, CDCl₃) δ 151.3, 140.6, 134.6, 129.1,

128.7, 128.2, 127.9, 127.7, 127.6, 127.6, 120.3, 117.7, 73.7 (d, *J* = 2.8 Hz), 71.4 (d, *J* = 1.8 Hz), 32.7 (d, *J* = 2.0 Hz); **HPLC** (Daicel Chiralpak® AD-H, *n*hexane/*i*PrOH = 95/5, flow rate 0.8 mL/min at a wavelength of 254 nm); *t*_R = 15.3 min (minor), *t*_R = 30.7 min (major).

(1*R*,2*R*)-2-(1-Methyl-1*H*-indol-3-yl)-1,2-diphenylethan-1-ol (13i)¹²



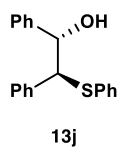
The crude mixture was purified by preparative TLC (*n*hexane/EtOAc = 3/1).

¹H NMR (600 MHz, CDCl₃) δ 7.46 (d, *J* = 8.0 Hz, 1H), 7.30 (d, *J* = 8.2 Hz, 1H), 7.25 – 7.12 (m, 11H), 7.10 – 7.07 (m, 1H), 7.06 – 7.02 (m, 1H), 5.33 (dd, *J* = 8.1, 2.4 Hz, 1H), 4.58 (d, *J* = 8.1 Hz, 1H), 3.80 (s, 3H), 2.52 (d, *J* = 2.7 Hz, 1H);

¹³C NMR (151 MHz, CDCl₃) δ 142.4, 141.9, 137.1, 128.6, 128.1, 128.0, 127.9, 127.3, 127.2, 126.8, 126.2, 121.9, 119.5, 119.1, 113.7, 109.2, 77.7 (d, *J* = 1.5 Hz), 52.2, 32.9 (q, *J* = 2.1 Hz);

HPLC (Daicel Chiralcel® OD-H, *n*hexane/*i*PrOH = 80/20, flow rate 0.8 mL/min at a wavelength of 254 nm); *t*_R = 16.3 min (minor), *t*_R = 24.9 min (major).

(1*S*,2*S*)-1,2-Diphenyl-2-(phenylthio)ethan-1-ol (13j)¹²

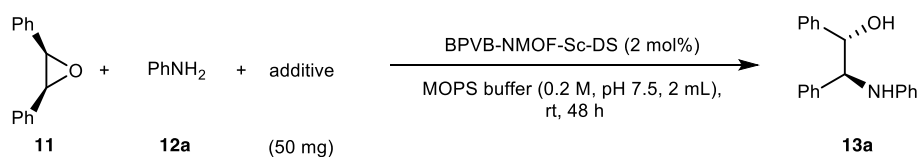


The crude mixture was purified by preparative TLC (dichloromethane/*n*hexane = 2/1). **¹H NMR** (600 MHz, CDCl₃) δ 7.31 – 7.28 (m, 2H), 7.23 – 7.20 (m, 3H), 7.19

– 7.11 (m, 8H), 7.05 – 7.01 (m, 2H), 4.94 (dd, *J* = 8.6, 2.1 Hz, 1H), 4.36 (d, *J* = 8.6

Hz, 1H), 3.30 (s, 1H); ^{13}C NMR (151 MHz, CDCl_3) δ 140.4, 139.2, 134.1, 132.4, 128.9, 128.5, 128.1, 128.0, 127.8, 127.4, 127.3, 126.9, 76.8, 64.0; HPLC (Daicel Chiralcel[®] OD-H, n hexane/ i PrOH = 95/5, flow rate 1.0 mL/min at a wavelength of 254 nm); t_{R} = 15.4 min (minor), t_{R} = 18.1 min (major).

8. Typical procedure for biocompatible epoxide ring-opening reactions



To a 3.5 mL vial equipped with a stirring bar were charged **11** (39.3 mg, 0.2 mmol), BPVB-NMOF-Sc-DS (0.004 mmol, 2 mol% based on Sc^{3+}), and an additive (50 mg) followed by adding MOPS buffer (0.2 M, pH 7.5, 2 mL) and subsequent aniline (0.3 mmol, 27.4 μL). It was flushed by argon before closing a cap to stir at room temperature. After 48 hours, the reaction mixture was filtered then the filtrate was extracted with EtOAc (3 x 10 mL). The combined organic phase was washed with brine, and dried over anhydrous Na_2SO_4 . The crude product was obtained after filtration and concentration. It was then purified by preparative thin-layer chromatography (n -hexane/EtOAc = 3/1) to give the desired product **13a**.

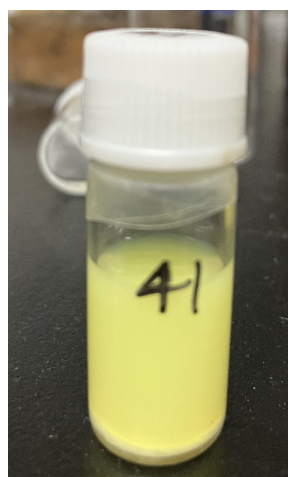
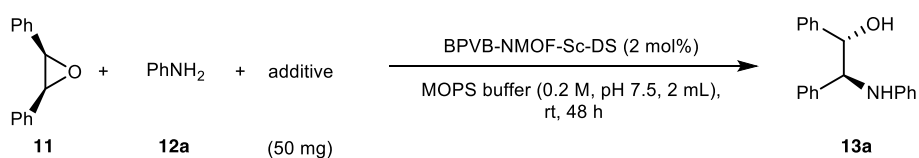


Figure S9. Appearance of the reaction in buffer in the presence of pepsin (after completion).

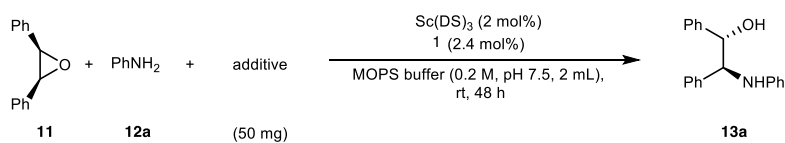
Table S12. Biocompatible conditions in BPVB-NMOF-Sc-DS-catalyzed asymmetric ring-opening reaction of epoxide.



Entry	Additive	Yield (%)	Ee (%)	Sc Leaching (%)	Zr Leaching (%)
1	glutathione	>99	85	UDL	UDL
2	lipase	85	87	3.1	0.8
3	pepsin	83	84	UDL	UDL
4	diastase	60	84	UDL	UDL

Respective limit of detection for Sc and Zr is 0.65% and 0.44%, respectively.

Table S13. Comparison of non-immobilized Sc(DS)₃ for biocompatible conditions.



Entry	Additive	Yield (%)	Ee (%)
1	glutathione	>99 (68) ^{a,b}	90 (88) ^{a,b}
2	lipase	59 (n.d.) ^{a,c}	87 (-) ^{a,c}
3	pepsin	39 (n.d.) ^{a,c}	84 (-) ^{a,c}
4	diastase	trace (n.d.) ^{a,c}	- (-) ^{a,c}

^a1 mol% Sc(DS)₃, 1.2 mol% Bolm's ligand. ^bThree halves equivalents of glutathione was used at 40°C, 24 h. ^cRun for 24 h.

9. General procedure for recovery and reuse experiments

To a 3.5 mL vial equipped with a stirring bar were charged **11** (0.4 mmol, 39.3 mg) and BPVB-NMOF-Sc-DS (0.008 mmol, 2 mol% based on Sc³⁺) followed by adding degassed water (2 mL). It was flushed by argon before closing a cap to stir at room temperature for 1 hour. Aniline (0.6 mmol, 54.8 μ L) was loaded and again argon-flushed before stirring at room temperature. After 24 h, the reaction mixture was carefully filtered and washed with H₂O and acetone, the obtained yellow solid was dried in *vacuo* at room temperature for 12 hours and directly applied for the next run (the reaction scale of the next run was calculated based on the remaining catalyst after recovery). On the other hand, the filtrate was extracted with EtOAc (3 x 15 mL). The combined organic phase was washed with brine, and dried over anhydrous Na₂SO₄. The crude product was obtained after filtration and concentration. It was then purified by preparative thin-layer chromatography (*n*-hexane/EtOAc = 3/1) to give the desired product **13a**. The leaching of metal ions was determined by ICP analysis in both aqueous solution and part of the crude product.

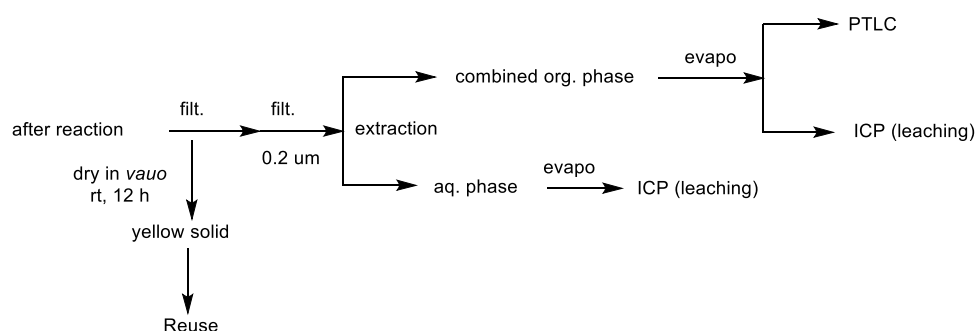
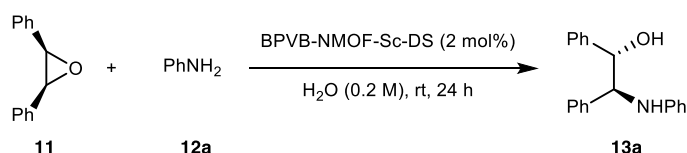


Table S14. Reuse experiment.



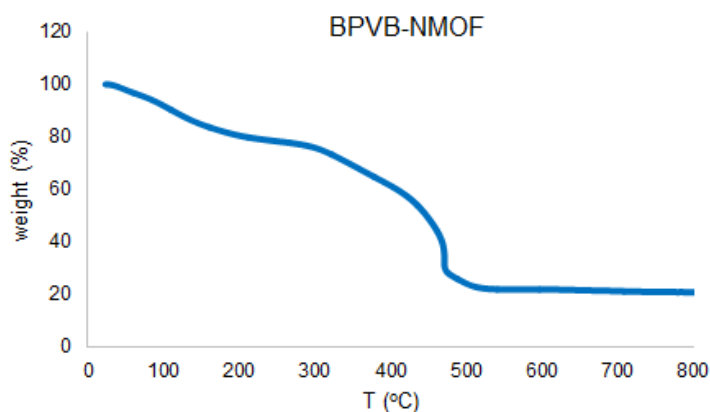
	1 st Run	2 nd Run	3 rd Run
Yield, Ee	96% yield, 87% ee	>99% yield, 81% ee	>99% yield, 78% ee
Sc Leaching	UDL	UDL	UDL
Zr Leaching	1.1	1.5	UDL

Respective limit of detection for Sc and Zr is 0.65% and 0.44%, respectively.

10. TG analysis

Thermogravimetric (TG) analysis of the prepared MOFs was conducted to assess their thermal characteristics. For BPVB-NMOF, a 20% solvent loss was detected, leading to a calculated yield of 47% (Figure S10a). Furthermore, the thermal stability of the MOFs before and after Sc-complexation were compared. Remarkably, after subjecting BPVB-NMOF-Sc-DS to temperatures exceeding 600 °C, a higher residue was observed. This observation indicates that the presence of Sc species has a substantial impact on the thermal stability of the MOF (Figure S10b).

a)



b)

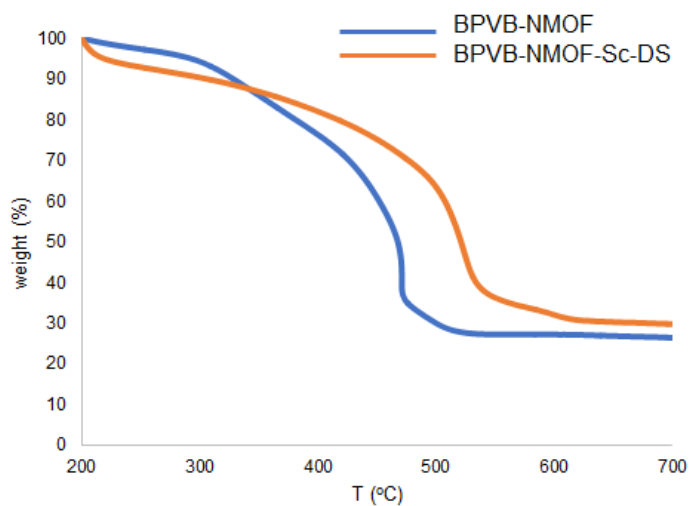
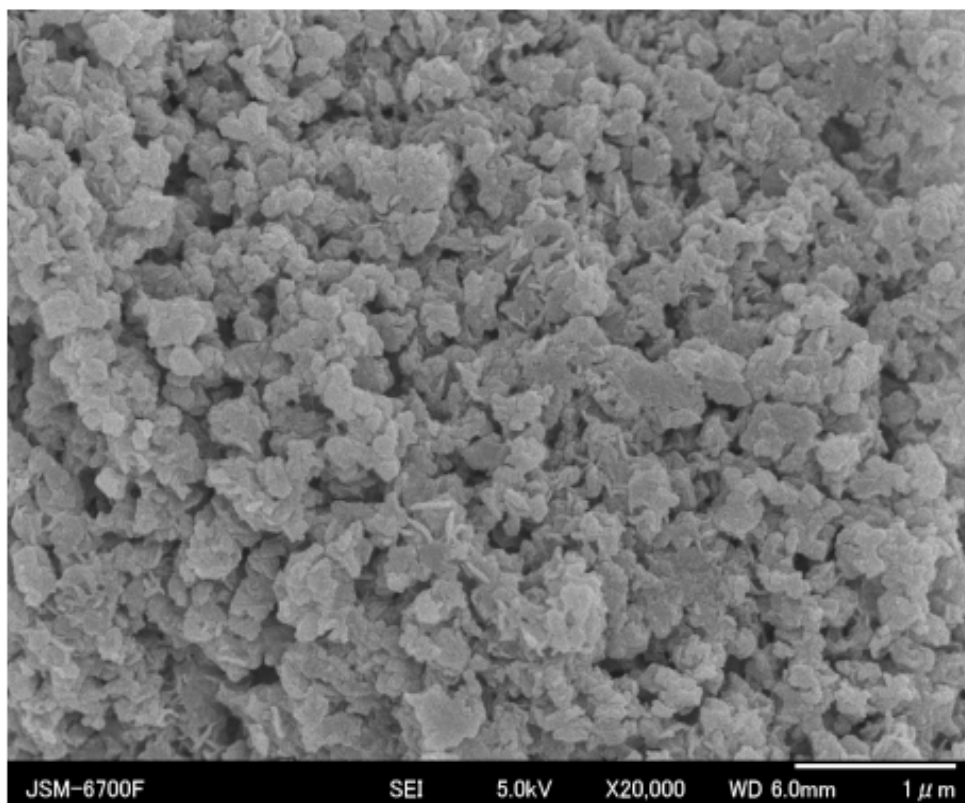


Figure S10. TG analysis. **a**, BPVB-NMOF. **b**, BPVB-NMOF-Sc-DS.

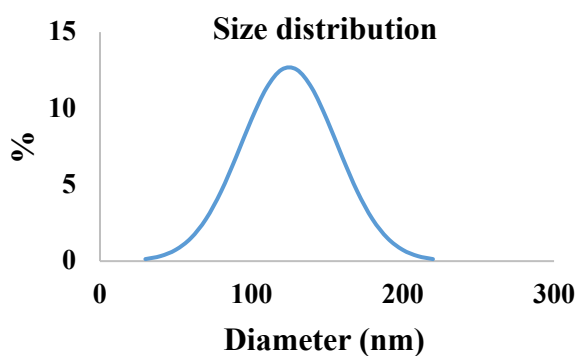
11. SEM analysis

The SEM image of BPVB-NMOF confirmed the successful preparation of nano-sized UiO-67 MOF. The analysis of particle size distribution provided a normal distribution curve, showcasing a well-defined pattern with an average particle diameter of 125 nm (Figure S11).

a)



b)



c)

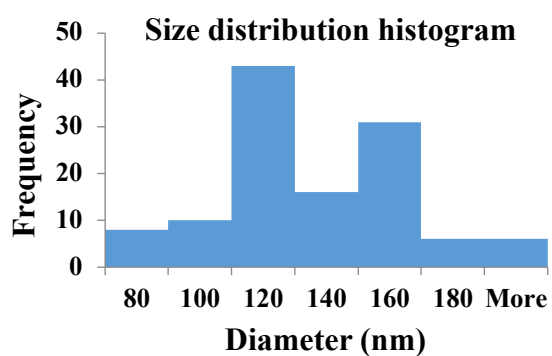


Figure S11. SEM Analysis of BPVB-NMOF. **a**, SEM Image of BPVB-NMOF. **b**, Size distribution curve. **c**, Size distribution histogram.

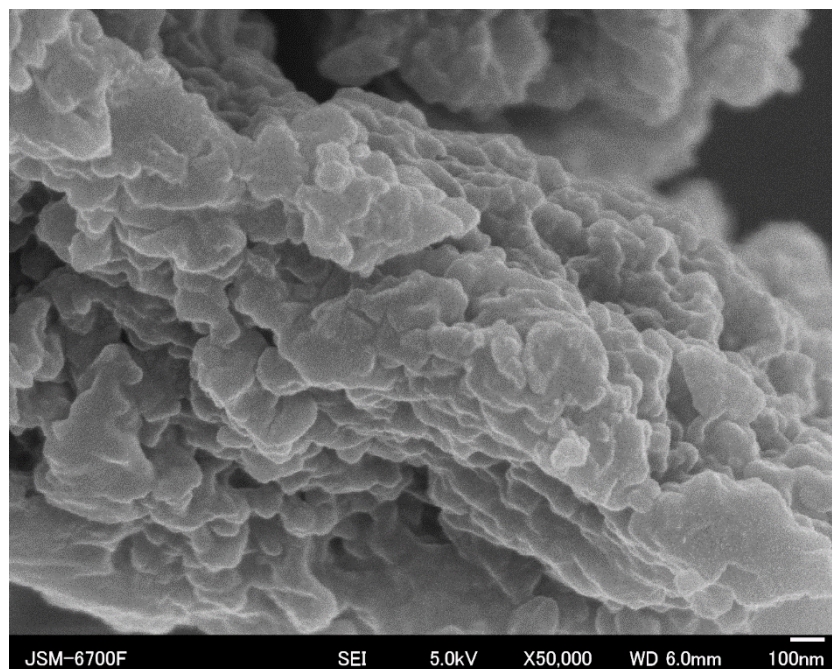


Figure S12. SEM Image of BPVB-NMOF-Sc-DS.

12. PXRD analysis

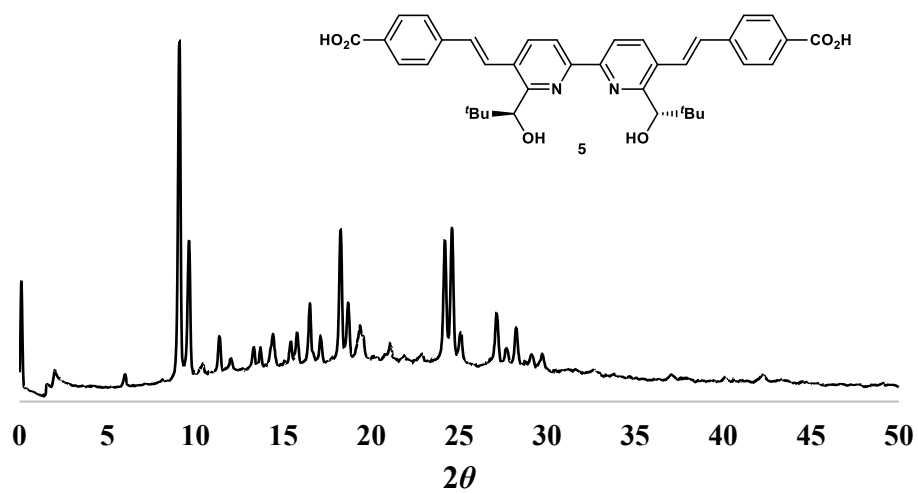


Figure S13. PXRD spectrum of chiral H₂BPVB 5.

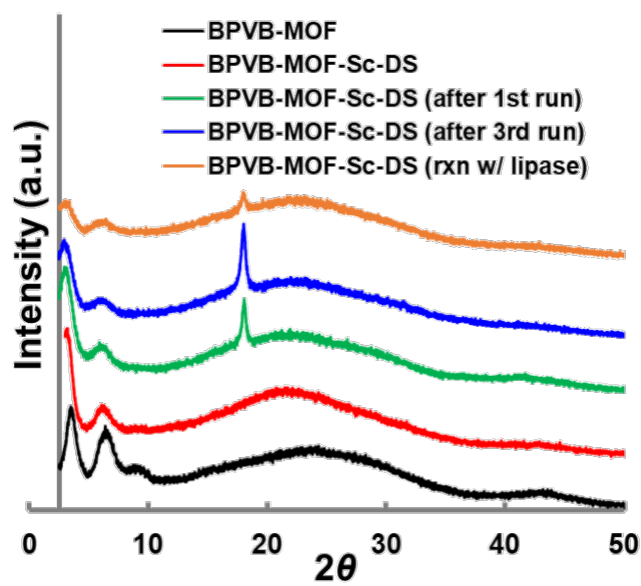


Figure S14. PXRD patterns of BPVB-NMOFs.

13. Water stability test of BPVB-NMOF and BPVB-NMOF-Sc-DS

To a 2 mL vial equipped with a stirring bar, BPVB-NMOF (10 mg), and degassed water (1 mL) were added. The vial was flushed with argon before closing the cap and stirring at room temperature for 24 hours. The resulting MOF was recovered by centrifugation, filtration, and drying in *vacuo* before PXRD and digestive $^1\text{H-NMR}$ analyses.

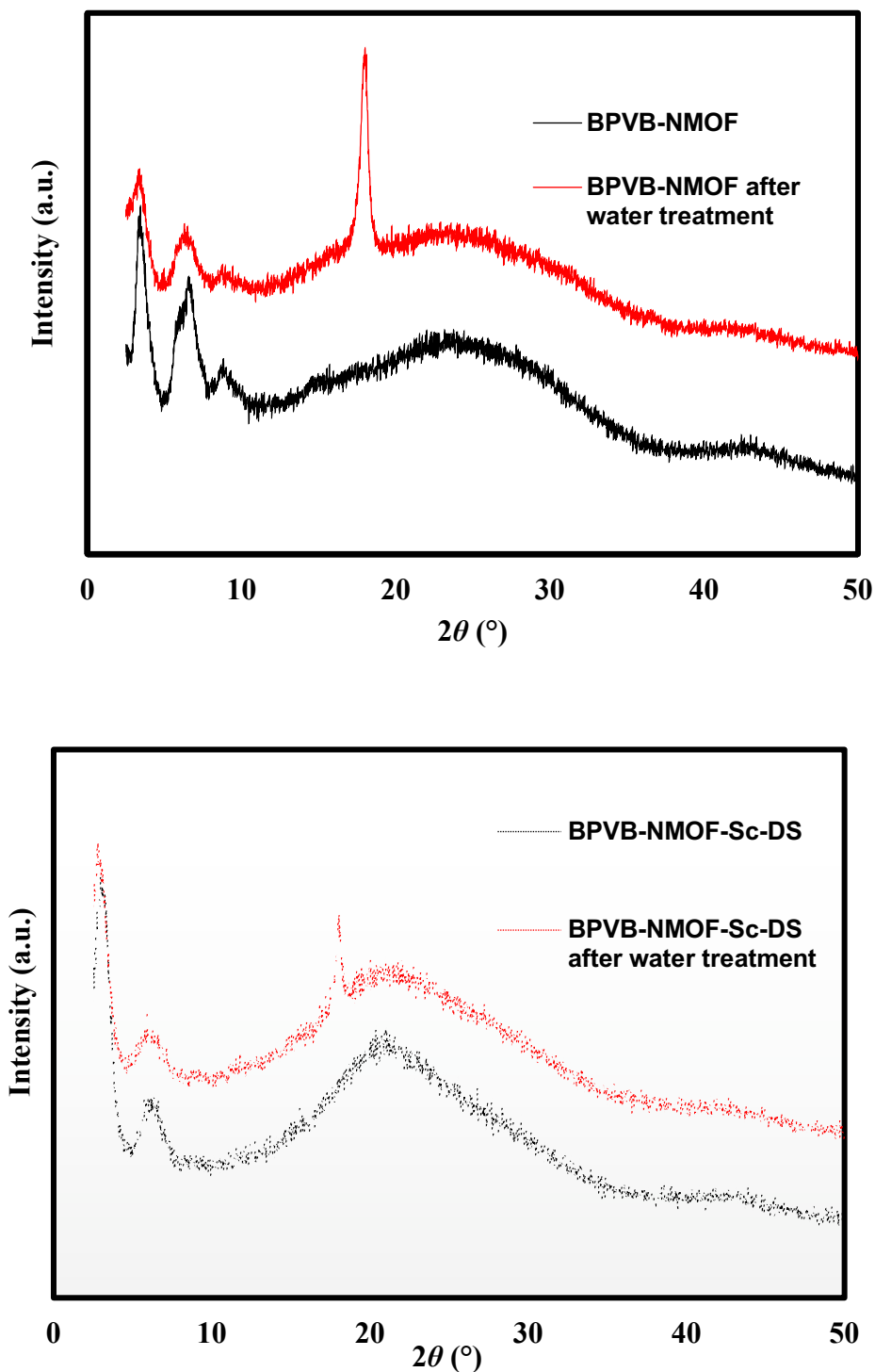


Figure S15. PXRD patterns of water-treated MOFs.

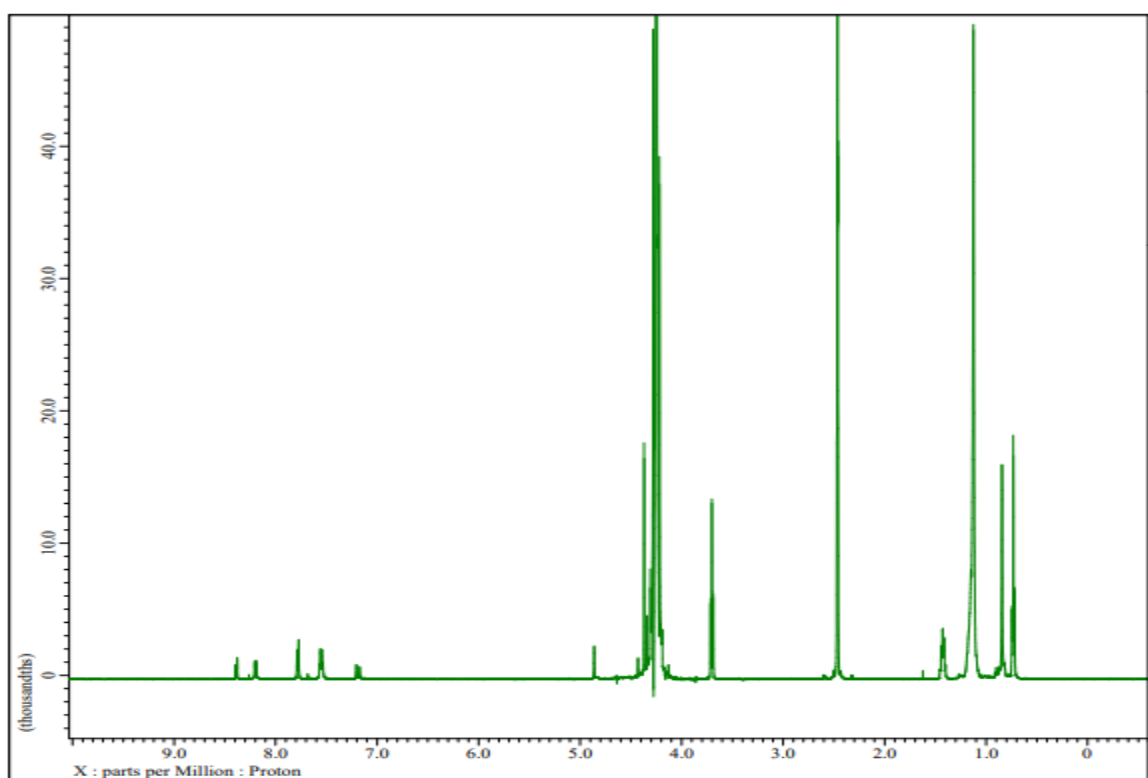
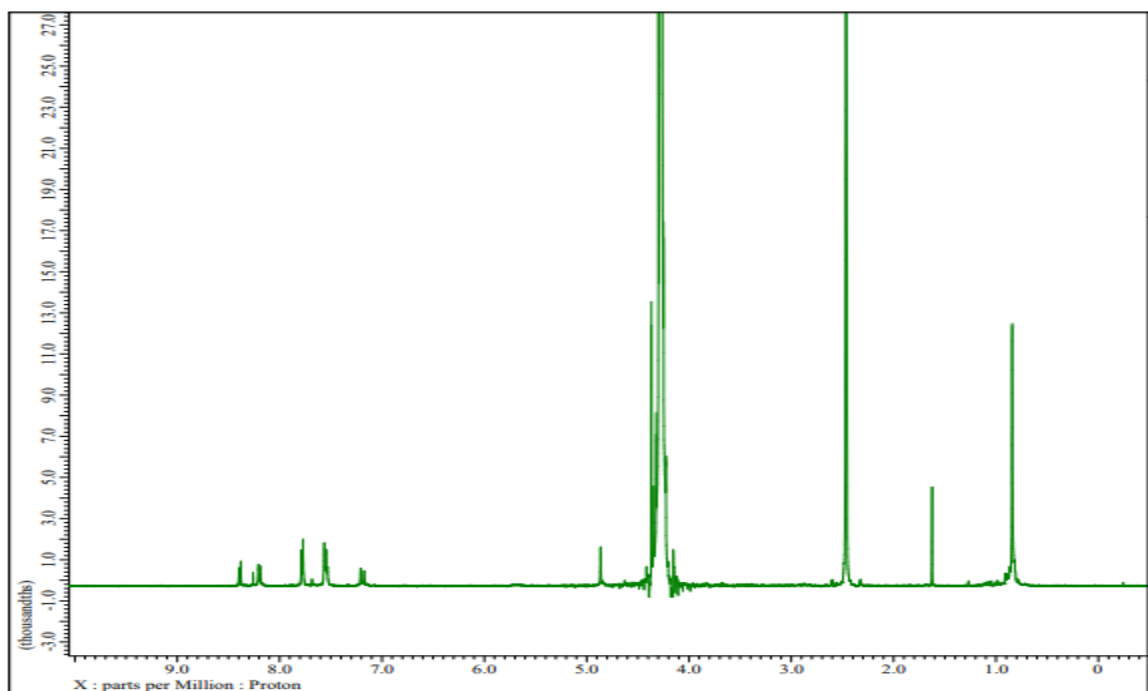


Figure S16. Digestive ¹H NMR spectra of BPVB-NMOF (above) and BPVB-NMOF-Sc-DS (below) ($K_3PO_4/D_2O/DMSO-d_6$).

14. STEM/EDS analysis

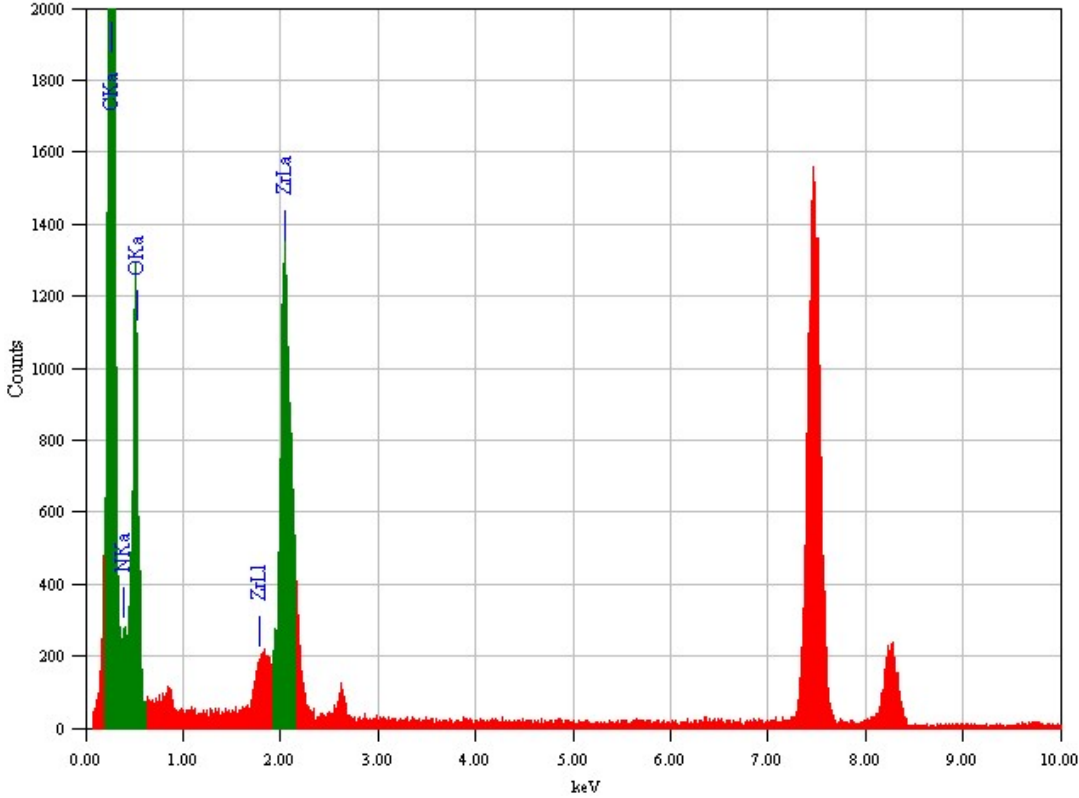
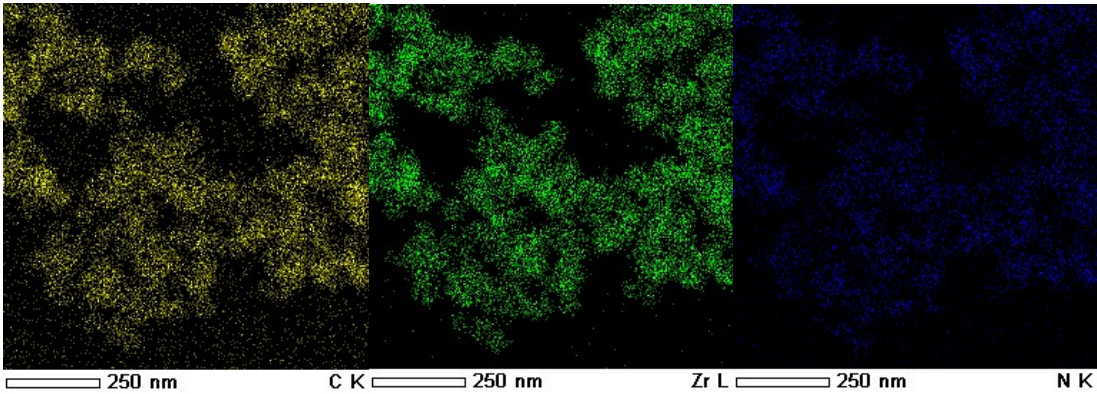
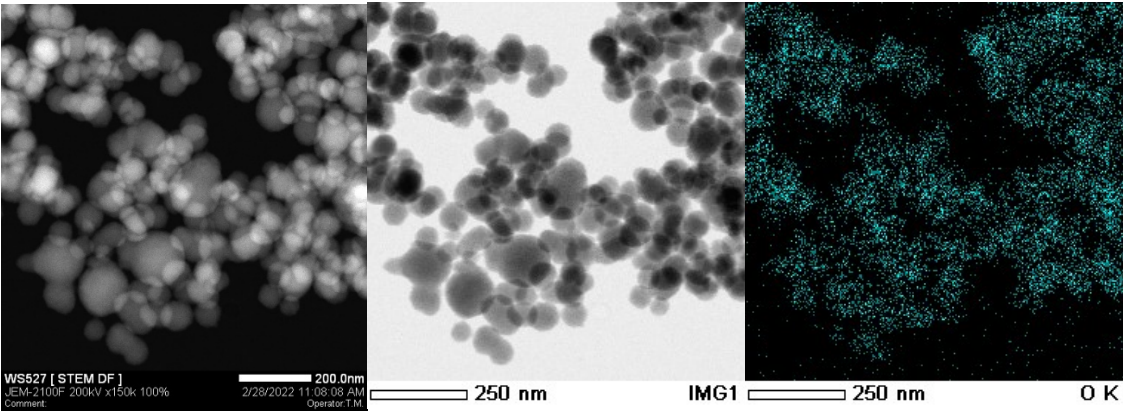


Figure S17. STEM/EDS analysis of BPV-MOF.

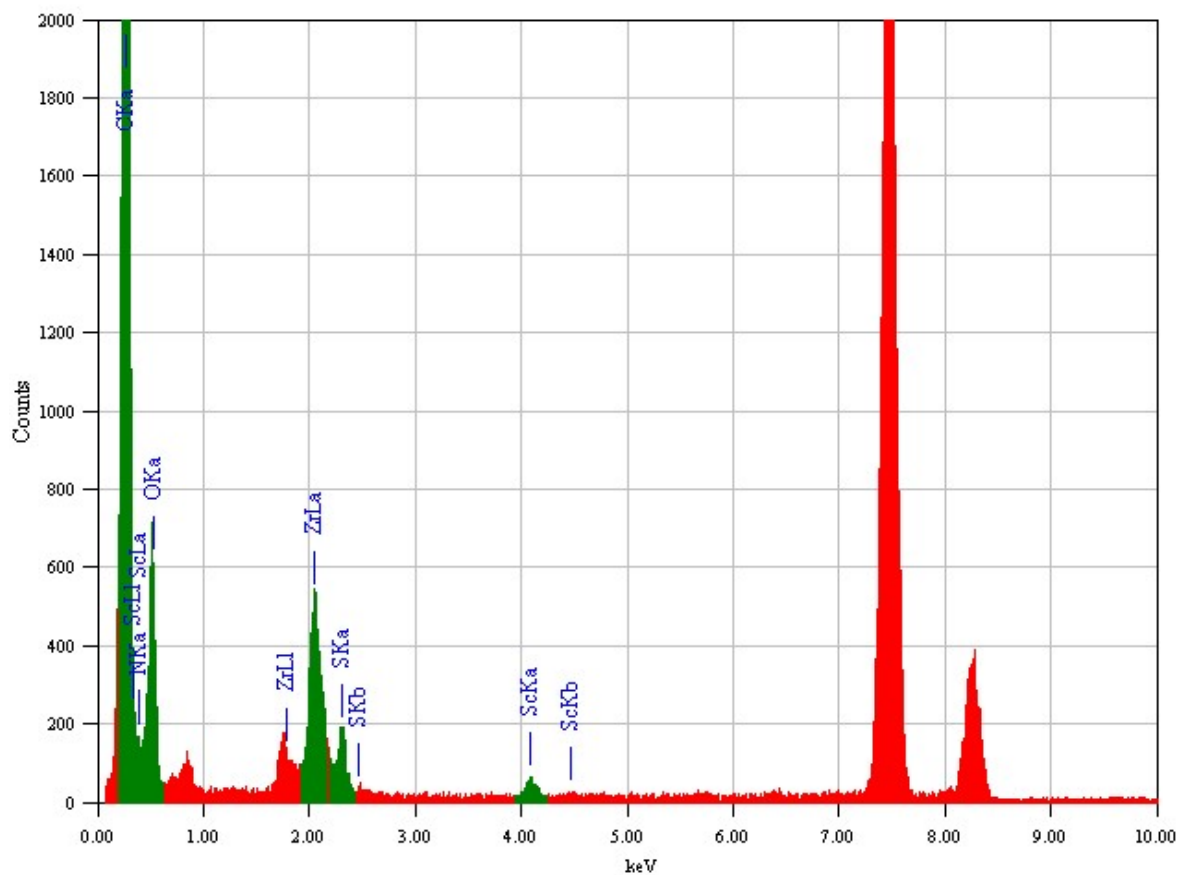
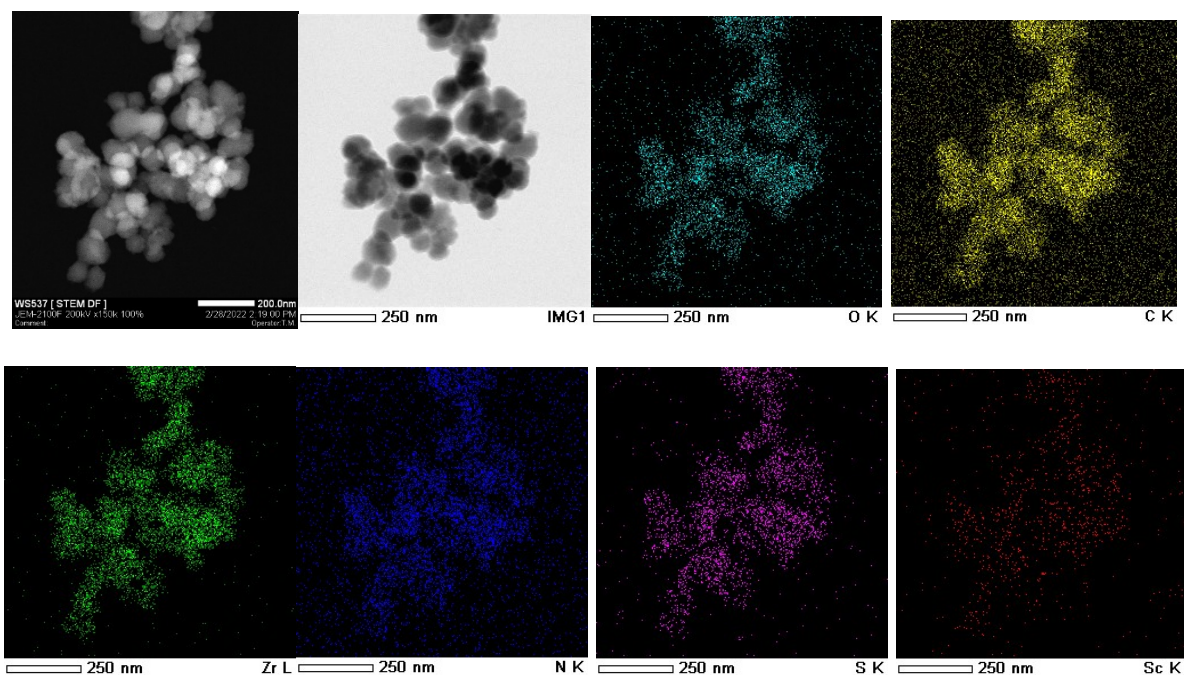


Figure S18. STEM/EDS analysis of BPV-MOF-Sc-DS.

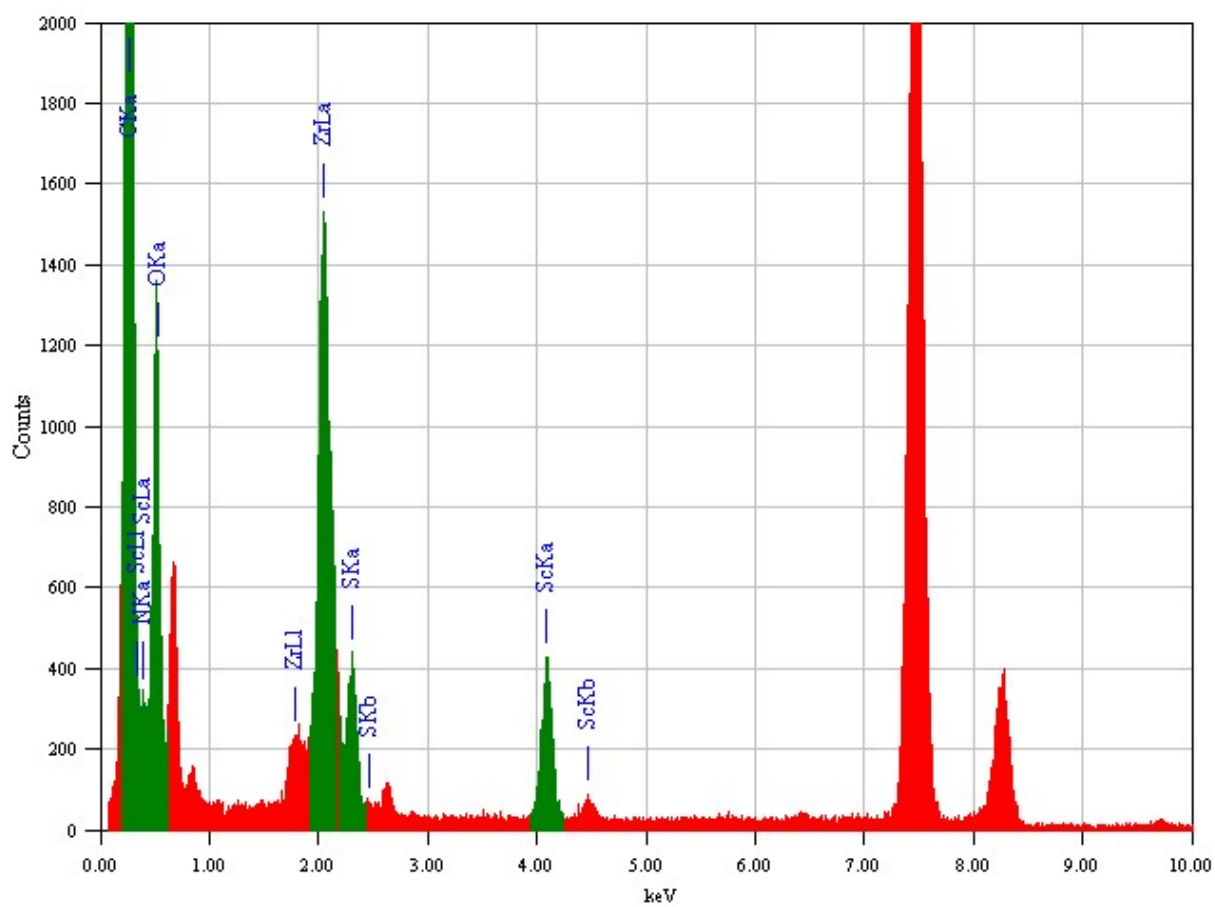
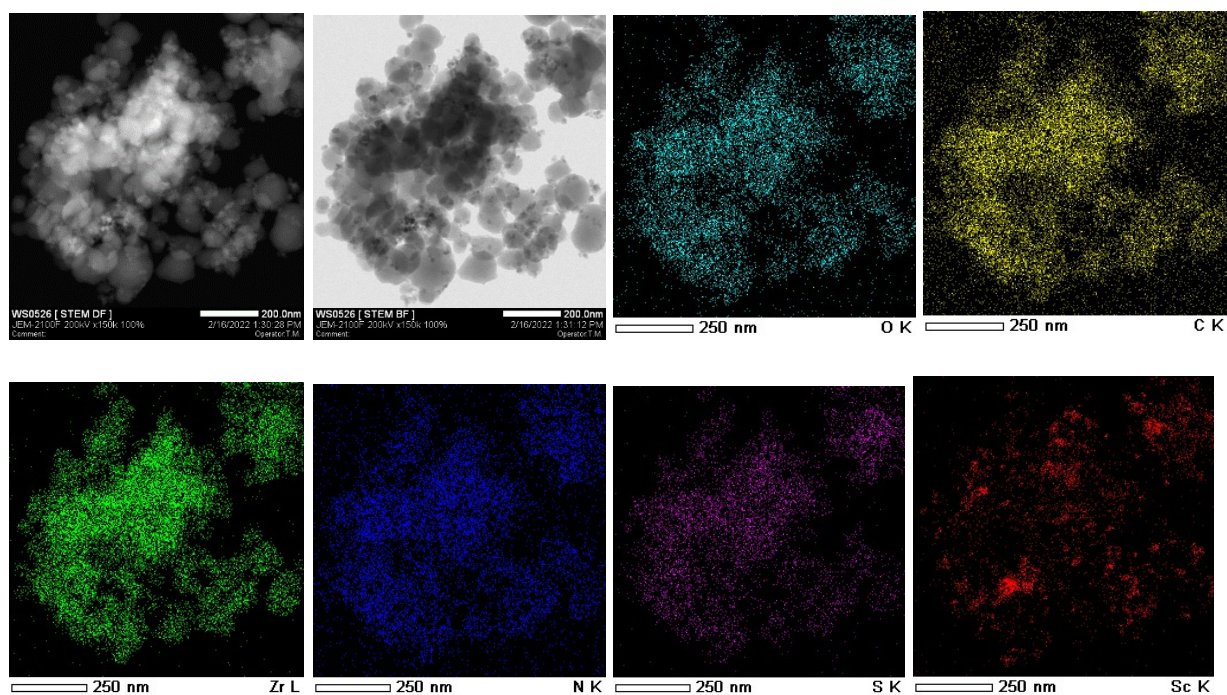


Figure S19. STEM/EDS analysis of BPV-MOF-Sc-OTf.

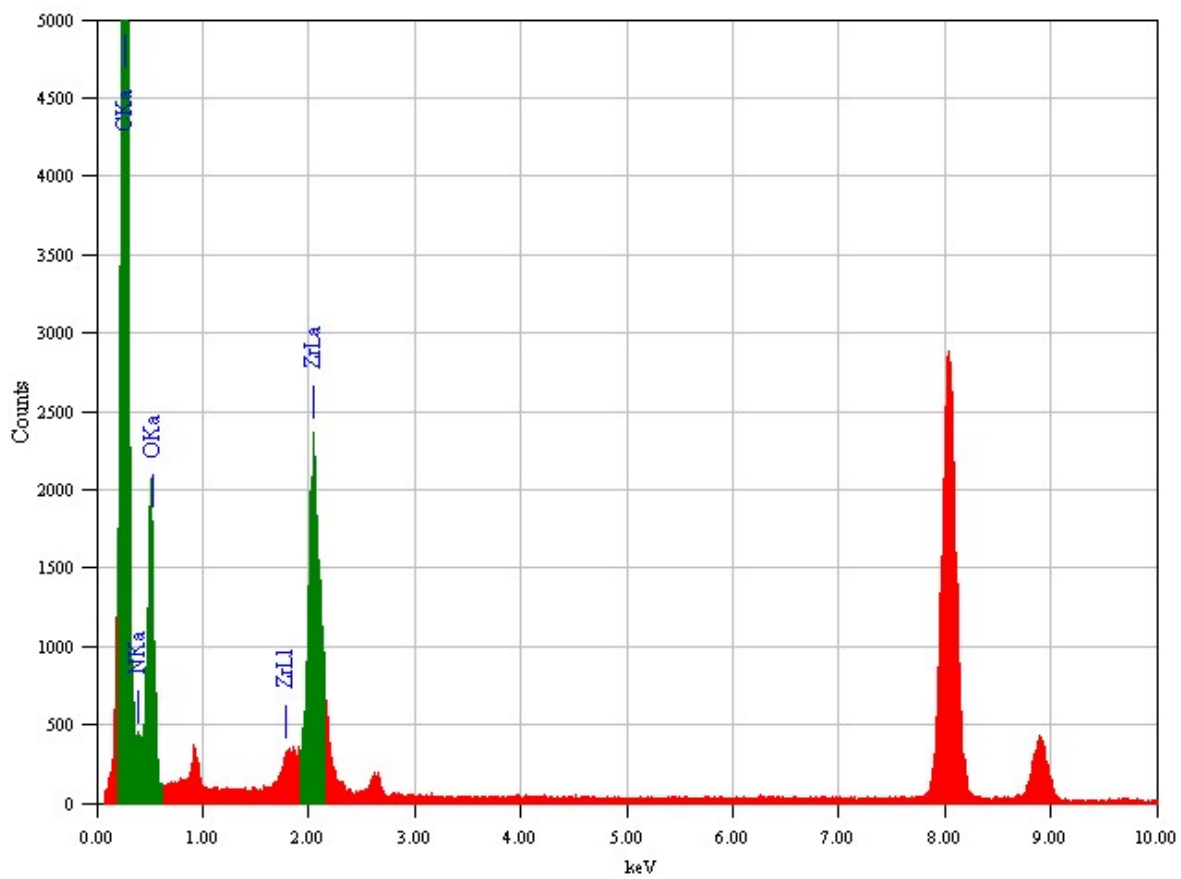
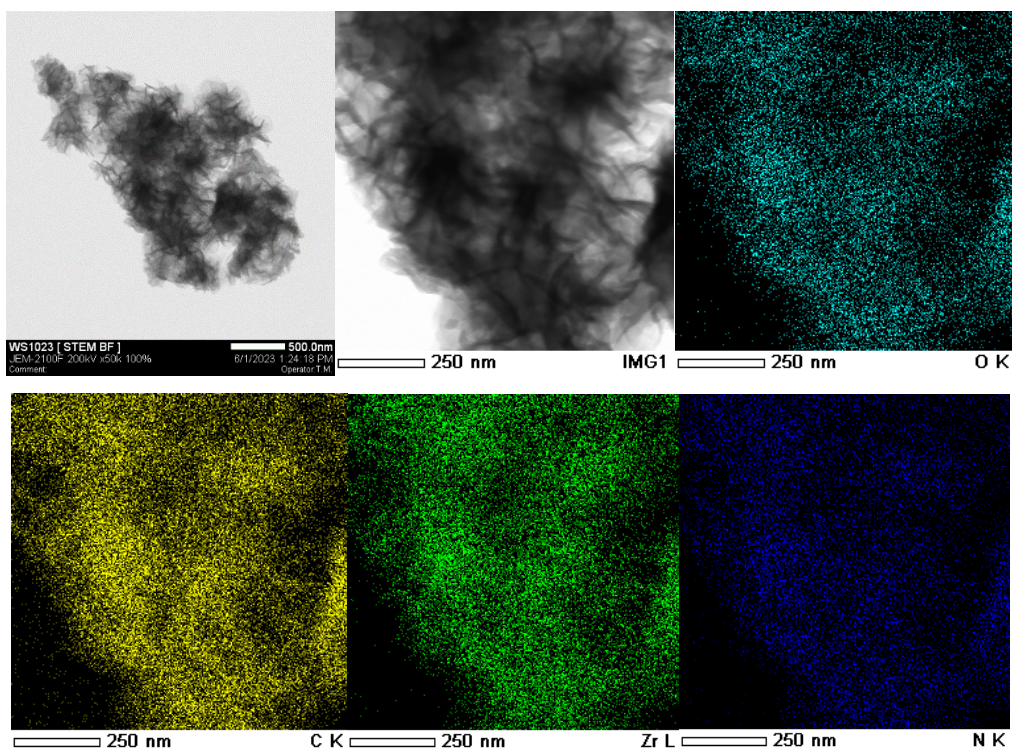


Figure S20. STEM/EDS analysis of BPVB-NMOF.
S42

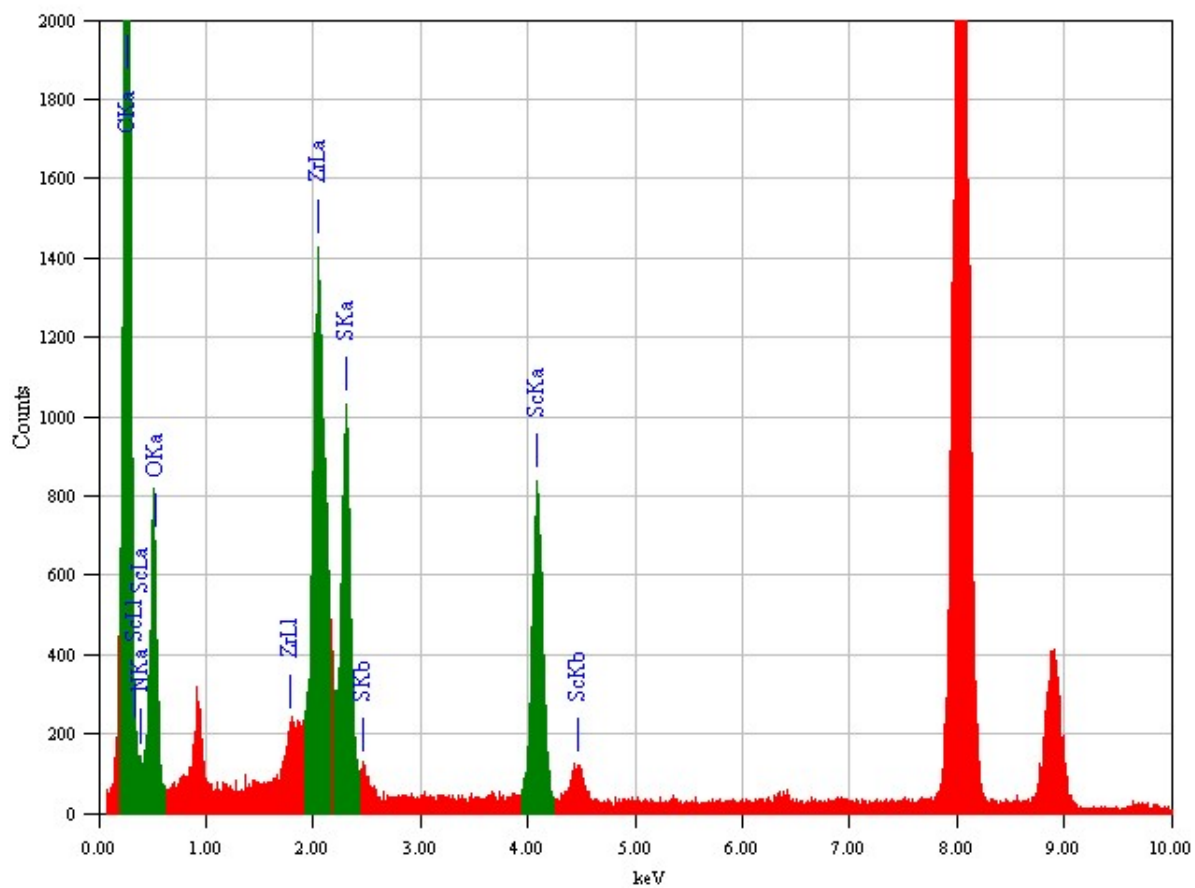
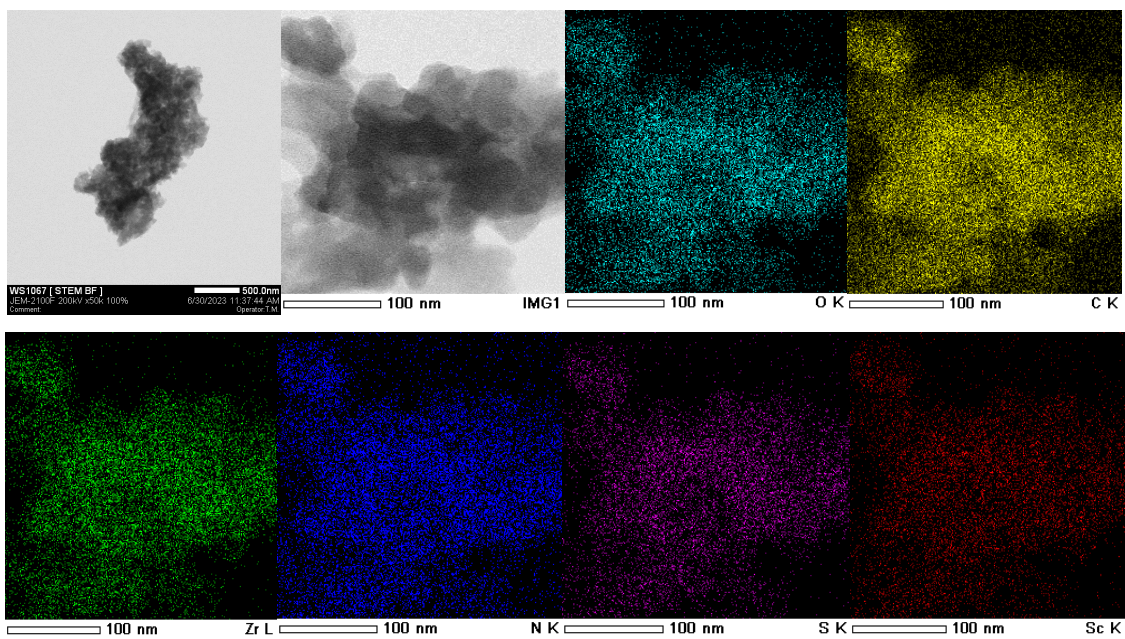


Figure S21. STEM/EDS analysis of BPVB-NMOF-Sc-DS.

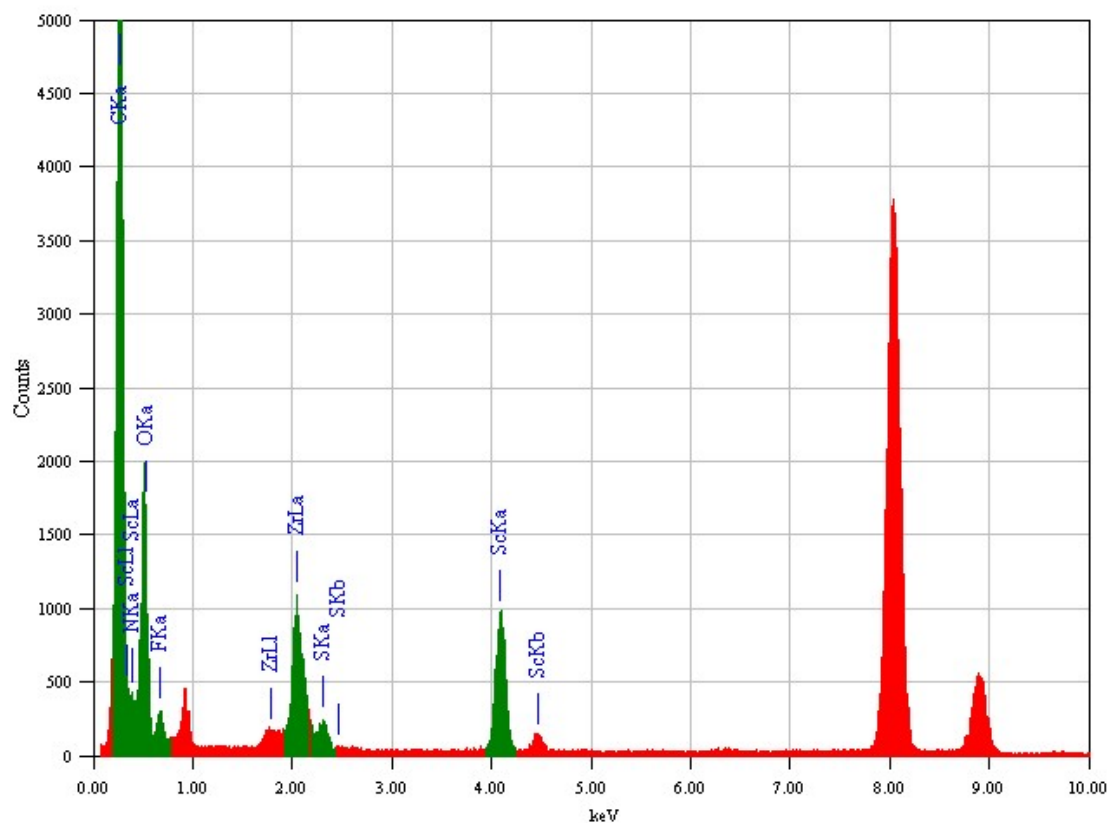
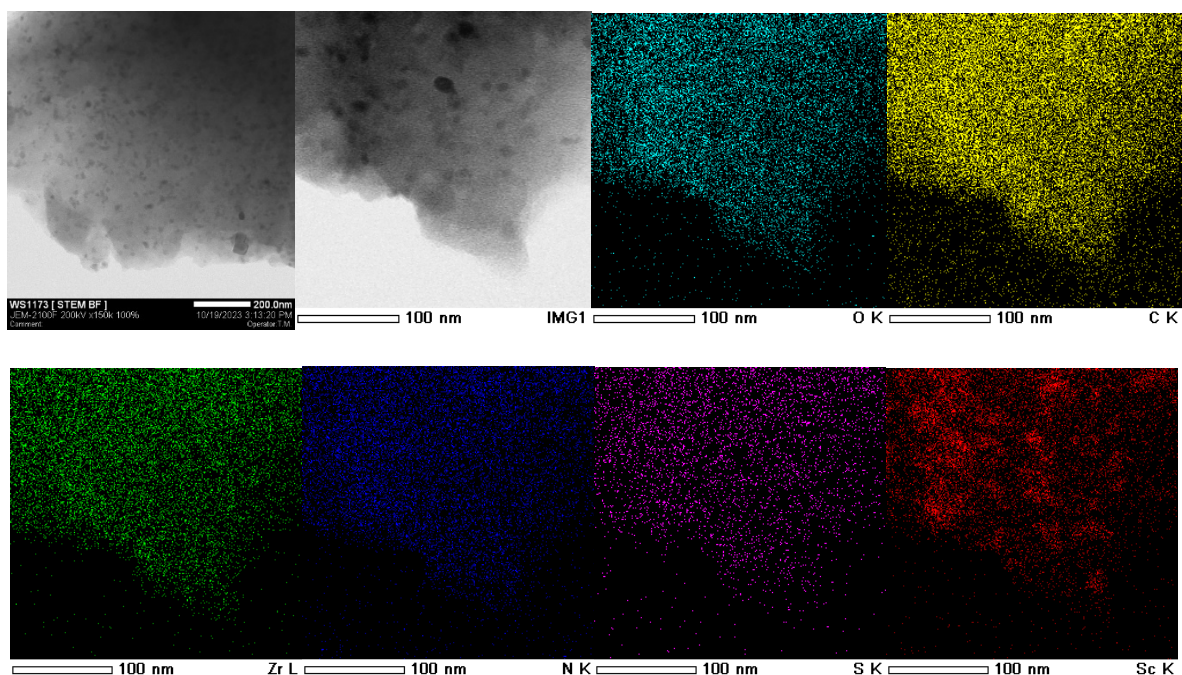
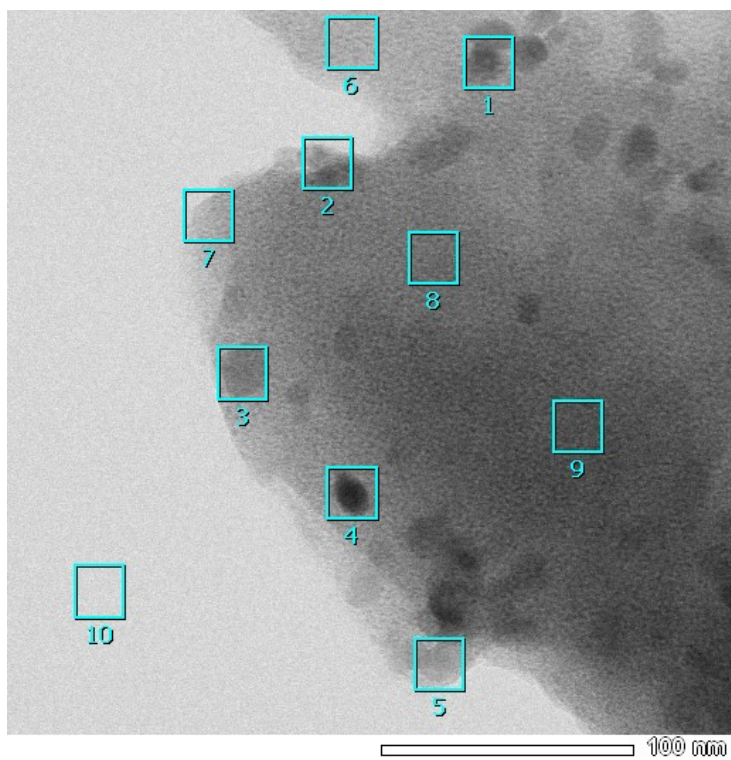
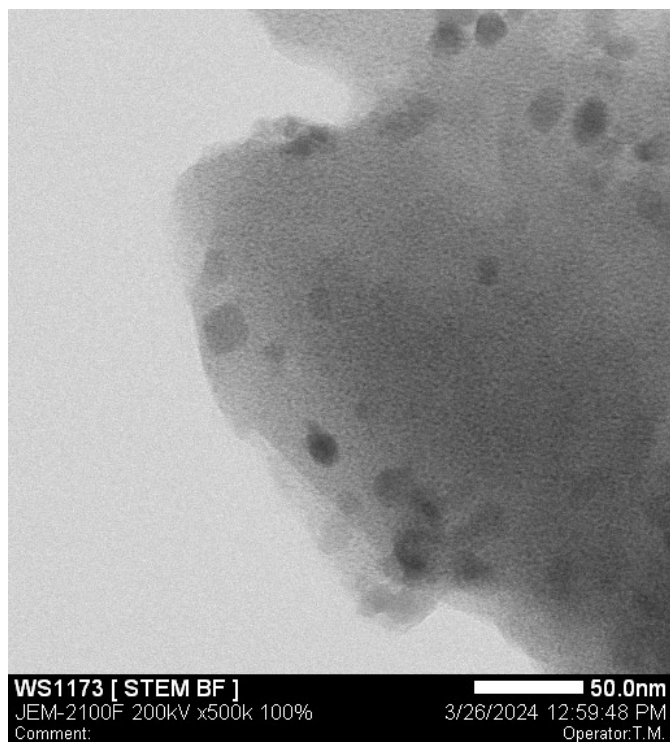
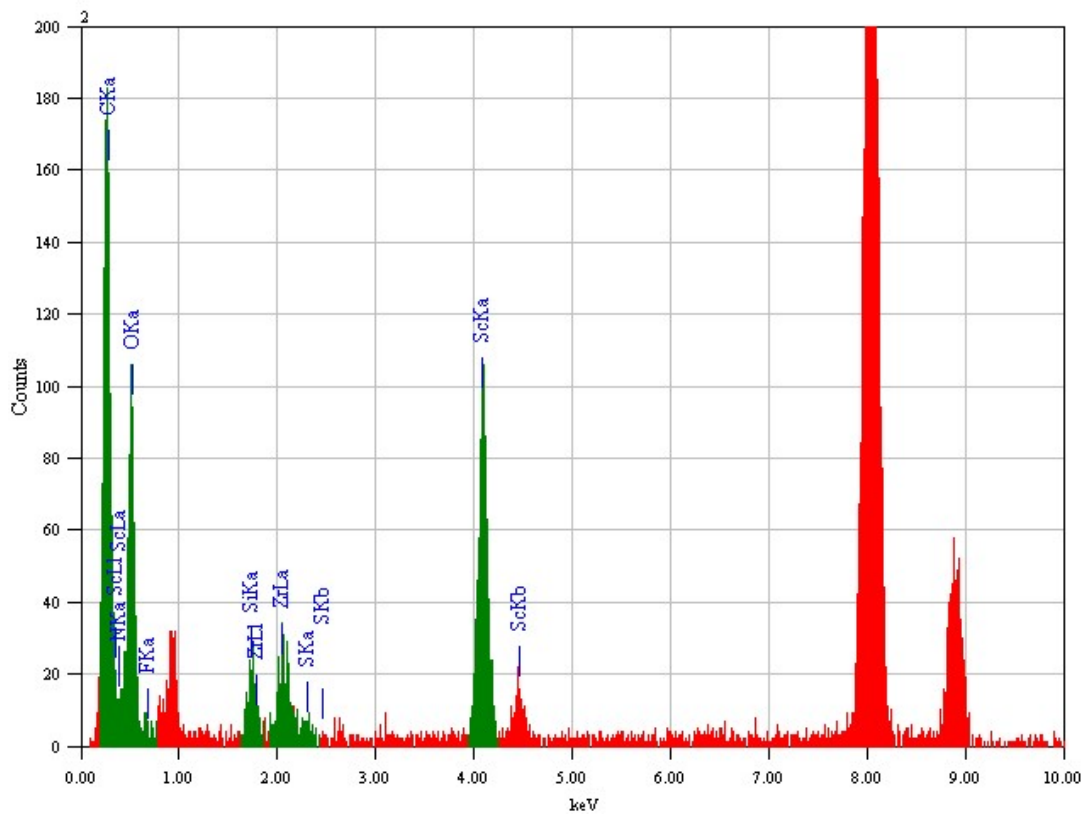
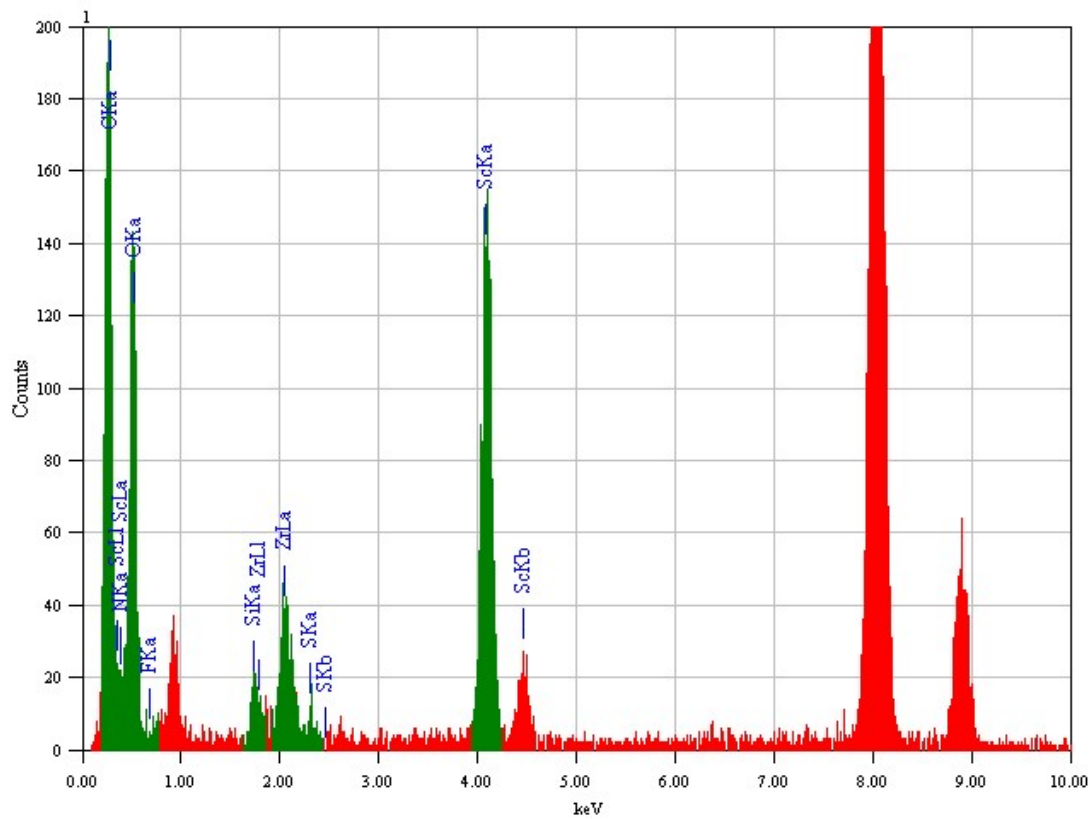
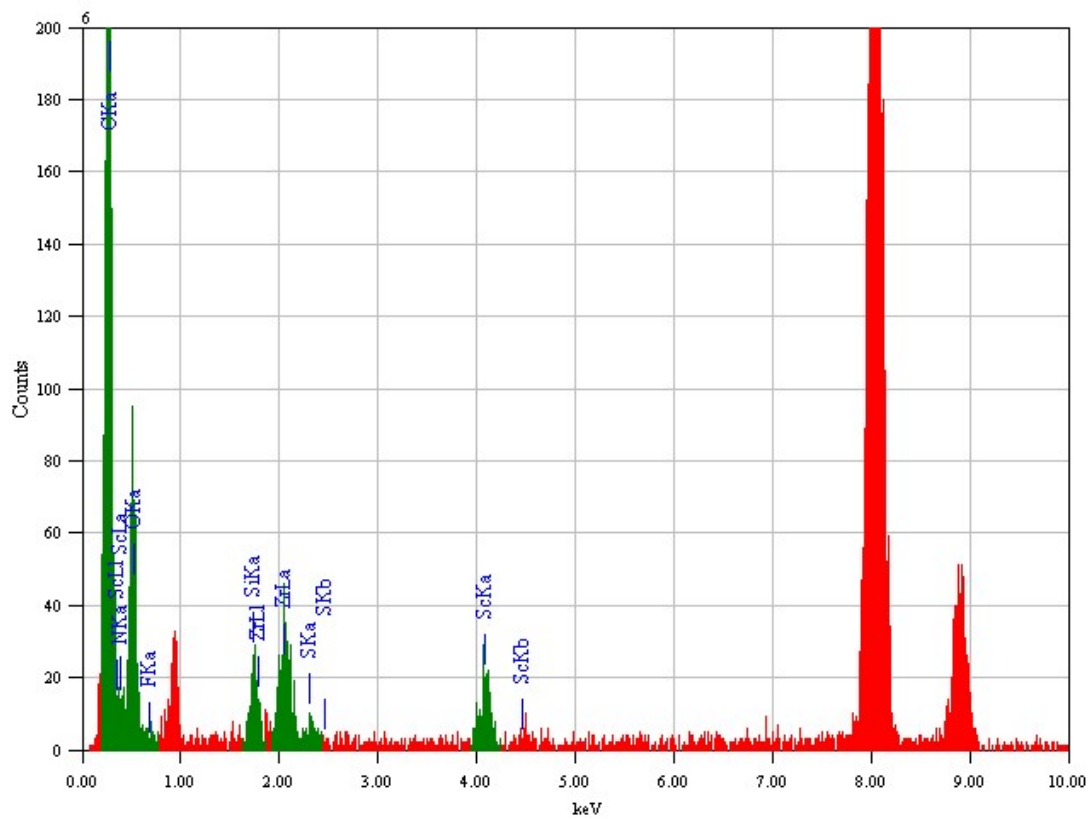
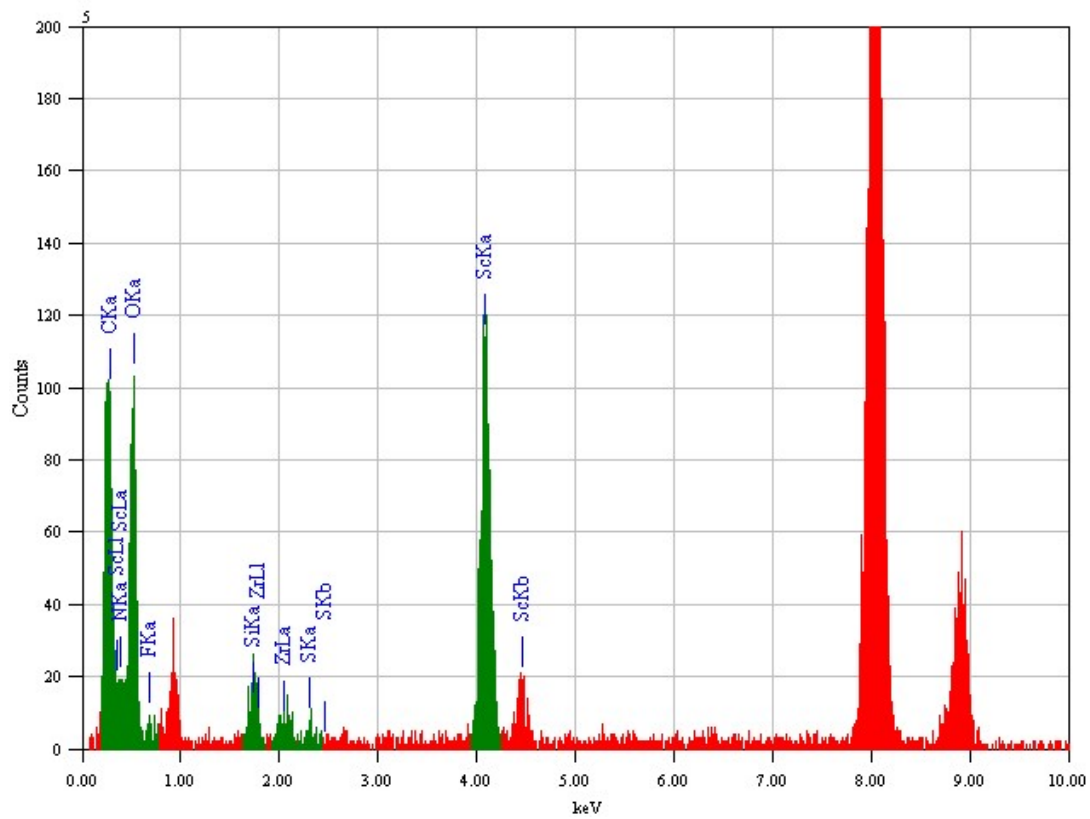


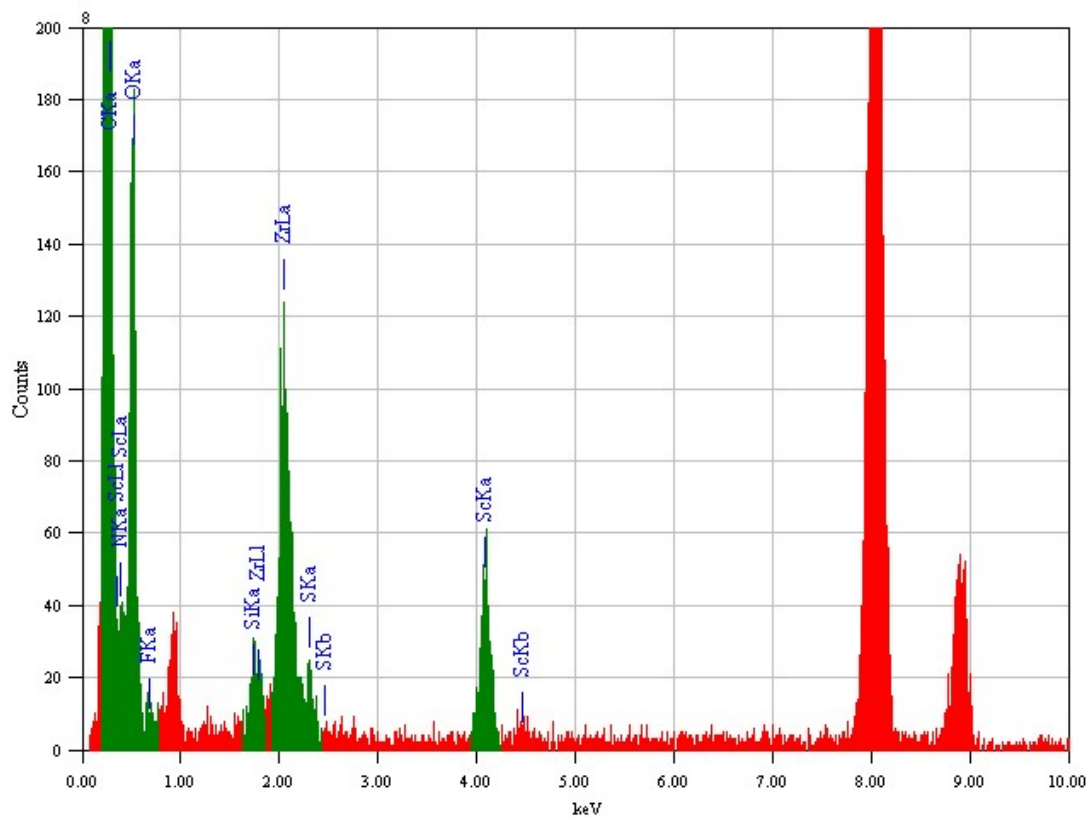
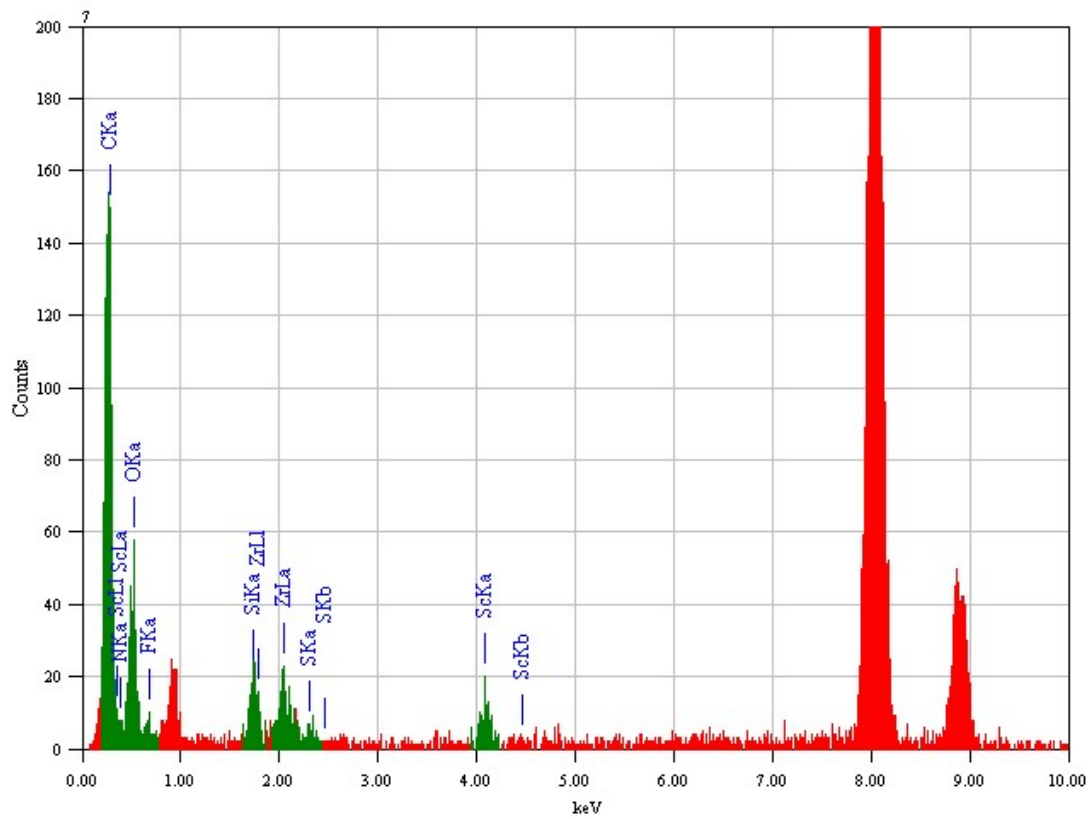
Figure S22. STEM/EDS analysis of BPVB-NMOF-Sc-OTf.

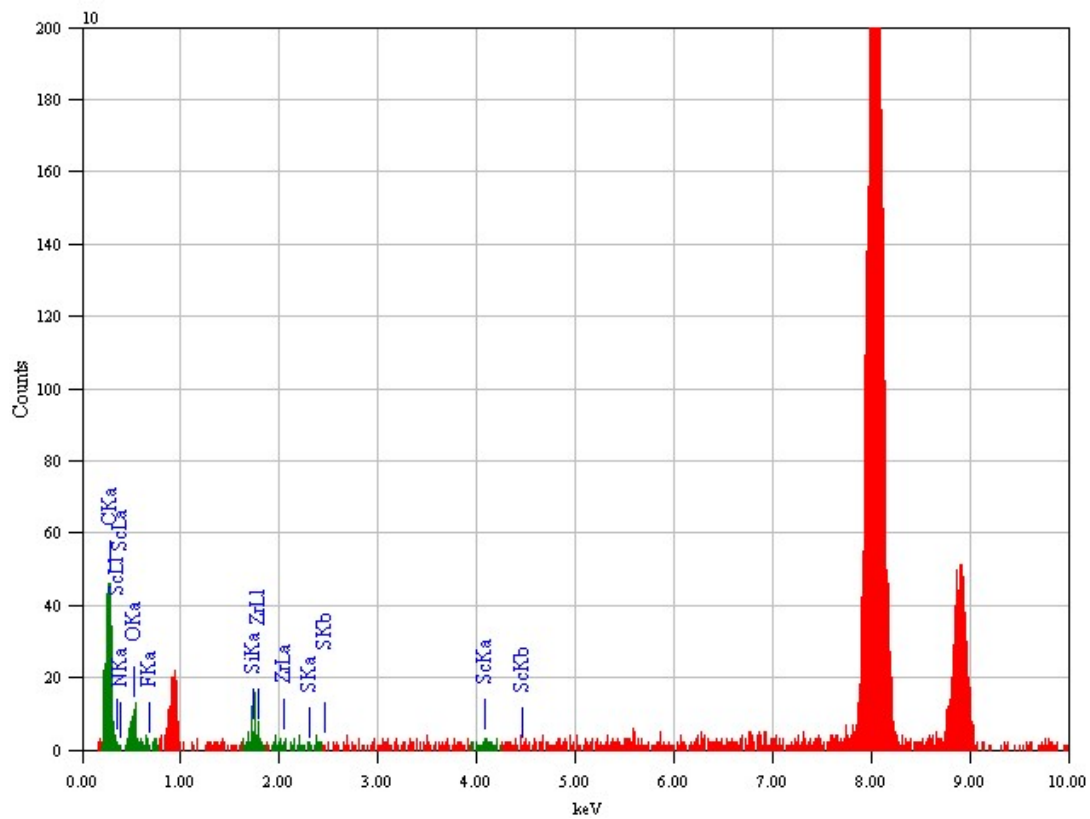
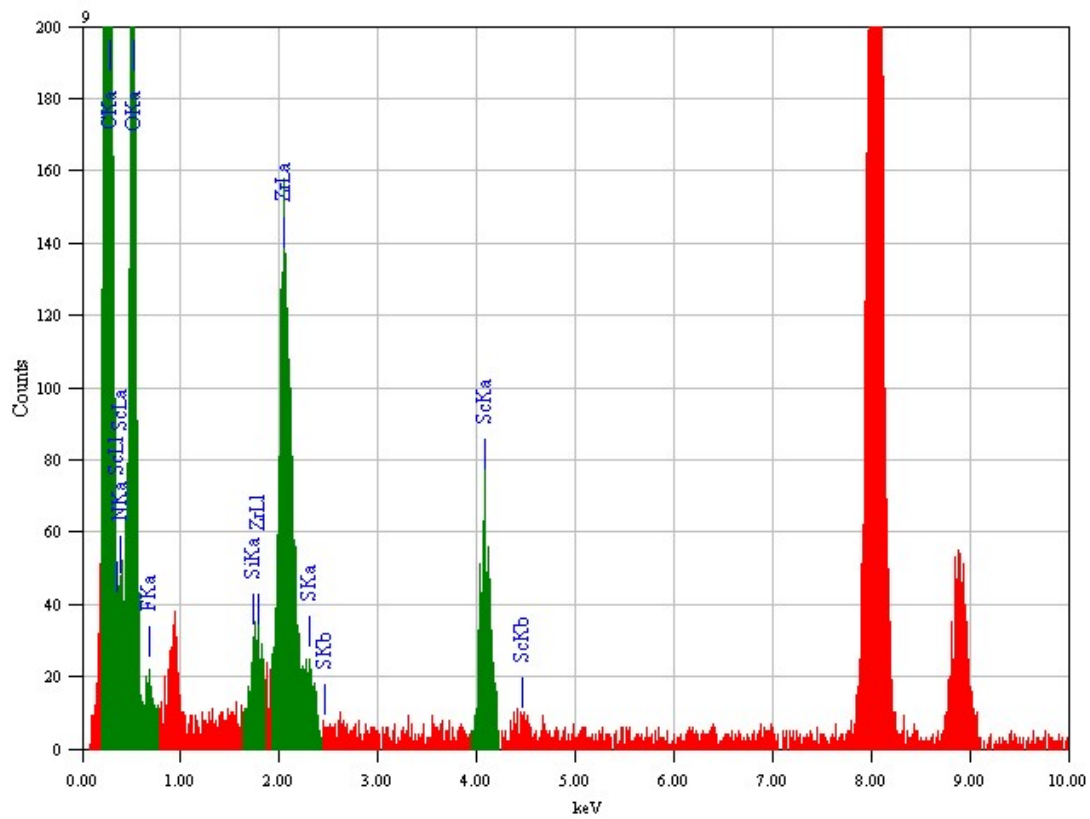
<Area analysis of BPVB-NMOF-Sc-OTf>











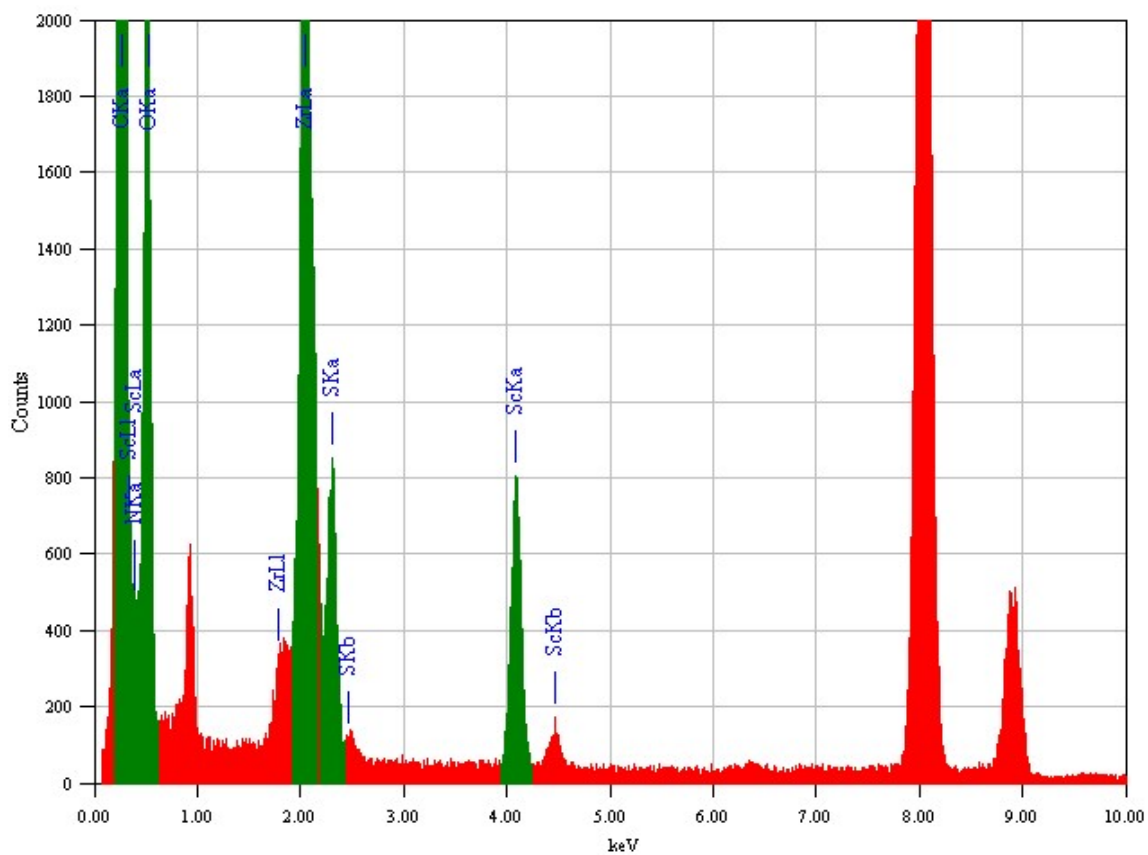
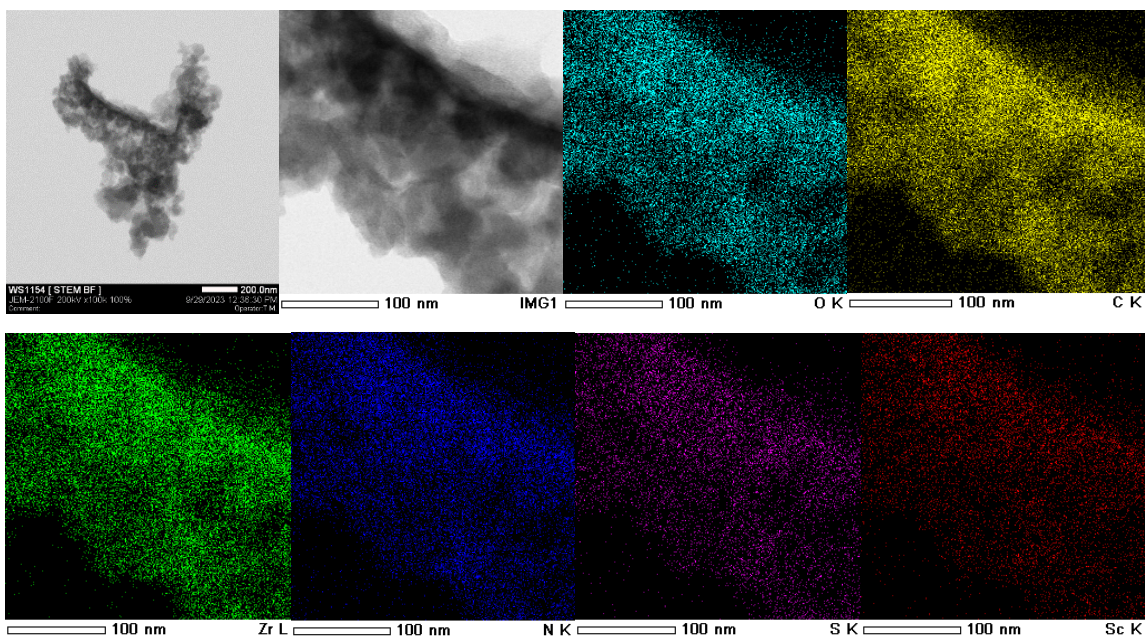


Figure S23. STEM/EDS analysis of BPVB-NMOF-Sc-DS (after the reaction with lipase).

15. N₂ adsorption/desorption isotherms

Nitrogen sorption experiments were conducted at 77 K after drying the samples (50-55 mg) at 50°C for 24 hours under vacuum.

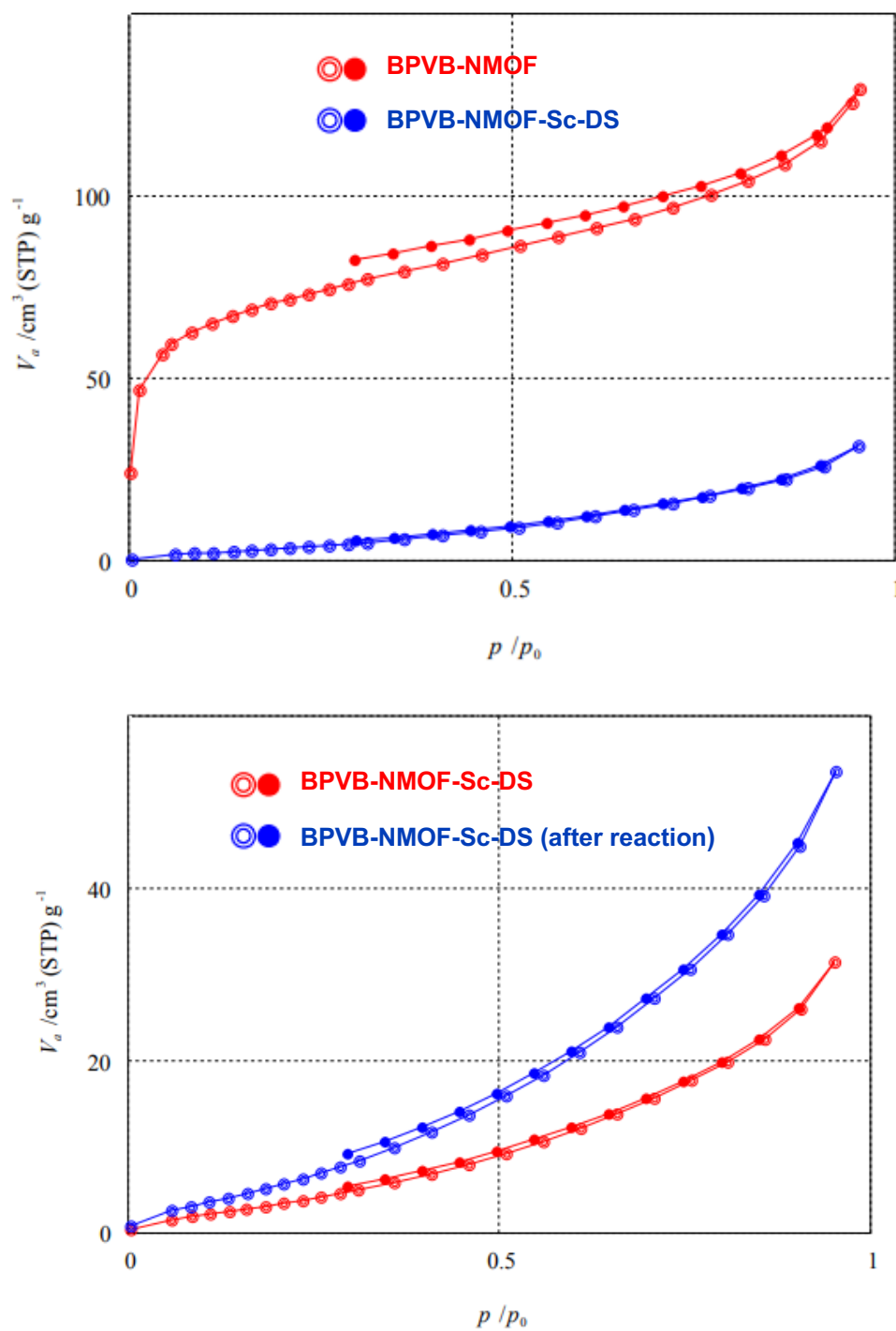


Figure S24. N₂ Adsorption/ desorption isotherms of BPVB-NMOF and BPVB-NMOF-Sc-DS.

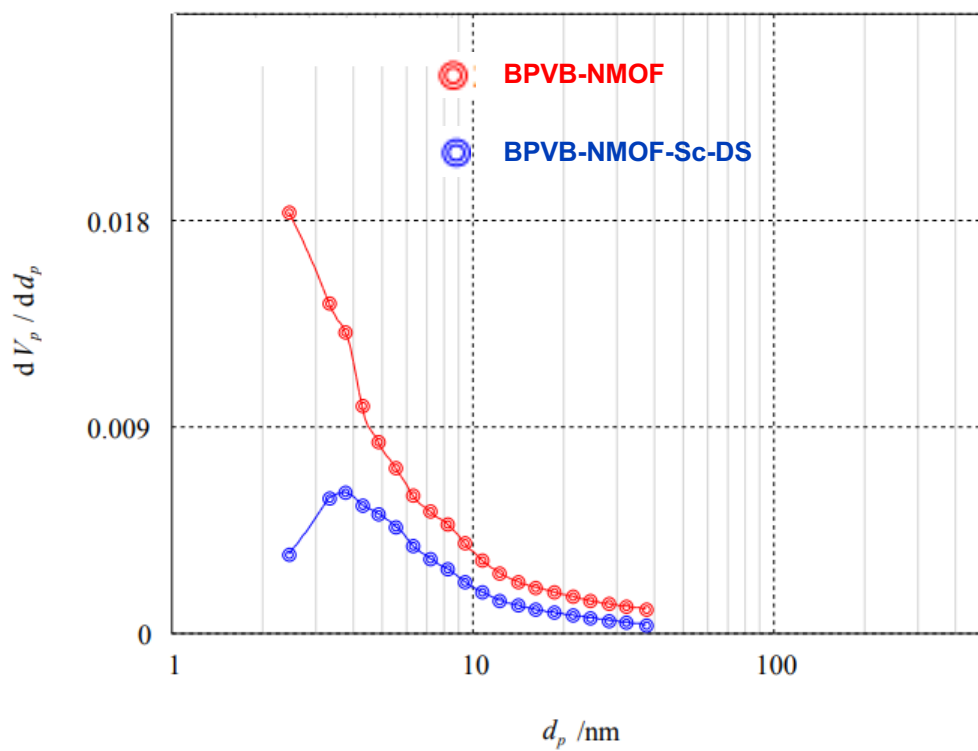


Figure S25. Pore size distributions of BPVB-NMOF (red) and BPVB-NMOF-Sc-DS (blue).

16. XPS study

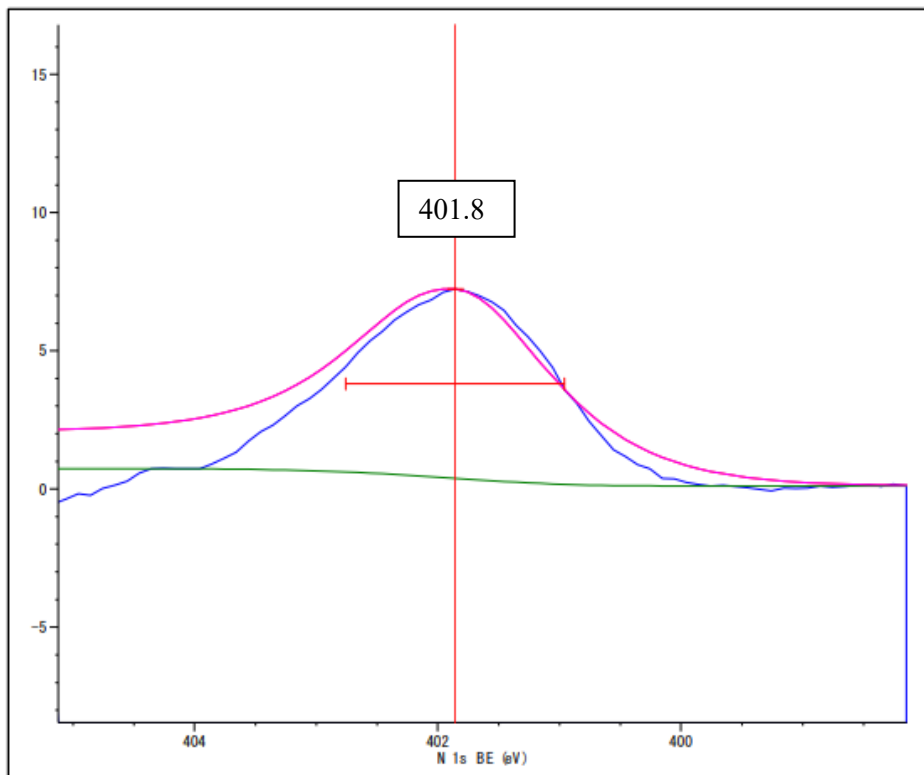


Figure S26. N 1s binding energy of BPVB-NMOF.

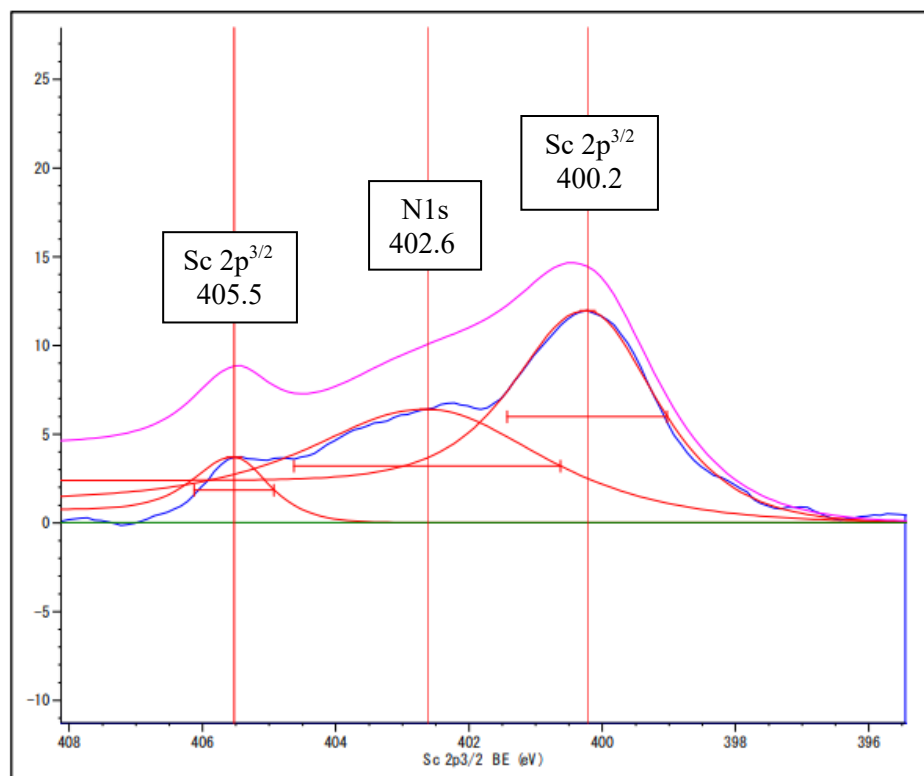


Figure S27. N 1s, Sc 2p^{3/2}, and Sc 2p^{1/2} binding energy of BPVB-NMOF-Sc-DS.

17. Computational details

All DFT geometry optimization and frequency calculations were performed with Gaussian 16 program.¹⁵ Optimization were conducted in the gas phase with the B3LYP functional and 6-31G+(d,p) basis sets for C, H, N, O and LanL2DZ for Sc. The optimization of Sc³⁺-H₂BPVB complex was performed with the solute electron density (SMD)¹⁶ implicit solvation model for solvents. All stationary points were characterized by vibrational frequency calculations to confirm the minima for ground state optimizations (no imaginary frequencies) or transition state calculations (one imaginary frequency) and to obtain zero-point energy (ZPE) corrections. All energy values are reported in Hartrees and are the sum of electronic and thermal free energies as computed by Gaussian 16.

Cartesian coordinate

The thermal corrections were computed at 298.15 K and 1 atm pressure. The Cartesian coordinates are in Å.

B3LYP optimized structures

H₂BPDC

C -0.66284400	0.33480300	-0.52846000	H -5.00654000	-0.54865200	-0.73837400
C 0.66278200	-0.33455400	-0.52840500	H -4.52780300	-2.56086900	-1.43940300
C -0.76761100	1.73180800	-0.55639500	H 5.00649200	0.54875700	-0.73844800
C -2.03927700	2.27858500	-0.57141000	H 4.52782000	2.56167300	-1.43820000
C -3.17227400	1.44655200	-0.56995800	H -2.77450500	-2.94433600	1.07789800
C -2.96822200	0.04654300	-0.50639300	H -3.36299300	-2.52591400	2.70328200
N -1.73512100	-0.46513400	-0.48839400	H -4.95982700	-0.50145100	2.97371800
N 1.73505900	0.46540300	-0.48841300	H -5.57483200	0.33242700	1.54089300
C 2.96814000	-0.04629300	-0.50648500	H -3.87862100	0.52076700	2.02398900
C 3.17217300	-1.44630500	-0.57004600	H -6.40882500	-1.94849800	0.64164900
C 2.03921900	-2.27835600	-0.57129000	H -5.28274800	-3.32656200	0.57650400
C 0.76754300	-1.73155700	-0.55621400	H 2.77415100	2.94334400	1.07897600
C -4.07809700	-0.98481300	-0.37243900	H 2.26720200	1.43285200	1.83946800
O -3.71716800	-2.09482000	-1.20374300	H 5.57549600	-0.33278800	1.54025300
C 4.07811300	0.98490600	-0.37230900	H 3.87937600	-0.52187200	2.02335100
O 3.71723000	2.09522200	-1.20317900	H 6.40873800	1.94875700	0.64180500
C -4.33202900	-1.42251400	1.10968500	H 5.28232700	3.32660600	0.57773200
C -3.10672500	-2.12242300	1.71710600	H 5.79115200	2.67324800	2.13379700
C -4.70600100	-0.19173500	1.95455900	H 4.96033200	0.50020100	2.97351300
C -5.52368100	-2.39961300	1.10727800	H -2.26695200	-1.43426800	1.83880400
C 4.33215500	1.42200700	1.10997800	H 3.36302400	2.52455100	2.70413100
C 3.10673400	2.12132300	1.71785300	H -5.79108700	-2.67403200	2.13308200
C 4.70652700	0.19092200	1.95421700	C -4.47319500	2.17336100	-0.61104200
C 5.52358200	2.39938800	1.10788700	O -4.60727800	3.32763100	-0.25023100
H 0.12904500	2.33847400	-0.57245000	O -5.51805600	1.47873900	-1.12988300
H -2.18728100	3.35236600	-0.59370100	H -6.27841300	2.08481500	-1.11366500
H 2.18718800	-3.35214500	-0.59348600	C 4.47316700	-2.17299800	-0.61135200
H -0.12912500	-2.33820700	-0.57214600	O 4.60771600	-3.32685000	-0.24942600
			O 5.51738600	-1.47876500	-1.13199900

H 6.27792700 -2.08461100 -1.11582400

H₂BPV

C -0.72616300 0.14816100 -0.55750700
C 0.72611900 -0.14810300 -0.55754400
C -1.19571000 1.47005500 -0.60175800
C -2.56443100 1.67255300 -0.61302200
C -3.45100100 0.57908200 -0.56892600
C -2.87530900 -0.71591300 -0.51702800
N -1.55493700 -0.90306200 -0.51421700
N 1.55489500 0.90311800 -0.51425200
C 2.87526800 0.71597300 -0.51706500
C 3.45095400 -0.57902900 -0.56897000
C 2.56437900 -1.67249500 -0.61308200
C 1.19566100 -1.46999800 -0.60180800
C -3.71139900 -1.97959600 -0.40723800
O -3.16938300 -2.91443400 -1.34012000
C 3.71135500 1.97966500 -0.40731300
O 3.16917700 2.91456800 -1.34002400
C -3.79480400 -2.55280900 1.04738700
C -2.42211100 -3.01673900 1.55817400
C -4.36784800 -1.47536400 1.98453100
C -4.76273000 -3.75267600 1.02954700
C 3.79497200 2.55276100 1.04735300
C 2.42234100 3.01663700 1.55836300
C 4.36815500 1.47527200 1.98435700
C 4.76289100 3.75263400 1.02947600
H -0.48659100 2.28723200 -0.64695800
H -2.96213900 2.67921800 -0.68930300
H 2.96209500 -2.67915700 -0.68937700
H 0.48654100 -2.28717300 -0.64700900
H -4.74277400 -1.74510000 -0.69735800
H -3.75552000 -3.68053400 -1.37253100
H 4.74268400 1.74521000 -0.69763300
H 3.75515000 3.68080100 -1.37224500
H -1.96331200 -3.72102800 0.85923400
H -2.53868800 -3.51222500 2.52857000
H -4.50635900 -1.88915200 2.98875700
H -5.34100900 -1.11119300 1.63678200
H -3.69669400 -0.61560100 2.06825100
H -5.74268400 -3.47156800 0.62487300
H -4.36926400 -4.59042800 0.44211700
H 1.96342800 3.72097600 0.85955100
H 1.73465700 2.17737500 1.68098900
H 5.34130200 1.11117300 1.63649500
H 3.69705500 0.61547100 2.06809000
H 5.74279100 3.47155300 0.62465100
H 4.36936200 4.59044300 0.44216900
H 4.91851000 4.12725500 2.04629900
H 4.50673800 1.88900600 2.98859600
H -1.73440000 -2.17749500 1.68077000
H 2.53904300 3.51204100 2.52878700
H -4.91821700 -4.12737500 2.04636100
C -4.89776600 0.79524000 -0.58587700

H -5.51940300 0.00415700 -0.99104000
C 4.89771400 -0.79521300 -0.58587500
H 5.51938500 -0.00415300 -0.99102600
C -5.52332500 1.90139700 -0.13742500
H -4.99229000 2.72717400 0.32311700
C 5.52322700 -1.90142200 -0.13748300
H 4.99215800 -2.72721400 0.32299200
C -6.97877000 2.09252100 -0.19884500
O -7.55432900 3.09211000 0.19369400
O -7.65648400 1.03897900 -0.73711400
H -8.59624200 1.28313300 -0.72435800
C 6.97866600 -2.09258700 -0.19889600
O 7.55419100 -3.09222100 0.19358100
O 7.65642500 -1.03901200 -0.73704600
H 8.59617600 -1.28319400 -0.72427900

H₂BPY

C 0.71163000 -0.20739500 -0.46935500
C -0.71162400 0.20732100 -0.46934700
C 1.06655800 -1.56458000 -0.51320000
C 2.41320100 -1.88710900 -0.51184400
C 3.37473500 -0.85916700 -0.46590800
C 2.91938200 0.48454200 -0.42020900
N 1.62233600 0.77756500 -0.42316100
N -1.62232900 -0.77763500 -0.42312800
C -2.91937900 -0.48460600 -0.42017200
C -3.37472700 0.85909300 -0.46588900
C -2.41318600 1.88704200 -0.51183600
C -1.06654800 1.56451100 -0.51319900
C 3.89232200 1.64603700 -0.36128100
O 3.46036500 2.58817900 -1.34632100
C -3.89234000 -1.64608600 -0.36125900
O -3.46041800 -2.58819200 -1.34633600
C 4.03389600 2.28233900 1.05989500
C 2.72563100 2.94396800 1.51941400
C 4.45618700 1.19566500 2.06451600
C 5.14736300 3.34572300 0.98861900
C -4.03394300 -2.28240400 1.05990900
C -2.72574200 -2.94416700 1.51942000
C -4.45611600 -1.19569700 2.06454400
C -5.14751600 -3.34567600 0.98864500
H 0.28973500 -2.31774300 -0.55284600
H 2.74138300 -2.92037500 -0.55035000
H -2.74137400 2.92030600 -0.55033900
H -0.28971700 2.31766600 -0.55285200
H 4.88209300 1.26026700 -0.63367300
H 4.17852600 3.21576200 -1.49359900
H -4.88210100 -1.26027600 -0.63363500
H -4.17840900 -3.21604900 -1.49328400
H 2.37125300 3.66314400 0.77619500
H 2.89211000 3.47158300 2.46524900
H 4.62793900 1.64473500 3.04829900
H 5.38189000 0.69916900 1.75577500
H 3.68161500 0.43107300 2.18104200

H 6.08809600 2.91539600 0.62527000
H 4.87017300 4.18391700 0.33922700
H -2.37147400 -3.66343100 0.77623300
H -1.93414900 -2.20712800 1.67254300
H -5.38172500 -0.69904100 1.75577000
H -3.68143000 -0.43123100 2.18112900
H -6.08822300 -2.91525300 0.62534500
H -4.87044900 -4.18388600 0.33921500
H -5.33437000 -3.76316500 1.98340100
H -4.62799600 -1.64476300 3.04830600
H 1.93413200 2.20684100 1.67261600
H -2.89225500 -3.47171100 2.46528900
H 5.33422400 3.76318800 1.98338400
C 4.75759700 -1.17723100 -0.46433000
C 5.94024400 -1.45568400 -0.45946200
C -4.75758000 1.17720500 -0.46431800
C -5.94020200 1.45575300 -0.45947100
C 7.36232200 -1.64943900 -0.42511100
O 8.17446500 -0.74668000 -0.34262700
O 7.70906500 -2.95728200 -0.49166400
H 8.68076400 -2.99187600 -0.46037900
C -7.36226700 1.64959500 -0.42518800
O -8.17451100 0.74691300 -0.34310500
O -7.70885800 2.95754000 -0.49128700
H -8.68055400 2.99222300 -0.46007400

H₂BPVB

C 0.74201700 -0.01101900 -0.59841000
C -0.73941000 -0.00548200 -0.60189700
C 1.46354200 -1.21375100 -0.64277200
C 2.84602400 -1.14432700 -0.65186600
C 3.50410700 0.09988700 -0.59977500
C 2.68265700 1.25464500 -0.54676000
N 1.35115500 1.18153600 -0.55101900
N -1.34866800 -1.19781200 -0.55271500
C -2.68017500 -1.27127100 -0.55386000
C -3.50160500 -0.11670100 -0.61361600
C -2.84321600 1.12728700 -0.66874400
C -1.46085200 1.19698200 -0.65457900
C 3.25829100 2.65518400 -0.42527500
O 2.58078200 3.46841100 -1.38411600
C -3.25526500 -2.67214100 -0.43256300
O -2.56871300 -3.48715800 -1.38332900
C 3.18986400 3.23992700 1.02505300
C 1.74118400 3.45899200 1.48789400
C 3.90987600 2.28099000 1.98942000
C 3.93410200 4.59025600 1.03026200
C -3.19752100 -3.25269500 1.01991400
C -1.75203500 -3.46551900 1.49546300
C -3.92886000 -2.29371500 1.97565100
C -3.93717900 -4.60551000 1.02237300
H 0.92899700 -2.15430400 -0.69354400
H 3.43384600 -2.05293000 -0.73442500
H -3.43056400 2.03559500 -0.75754600

H -0.92629600 2.13741400 -0.70740300
H 4.32450400 2.61815000 -0.68108600
H 2.98589000 4.34446200 -1.37569100
H -4.31932700 -2.63755100 -0.69737900
H -2.97615900 -4.36215400 -1.37950800
H 1.19101300 4.07483100 0.77138200
H 1.73799800 3.96555600 2.45978500
H 3.94233900 2.71548200 2.99409400
H 4.94111900 2.08742800 1.67411200
H 3.39408900 1.31874600 2.05700800
H 4.96246700 4.48289100 0.66409100
H 3.42439100 5.34559100 0.42028000
H -1.19361800 -4.08056800 0.78471300
H -1.22037300 -2.51764300 1.59913600
H -4.95858400 -2.10572800 1.65209300
H -3.41777400 -1.32901300 2.04408900
H -4.96249200 -4.50287300 0.64642700
H -3.41915500 -5.36079200 0.41945600
H -3.99489500 -5.00314900 2.04080300
H -3.96705200 -2.72521500 2.98141500
H 1.20521100 2.51326800 1.58855300
H -1.75516900 -3.97033300 2.46825600
H 3.98372500 4.99083600 2.04796800
C 4.96687400 0.16775900 -0.60909300
H 5.41110200 1.04555300 -1.06794200
C -4.96419300 -0.18496700 -0.62643200
H -5.40659400 -1.06805500 -1.07651600
C 5.78276800 -0.76742400 -0.07903700
H 5.33833600 -1.60742500 0.45143600
C -5.78229300 0.75563900 -0.10939300
H -5.33996000 1.60324300 0.41060600
C 7.24538100 -0.74852900 -0.09461800
C 7.99746400 0.15600100 -0.87210900
C 7.94519500 -1.67571100 0.70315400
C 9.38532300 0.14506400 -0.83923400
H 7.49219300 0.86359300 -1.52061100
C 9.33380700 -1.69195500 0.73951400
H 7.38373300 -2.38546300 1.30399200
C 10.06711000 -0.77873100 -0.02989200
H 9.95024500 0.84436200 -1.44426600
H 9.86934500 -2.40423000 1.35740600
C -7.24472100 0.73470300 -0.12705700
C -7.94607200 1.68386500 0.64159300
C -7.99567300 -0.19403800 -0.87835900
C -9.33626500 1.70216400 0.67720100
H -7.38569200 2.41141400 1.22183300
C -9.38188100 -0.18182900 -0.84538800
H -7.48973900 -0.92158700 -1.50377000
C -10.06665100 0.76471400 -0.06581400
H -9.85913000 2.43770300 1.27694100
H -9.95920200 -0.89460200 -1.42392800
C 11.54560200 -0.83033500 0.03661200
O 12.18870600 -1.60878000 0.71689400
O 12.15058500 0.09789300 -0.75257700

H 13.10717700 -0.02265600 -0.63534200
C -11.54711200 0.73619500 -0.06662600
O -12.23110100 -0.05428800 -0.69103200
O -12.10268300 1.69954700 0.71652100
H -13.06522100 1.59145700 0.64471800

Sc³⁺-H₂BPVB

C 0.73267700 -0.99795800 -0.01013400
C -0.73267600 -0.99794700 0.01073300
C 1.51863800 -2.14508600 -0.12221800
C 2.89443000 -2.00731000 -0.20302100
C 3.51149800 -0.74319900 -0.12736100
C 2.65348700 0.36606000 0.04302600
N 1.31355100 0.22329400 0.06294300
N -1.31354400 0.22328200 -0.06264200
C -2.65346200 0.36609500 -0.04283100
C -3.51148700 -0.74313000 0.12776200
C -2.89443500 -2.00722200 0.20381300
C -1.51864500 -2.14505400 0.12308500
C 3.13131700 1.78630500 0.22925600
O 2.03098100 2.59211500 -0.28381600
C -3.13132900 1.78628100 -0.22927800
O -2.03100800 2.59221600 0.28371600
Sc -0.00001600 2.04565100 -0.00006200
C 3.47407600 2.19555500 1.69983500
C 2.30384200 1.92028400 2.65359400
C 4.71229700 1.42034700 2.17951800
C 3.80513100 3.69967400 1.70920900
C -3.47407500 2.19541100 -1.69986500
C -2.30379200 1.92013900 -2.65357600
C -4.71223500 1.42010900 -2.17951500
C -3.80520600 3.69952100 -1.70934500
H 1.06442000 -3.12528200 -0.18947800
H 3.50198700 -2.89137300 -0.35630600
H -3.50204500 -2.89121200 0.35731500
H -1.06444000 -3.12524000 0.19056000
H 3.99643100 1.99306000 -0.40329600
H 2.28002100 3.52912400 -0.34432100
H -3.99643300 1.99304300 0.40328700
H -2.28018600 3.52920000 0.34403700
H 1.40910300 2.48661500 2.36579400
H 2.57830600 2.24337900 3.66258300
H 4.97905700 1.77257800 3.18089300
H 5.57220600 1.58537000 1.52338800
H 4.52429100 0.34583500 2.24421800
H 4.58614000 3.93816800 0.97845300

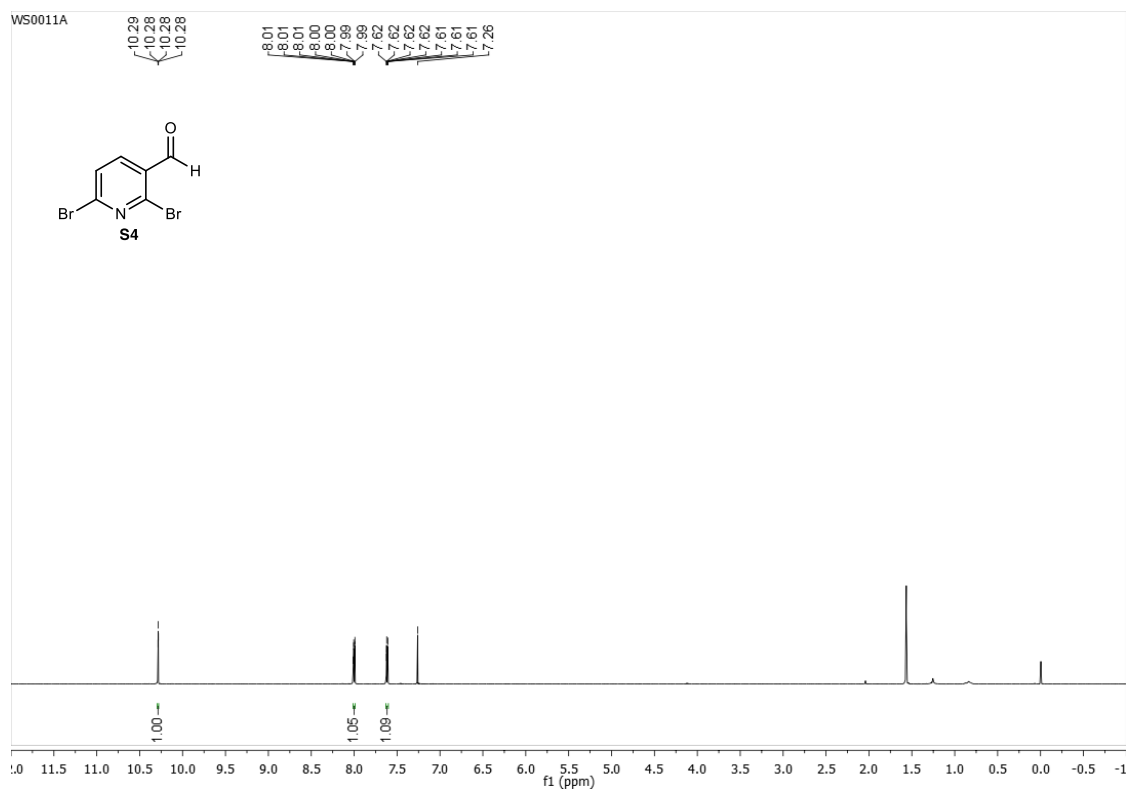
H 2.92566300 4.31913500 1.50040600
H -1.40912600 2.48665100 -2.36594200
H -2.05137300 0.85668100 -2.69699400
H -5.57214800 1.58501300 -1.52336100
H -4.52413800 0.34561500 -2.24426900
H -4.58625700 3.93804100 -0.97864200
H -2.92577600 4.31904500 -1.50055400
H -4.17016800 3.98334300 -2.70114700
H -4.97906300 1.77234800 -3.18087200
H 2.05157000 0.85681400 2.69729300
H -2.57838500 2.24289500 -3.66263800
H 4.17013400 3.98356200 2.70097400
C 4.95724700 -0.58161900 -0.25694100
H 5.30944100 0.41381900 -0.50042200
C -4.95725300 -0.58156400 0.25717200
H -5.30948200 0.41386900 0.50065900
C 5.85745500 -1.57218700 -0.07680000
H 5.51086700 -2.56646300 0.19663200
C -5.85742700 -1.57212100 0.07681300
H -5.51079600 -2.56637400 -0.19665000
C 7.30977300 -1.44403600 -0.18483700
C 7.96988800 -0.22026700 -0.42351700
C 8.09793000 -2.60122200 -0.02936300
C 9.35676000 -0.16692500 -0.50759500
H 7.39979300 0.69593800 -0.53684600
C 9.48662200 -2.54408700 -0.11958400
H 7.60750600 -3.55185300 0.16158000
C 10.13807300 -1.32613600 -0.36005100
H 9.84710400 0.78327800 -0.68781100
H 10.07345200 -3.44791300 0.00024200
C -7.30976100 -1.44398200 0.18470900
C -8.09788900 -2.60120100 0.02929300
C -7.96990400 -0.22020300 0.42320100
C -9.48658300 -2.54407700 0.11940500
H -7.60742300 -3.55184100 -0.16149700
C -9.35678900 -0.16687300 0.50720300
H -7.39984800 0.69603600 0.53645900
C -10.13806900 -1.32610100 0.35972400
H -10.07341500 -3.44790400 -0.00037800
H -9.84714700 0.78334700 0.68729500
C -11.65113600 -1.26198000 0.45243000
O -12.18703500 -0.12097400 0.62019300
O -12.29456200 -2.35403500 0.35465700
C 11.65114200 -1.26195600 -0.45283600
O 12.29456100 -2.35407500 -0.35566300
O 12.18702300 -0.12088000 -0.62010300

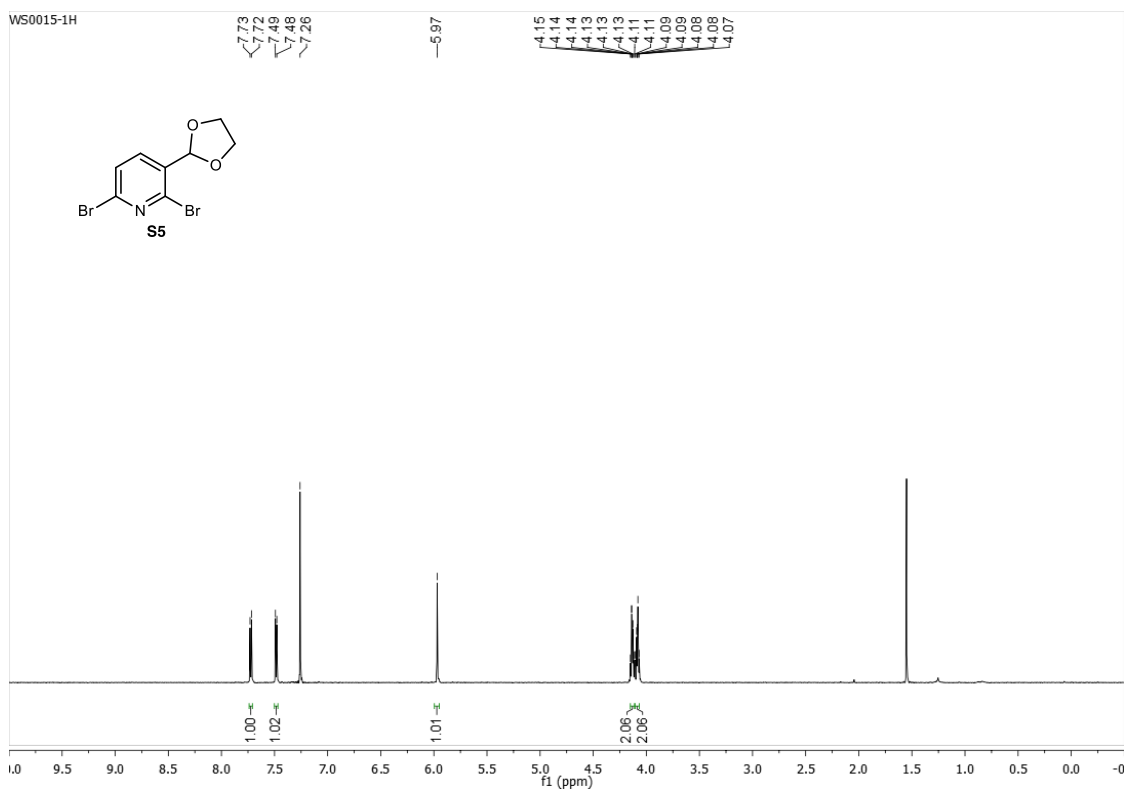
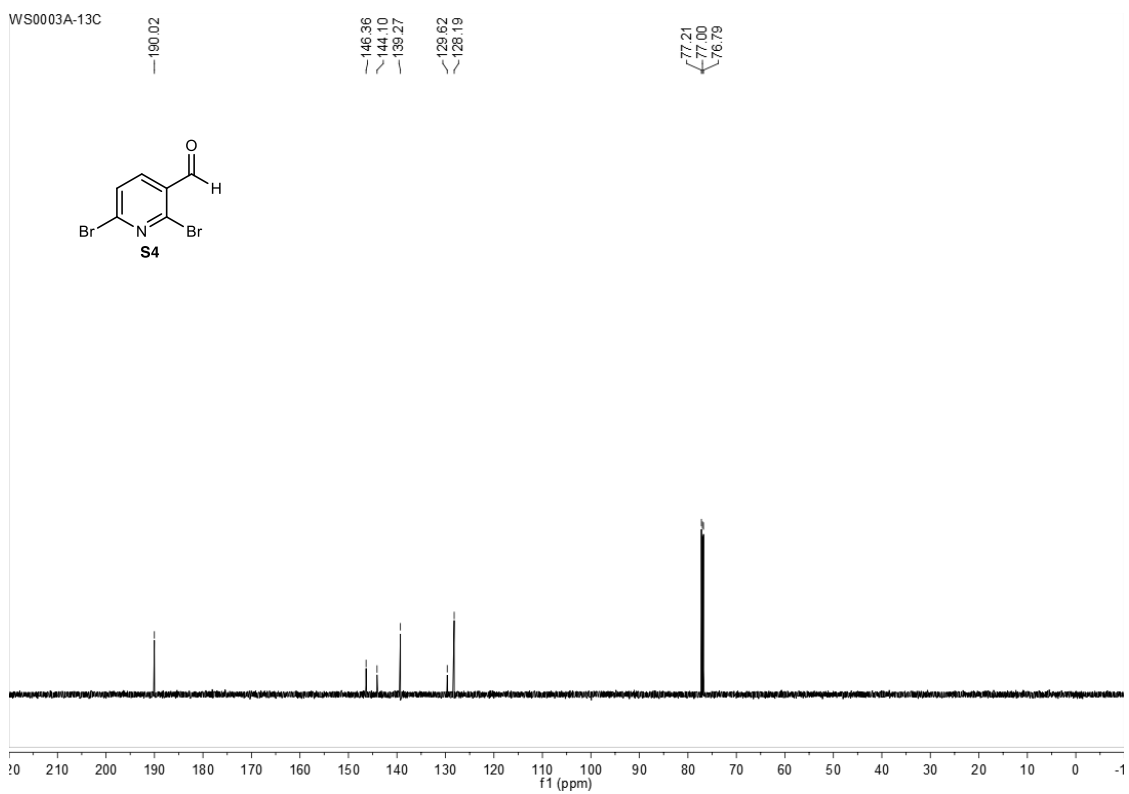
18. References

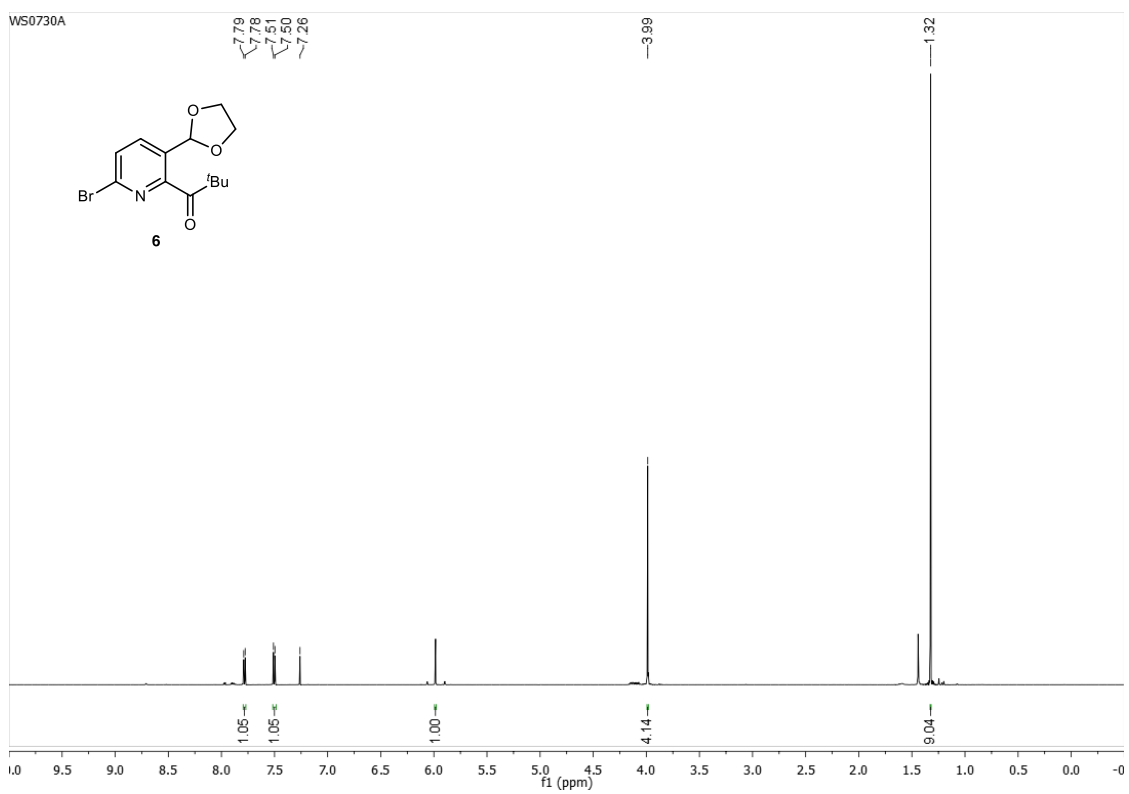
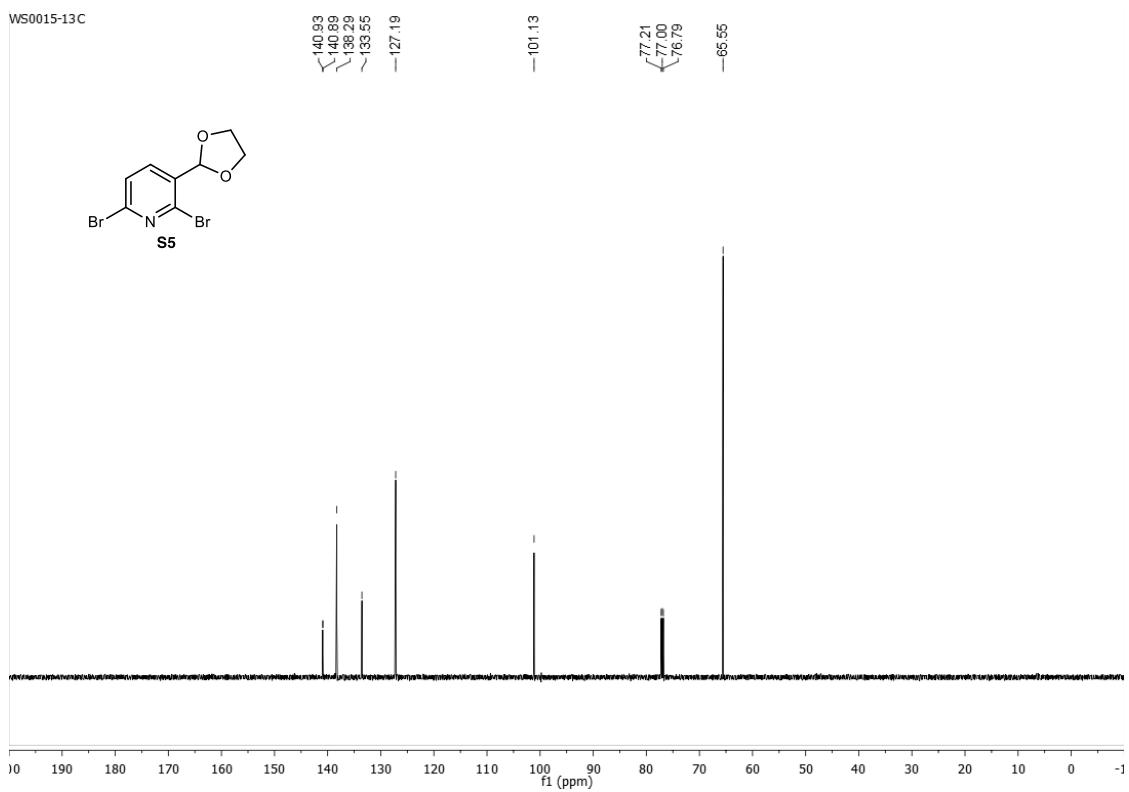
1. K. Manna, T. Zhang, F. X. Greene, W. Lin, Bipyridine- and phenanthroline-based metal-organic frameworks for highly efficient and tandem catalytic organic transformations via directed C-H activation. *J. Am. Chem. Soc.* **2015**, *137*, 2665–2673.
2. C. Chen, P. Pan, Z. Deng, D. Wang, Q. Wu, L. Xu, T. Hou, S. Cui, Discovery of 3,6-diaryl-1*H*-pyrazolo[3,4-*b*]pyridines as potent anaplastic lymphoma kinase (ALK) inhibitors. *Bioorg. Med. Chem. Lett.* **2019**, *29*, 912–916.
3. P. Bałczewski, A. Bodzioch, E. Rózycka-Sokołowska, B. Marciniak, P. Uznanski, First approach to nitrogen-containing fused aromatic hydrocarbons as targets for organoelectronics utilizing a new transformation of *o*-protected diaryl methanols. *Chem. Eur. J.* **2010**, *16*, 2392–2400.
4. C. Bolm, M. Zehnder, D. Bur, Optically active bipyridines in asymmetric catalysis. *Angew. Chem. Int. Ed. Engl.* **1990**, *29*, 205–207.
5. J. Mao, B. Wan, F. Wu, S. Lu, First example of asymmetric transfer hydrogenation in water induced by a chiral amino alcohol hydrochloride. *Tetrahedron Lett.* **2005**, *46*, 7341–7344.
6. K. C. Nicolaou, C. F. Claiborne, P. G. Nantermet, E. A. Couladouros, E. J. Sorensen, Synthesis of novel toxoids. *J. Am. Chem. Soc.* **1994**, *116*, 1591–1592.
7. X. Wu, S. Sun, S. Xu, J. Cheng, Rh-Catalyzed annulation of *ortho*-C-H bonds of 2-arylimidazoles with 1,4,2-dioxazol-5-ones toward 5-arylimidazo[1,2-*c*]quinazolines. *Adv. Synth. Catal.* **2018**, *360*, 1111–1115.
8. Z. Dogan, R. Paulini, J. A. R. Stütz, S. Narayanan, C. Richert, 5'-Tethered stilbene derivatives as fidelity- and affinity-enhancing modulators of DNA duplex stability. *J. Am. Chem. Soc.* **2004**, *126*, 4762–4763.
9. Md. M. Baag, A. Kar, N. P. Argade, *N*-Bromosuccinimide-dibenzoyl peroxide/azabisisobutyronitrile: a reagent for *Z*- to *E*-alkene isomerization. *Tetrahedron* **2003**, *59*, 6489–6492.
10. S. Lauzon, T. Ollevier, 2,2'-Bipyridine- α,α' -trifluoromethyl-diol ligand: synthesis and application in the asymmetric Et₂Zn alkylation of aldehydes. *Chem. Commun.*, **2021**, *57*, 11025–11028.
11. J. M. Gawel, A. E. Shouksmith, Y. S. Raouf, N. Nawar, K. Toutah, S. Bukhari, P. Manaswiyoungkul, O. O. Olaoye, J. Israelian, T. B. Radu, A. D. Cabral, D. Sina, A. Sedighi, E. D. de Araujo, P. T. Gunning, PTG-0861: A novel HDAC6-selective inhibitor as a

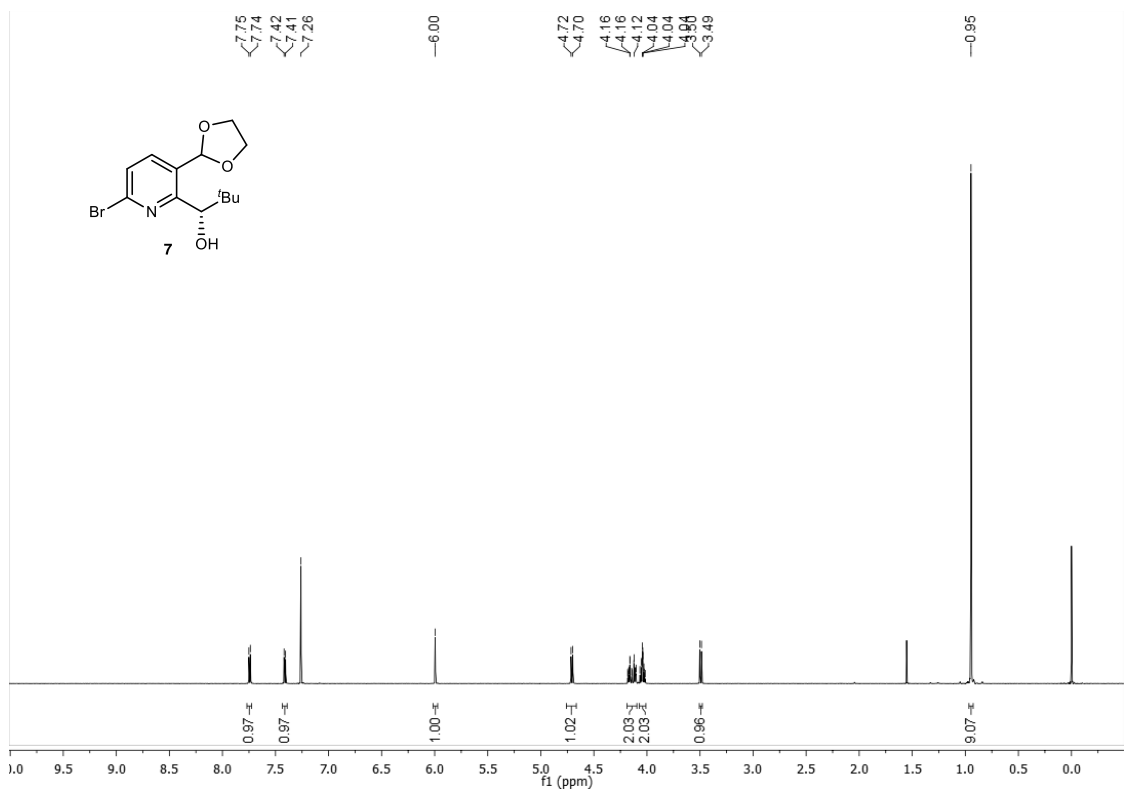
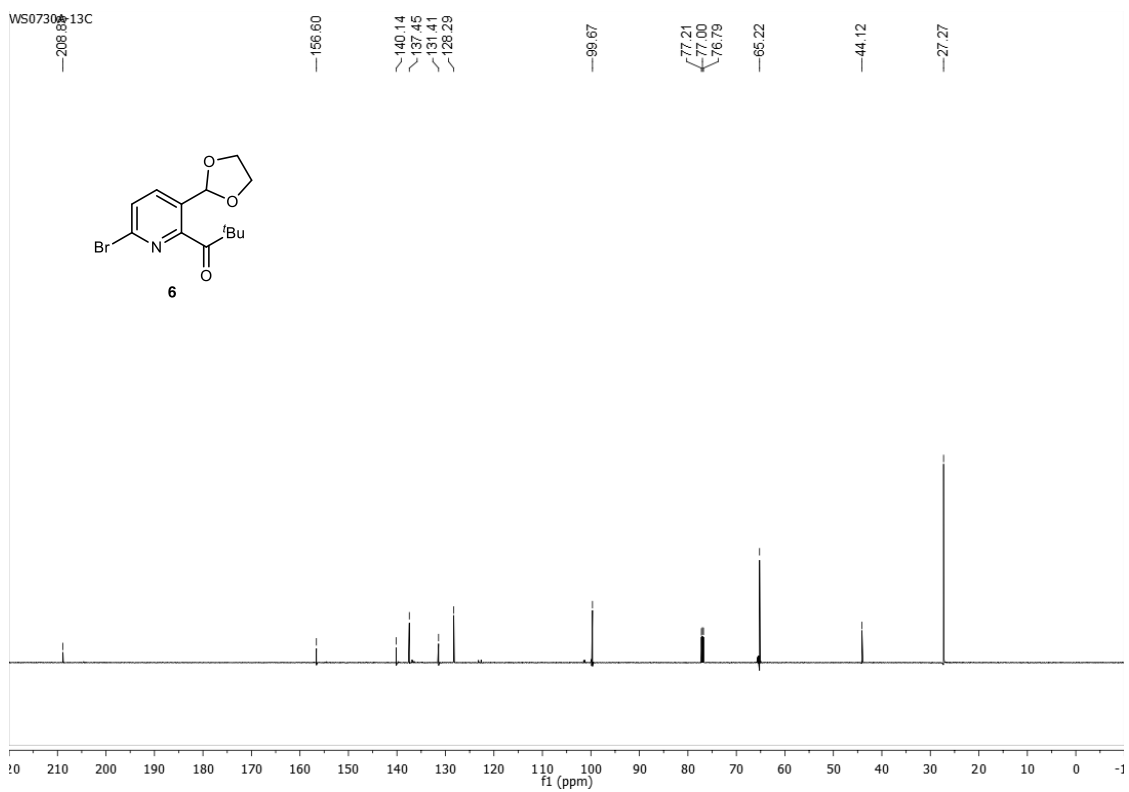
- therapeutic strategy in acute myeloid leukaemia. *Eur. J. Med. Chem.* **2020**, *201*, 112411–112435.
12. T. Kitanosono, F. Lu, K. Masuda, Y. Yamashita, S. Kobayashi, Efficient recycling of catalyst-solvent couples from Lewis acid catalyzed asymmetric reactions in water. *Angew. Chem. Int. Ed.* **2022**, *61*, e202202335.
 13. B. Gao, Y. Wen, Z. Yang, X. Huang, X. Liu, X. Feng, Asymmetric ring opening of meso-epoxides with aromatic amines catalyzed by a new proline-based *N,N'*-dioxide-indium tris(triflate) complex. *Adv. Synth. Catal.* **2008**, *350*, 385–390.
 14. C. Ogawa, S. Azoulay, S. Kobayashi, Bismuth triflate-chiral bipyridine complex catalyzed asymmetric ring opening reactions of *meso*-epoxide in water. *Heterocycles*, **2005**, *66*, 201–206.
 15. Gaussian 16, Revision B.01, M. J. Frisch, G. W. Trucks, H. B. Schlegel, G. E. Scuseria, M. A. Robb, J. R. Cheeseman, G. Scalmani, V. Barone, G. A. Petersson, H. Nakatsuji, X. Li, M. Caricato, A. V. Marenich, J. Bloino, B. G. Janesko, R. Gomperts, B. Mennucci, H. P. Hratchian, J. V. Ortiz, A. F. Izmaylov, J. L. Sonnenberg, D. Williams-Young, F. Ding, F. Lipparini, F. Egidi, J. Goings, B. Peng, A. Petrone, T. Henderson, D. Ranasinghe, V. G. Zakrzewski, J. Gao, N. Rega, G. Zheng, W. Liang, M. Hada, M. Ehara, K. Toyota, R. Fukuda, J. Hasegawa, M. Ishida, T. Nakajima, Y. Honda, O. Kitao, H. Nakai, T. Vreven, K. Throssell, J. A. Montgomery, Jr., J. E. Peralta, F. Ogliaro, M. J. Bearpark, J. J. Heyd, E. N. Brothers, K. N. Kudin, V. N. Staroverov, T. A. Keith, R. Kobayashi, J. Normand, K. Raghavachari, A. P. Rendell, J. C. Burant, S. S. Iyengar, J. Tomasi, M. Cossi, J. M. Millam, M. Klene, C. Adamo, R. Cammi, J. W. Ochterski, R. L. Martin, K. Morokuma, O. Farkas, J. B. Foresman, D. J. Fox, *Gaussian, Inc., Wallingford CT, 2016*.
 16. A. V. Marenich, C. J. Cramer, D. G. Truhlar, Universal Solvation Model Based on the Generalized Born Approximation with Asymmetric Descreening. *J. Chem. Theory Comput.* **2009**, *5*, 2447–2467.

19. ¹H & ¹³C NMR spectra and HPLC chromatograms

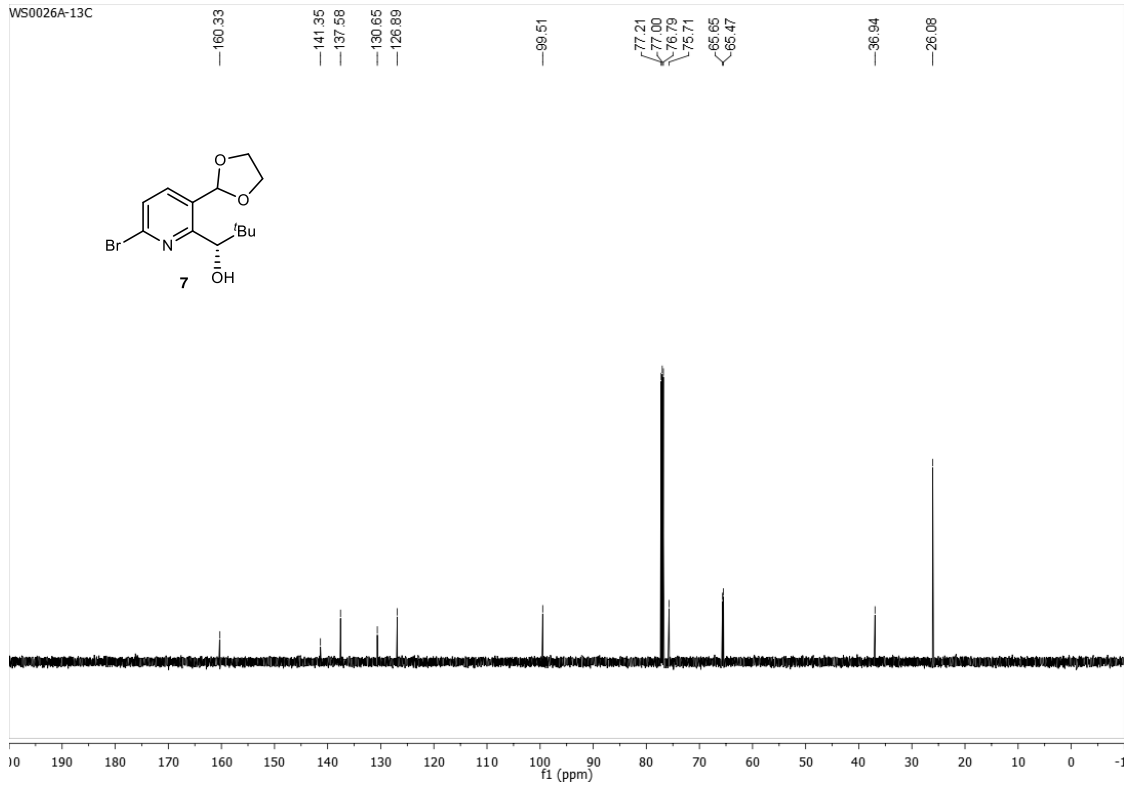


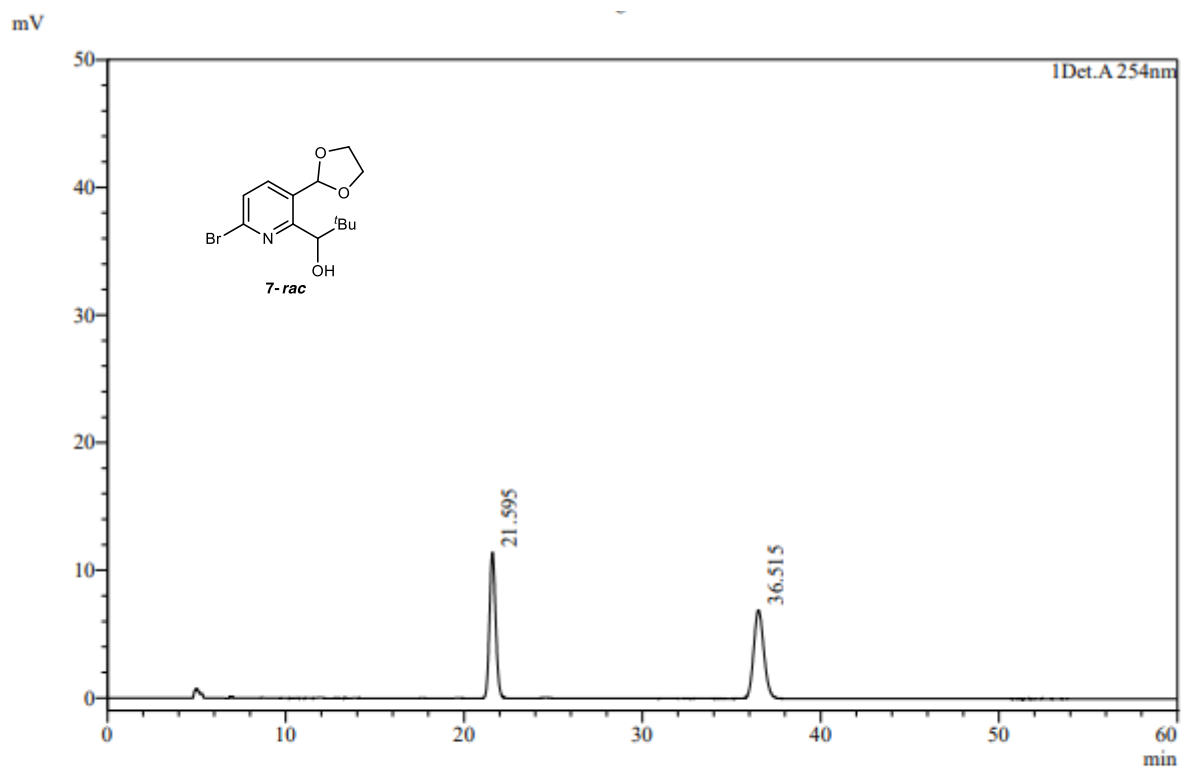






WS0026A-13C

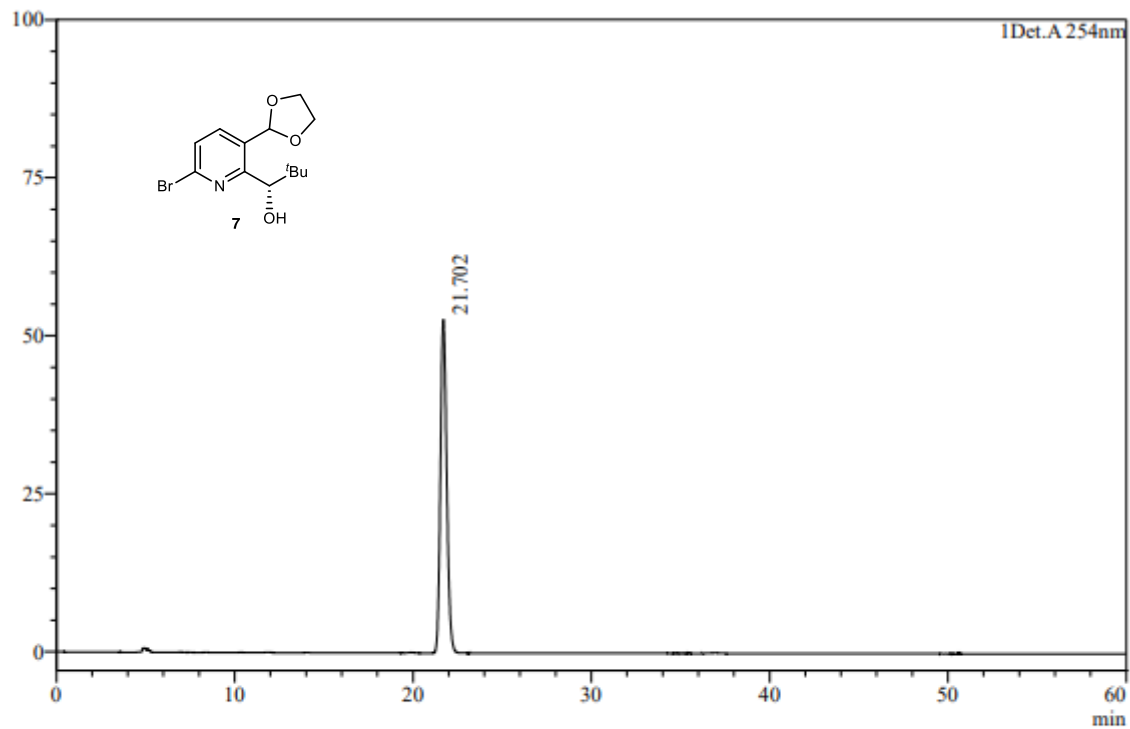




Peak Table

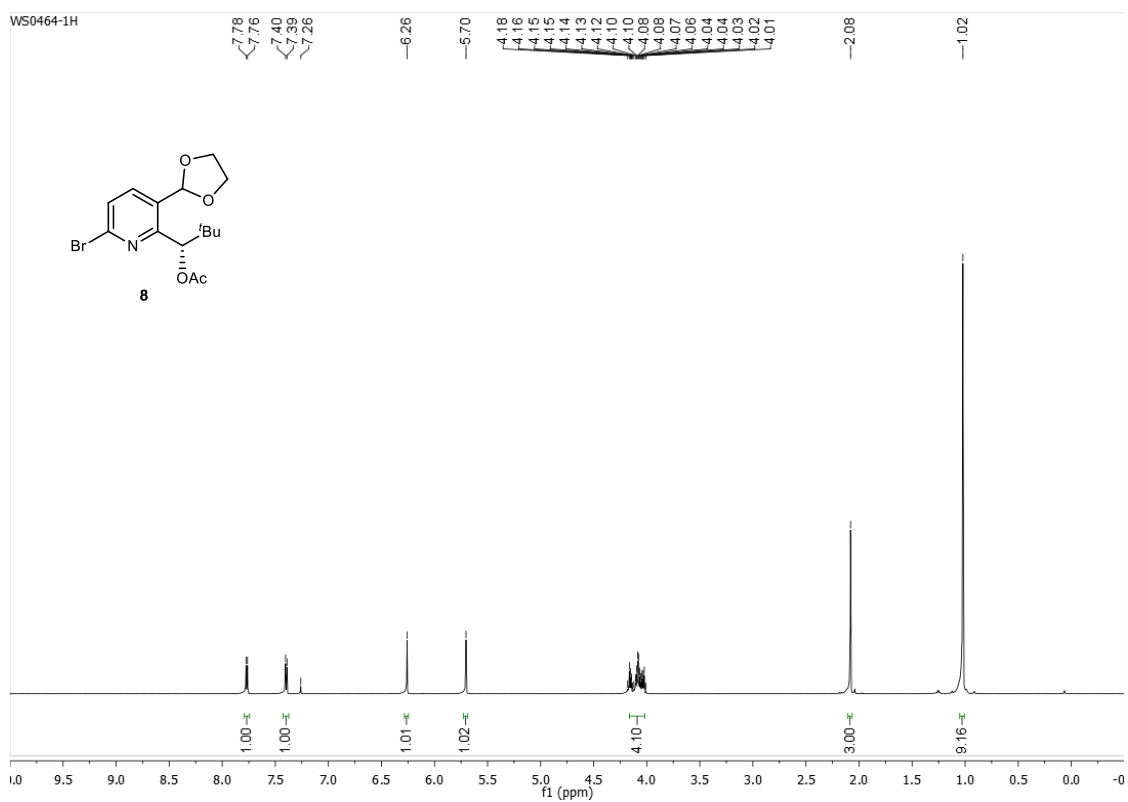
Peak#	Ret. Time	Area	Area%	Height	Conc.
1	21.595	274058	50.079	11409	50.079
2	36.515	273191	49.921	6907	49.921
Total		547249	100.000	18315	

mV

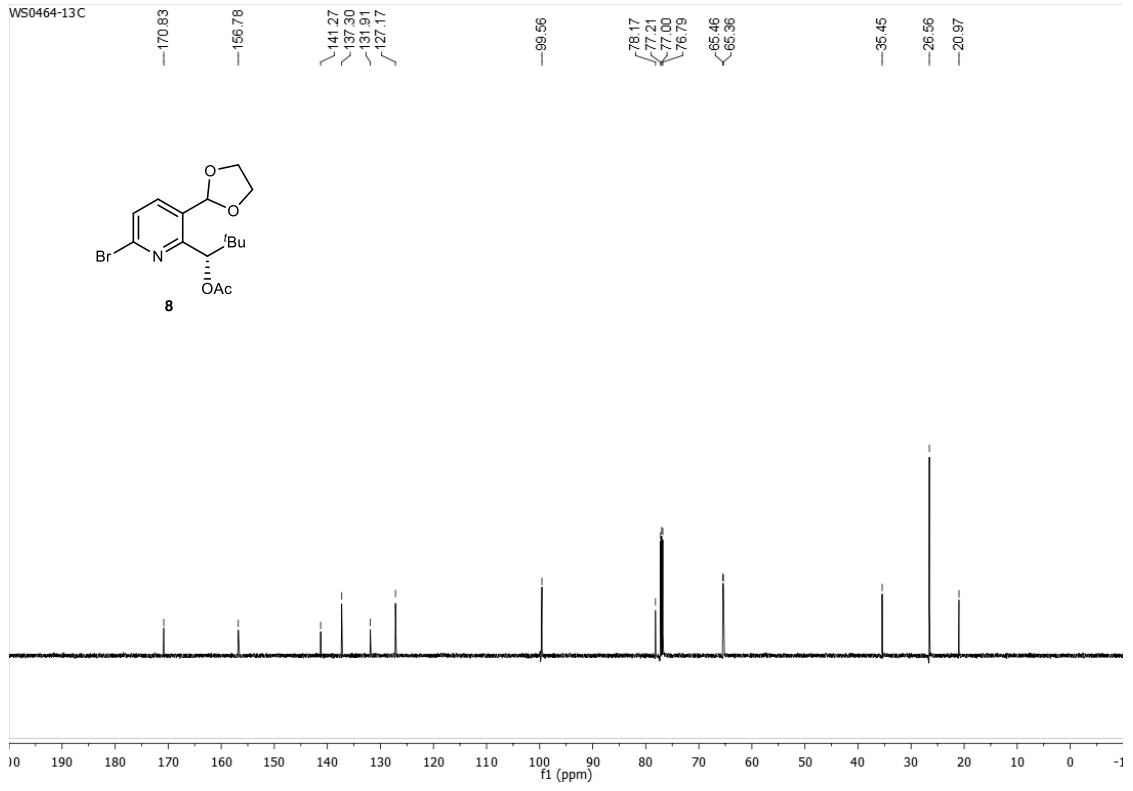
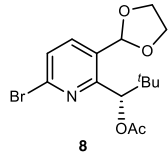


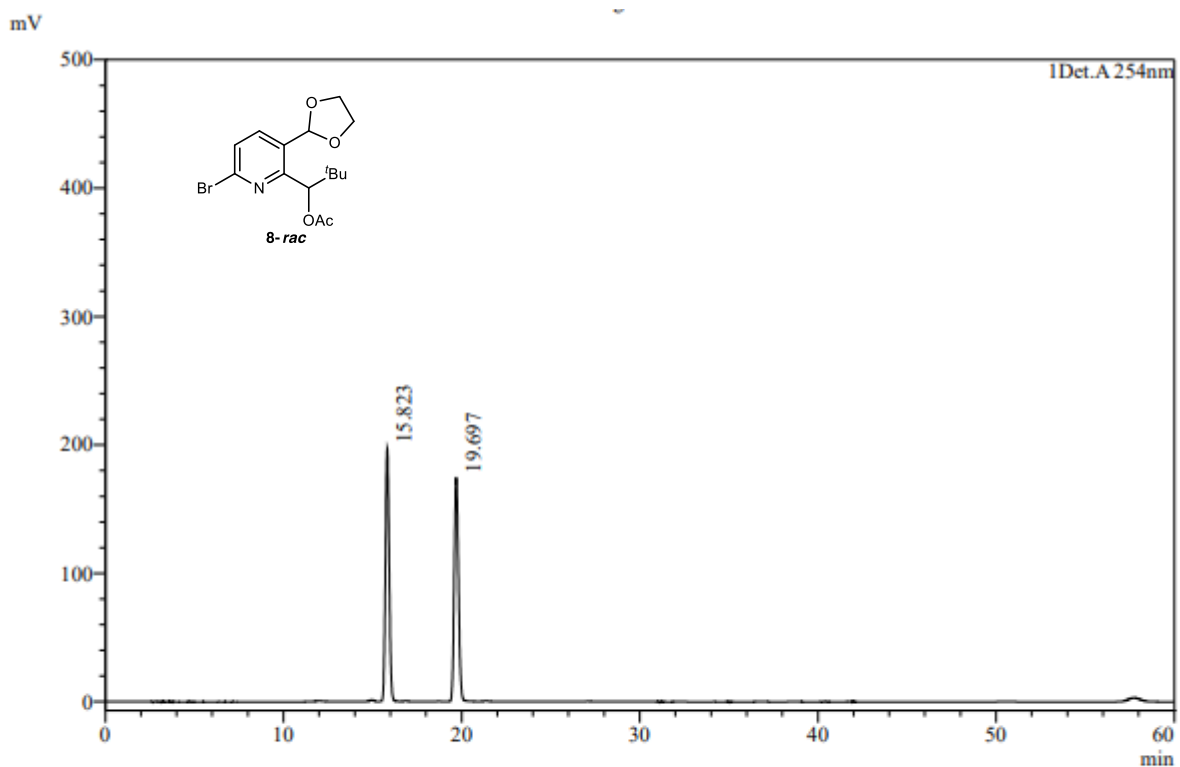
Peak Table

Peak#	Ret. Time	Area	Area%	Height	Conc.
1	21.702	1296040	100.000	52724	100.000
Total		1296040	100.000	52724	



WS0464-13C

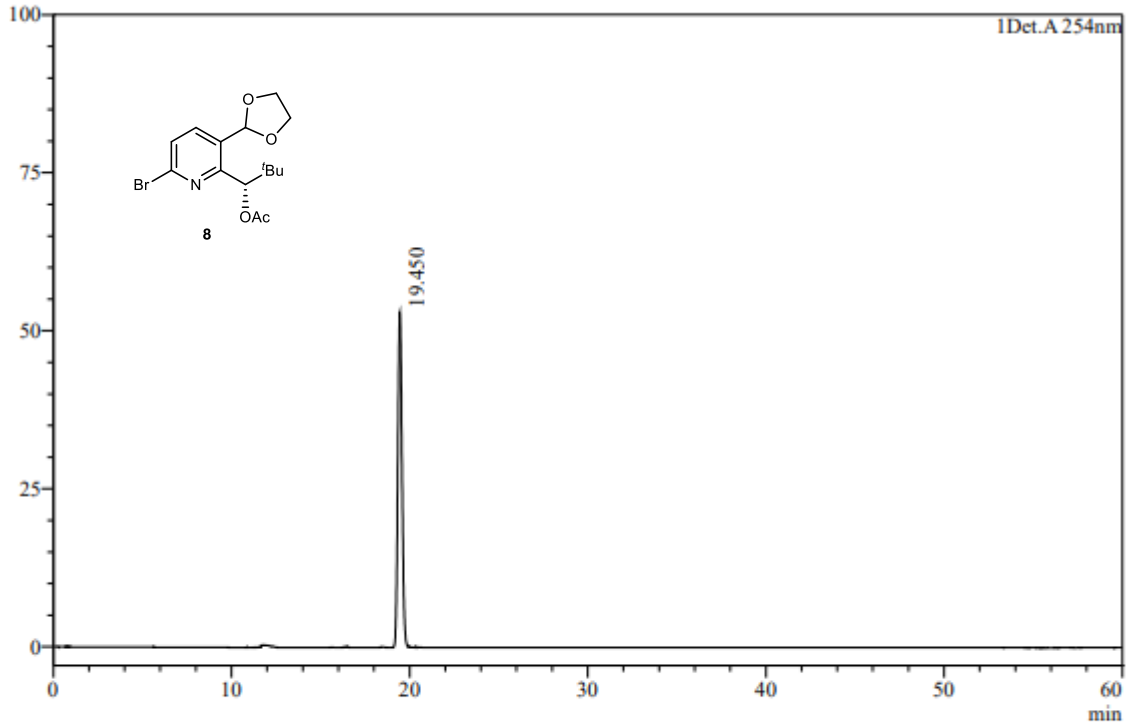




Peak Table

Peak#	Ret. Time	Area	Area%	Height	Conc.
1	15.823	2887304	50.048	196682	50.048
2	19.697	2881813	49.952	174069	49.952
Total		5769117	100.000	370752	

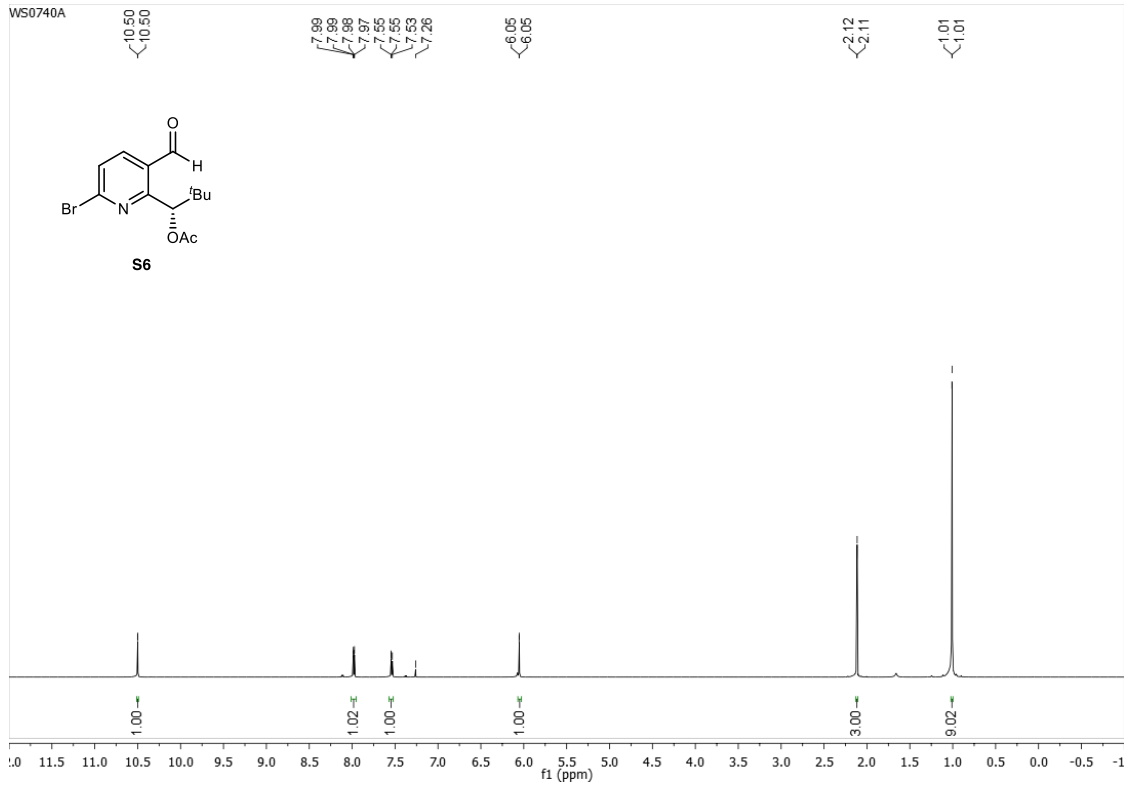
mV

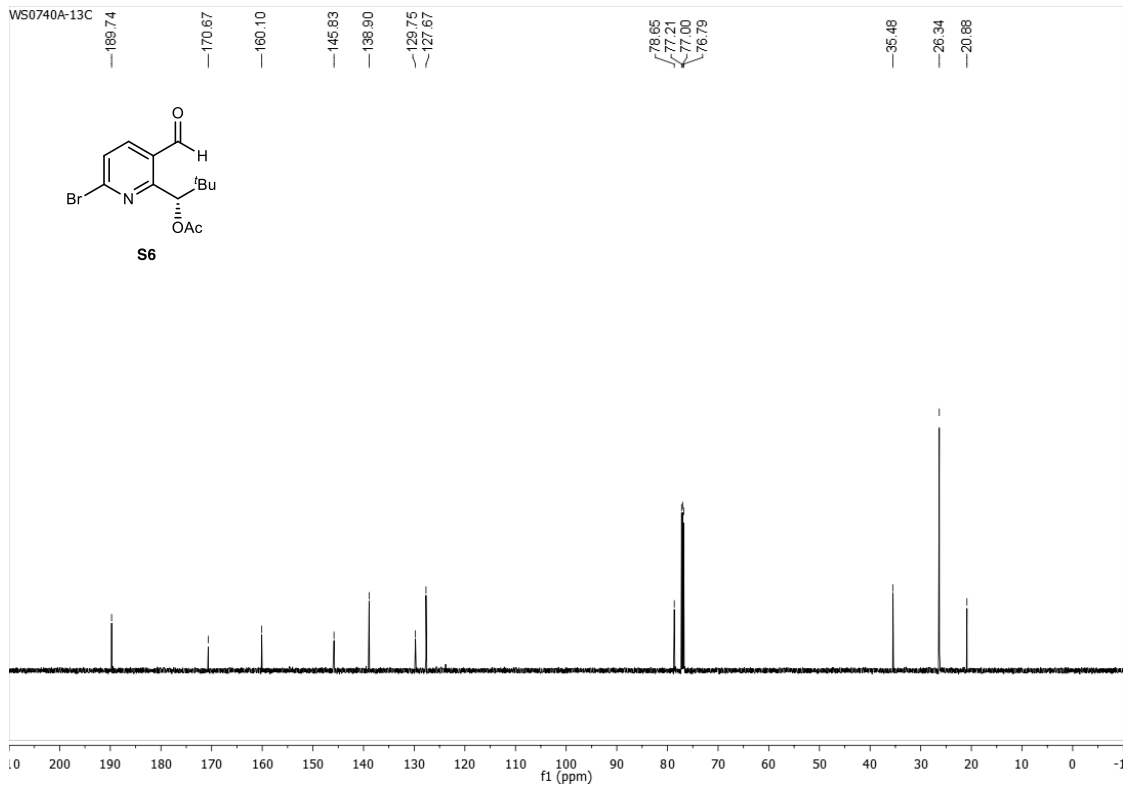


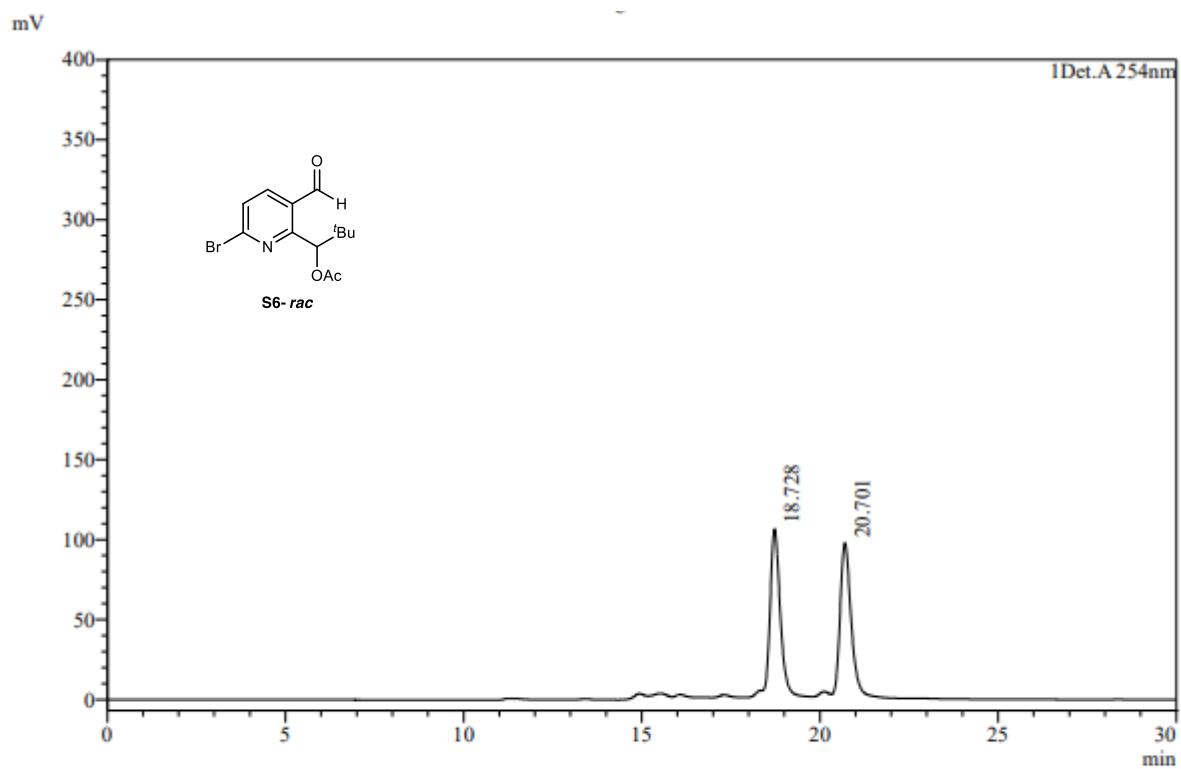
Peak Table

Peak#	Ret. Time	Area	Area%	Height	Conc.
1	19.450	868318	100.000	52963	100.000
Total		868318	100.000	52963	

WS0740A

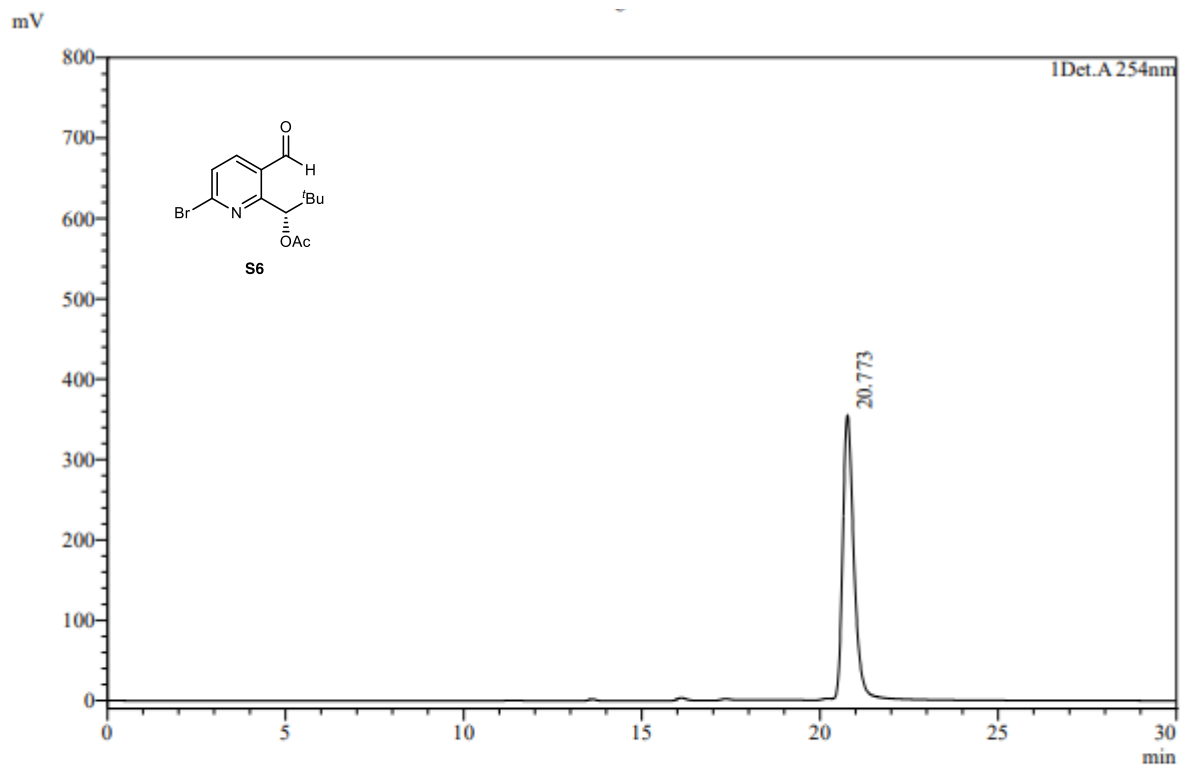






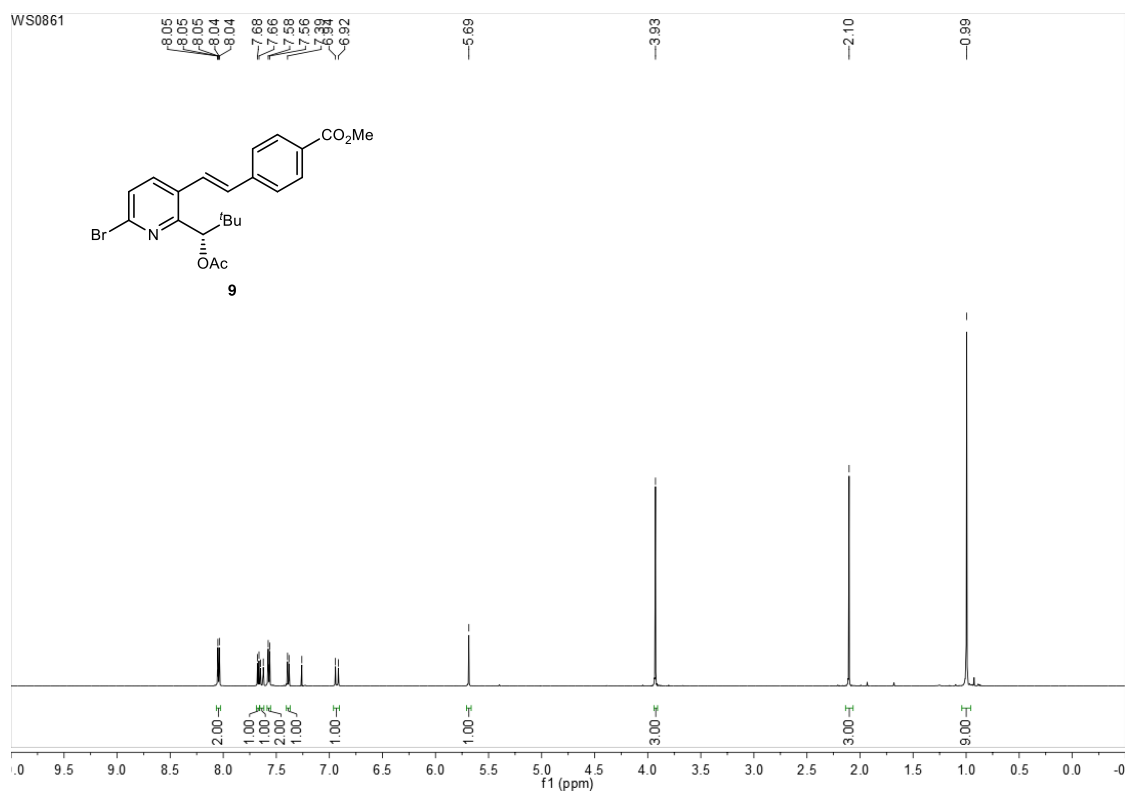
Peak Table

Peak#	Ret. Time	Area	Area%	Height	Conc.
1	18.728	1948051	49.927	102636	49.927
2	20.701	1953769	50.073	94773	50.073
Total		3901819	100.000	197409	

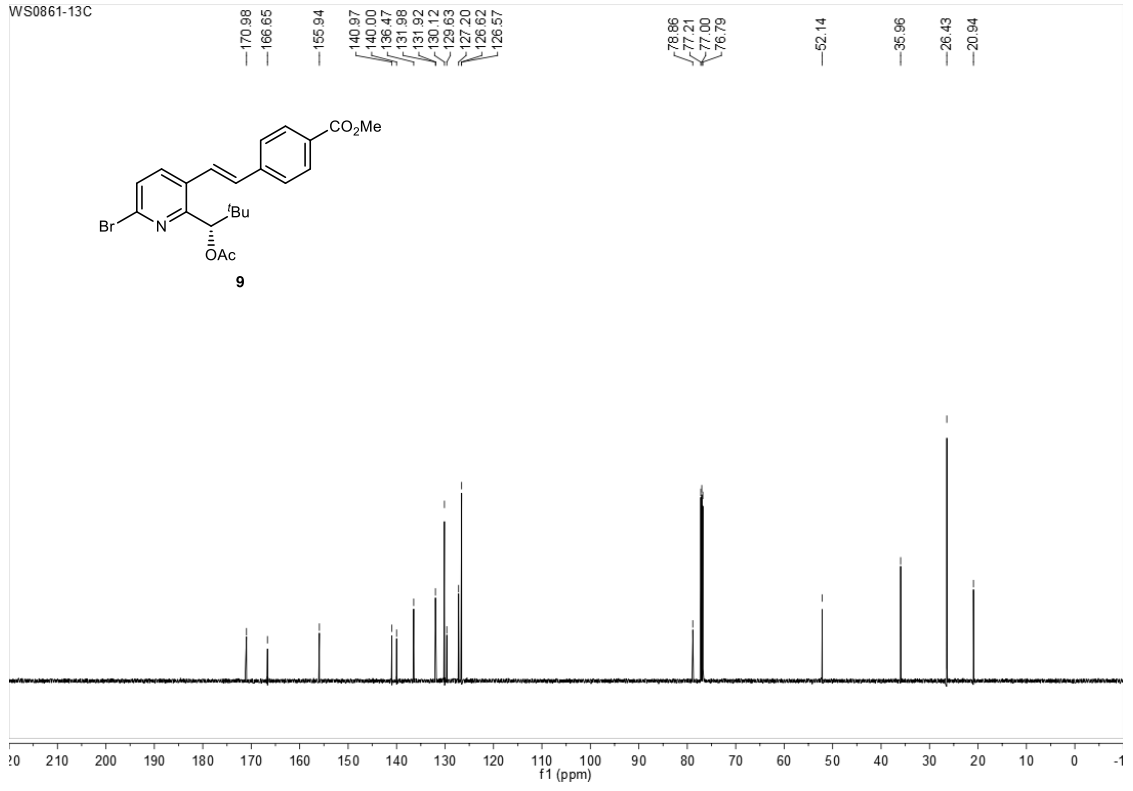


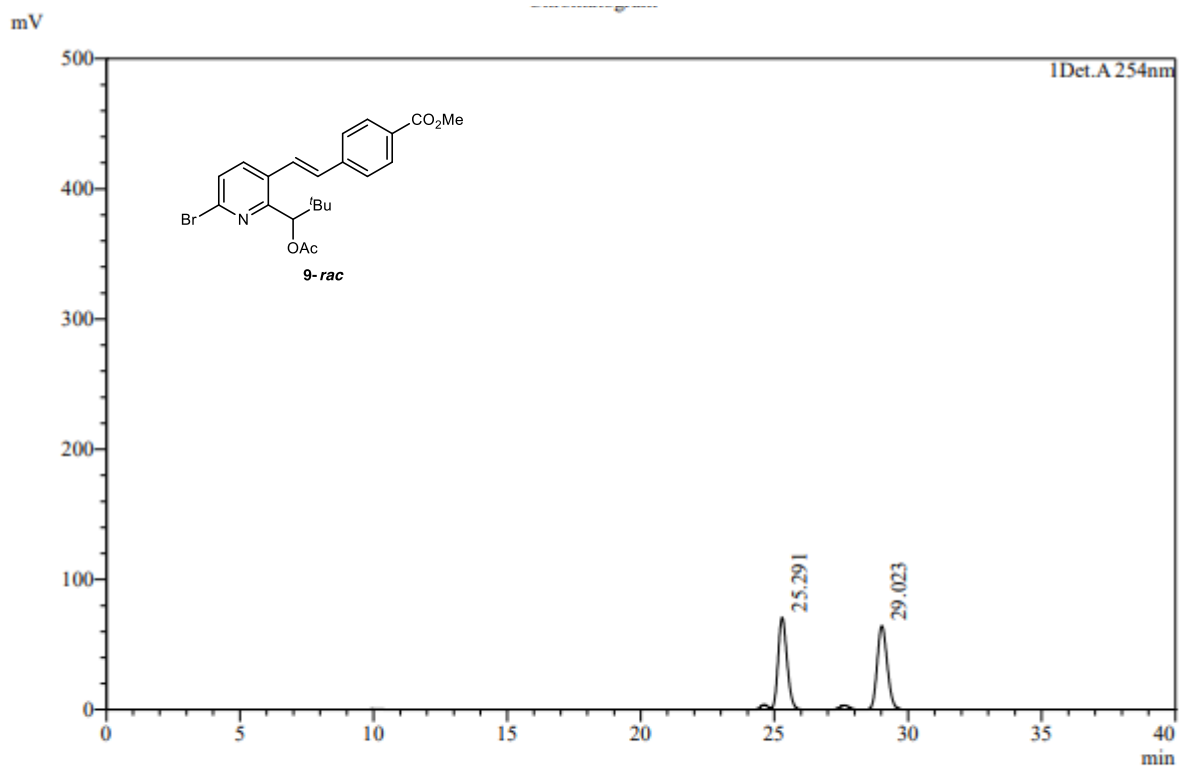
Peak Table

Peak#	Ret. Time	Area	Area%	Height	Conc.
1	20.773	7652002	100.000	353064	100.000
Total		7652002	100.000	353064	



WS0861-13C

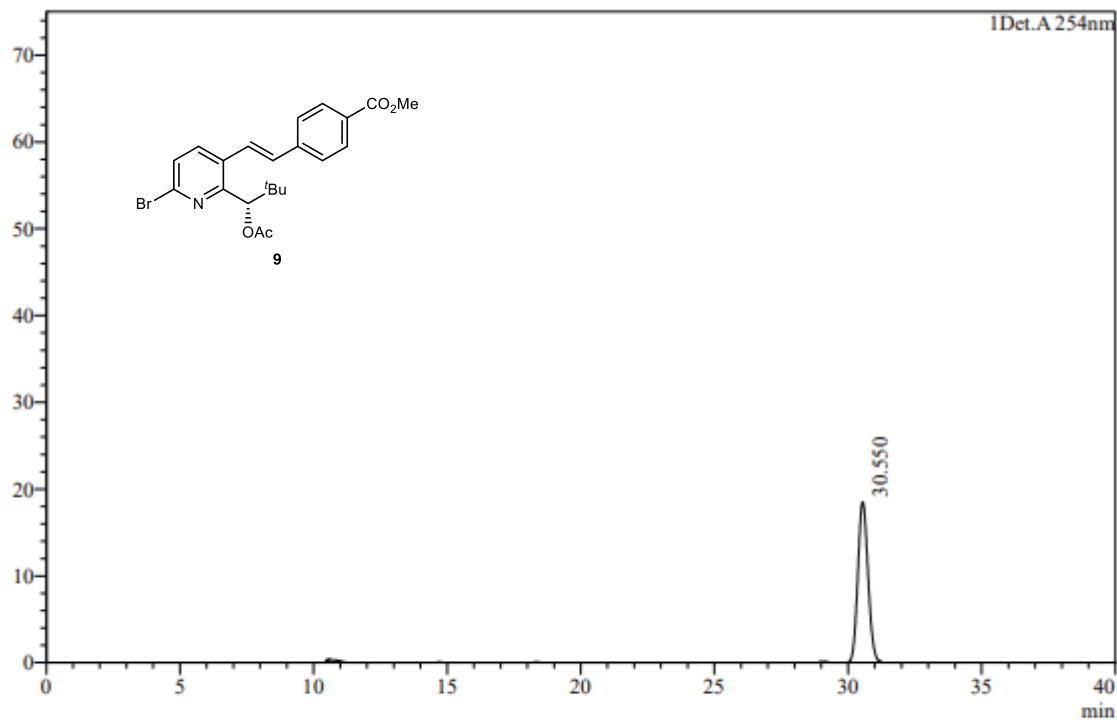




Peak Table

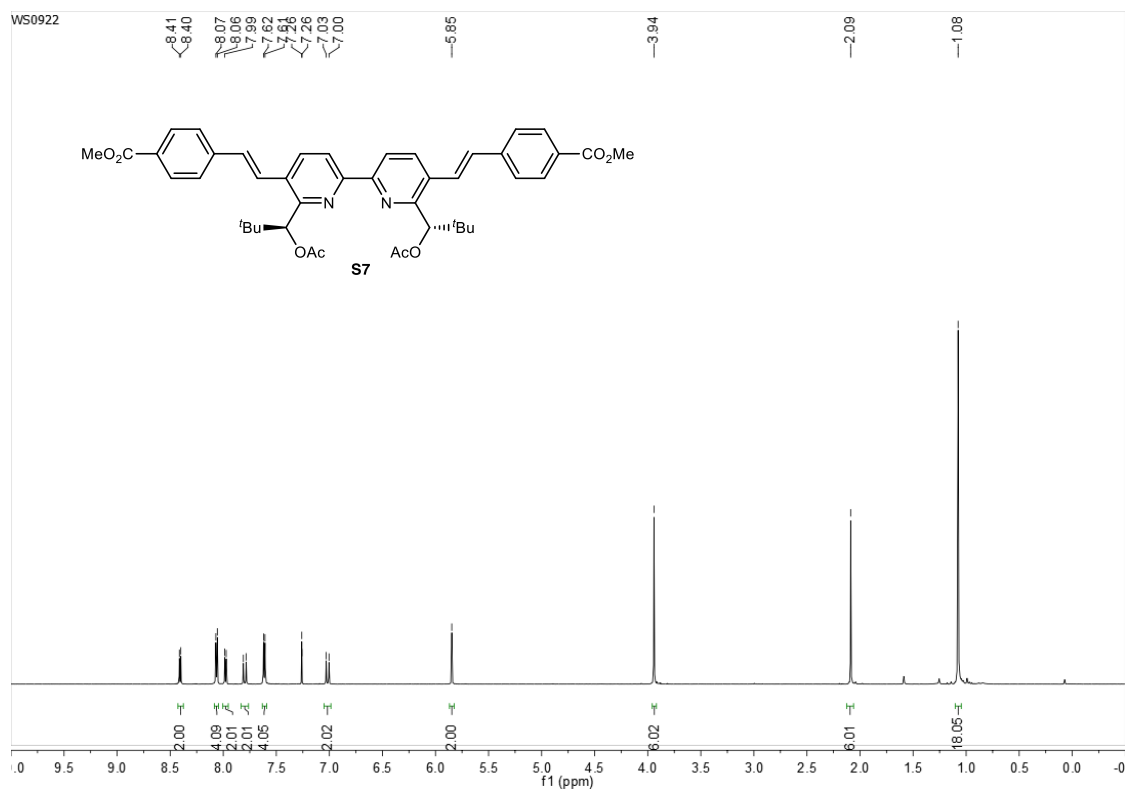
Peak#	Ret. Time	Area	Area%	Height	Conc.
1	25.291	1492350	50.380	68120	50.380
2	29.023	1469862	49.620	60884	49.620
Total		2962212	100.000	129004	

mV

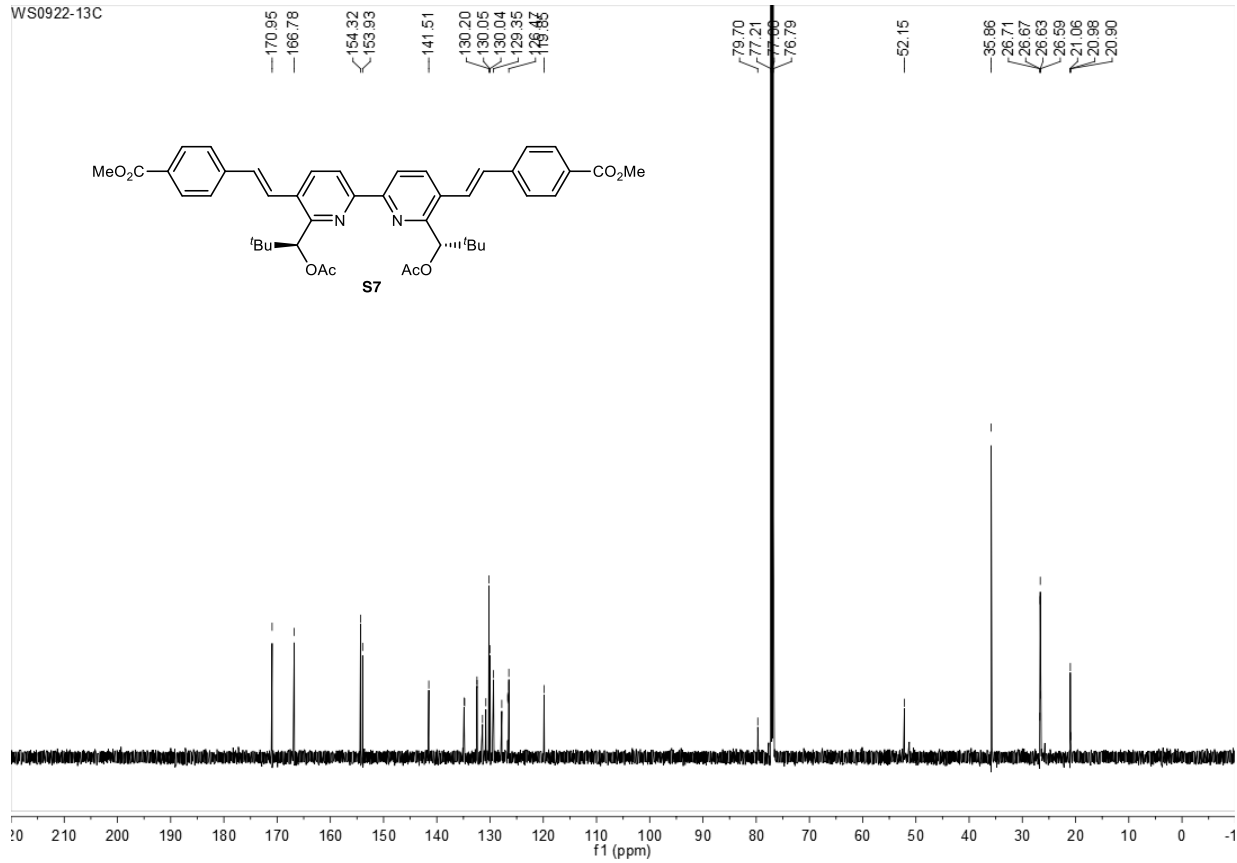


Peak Table

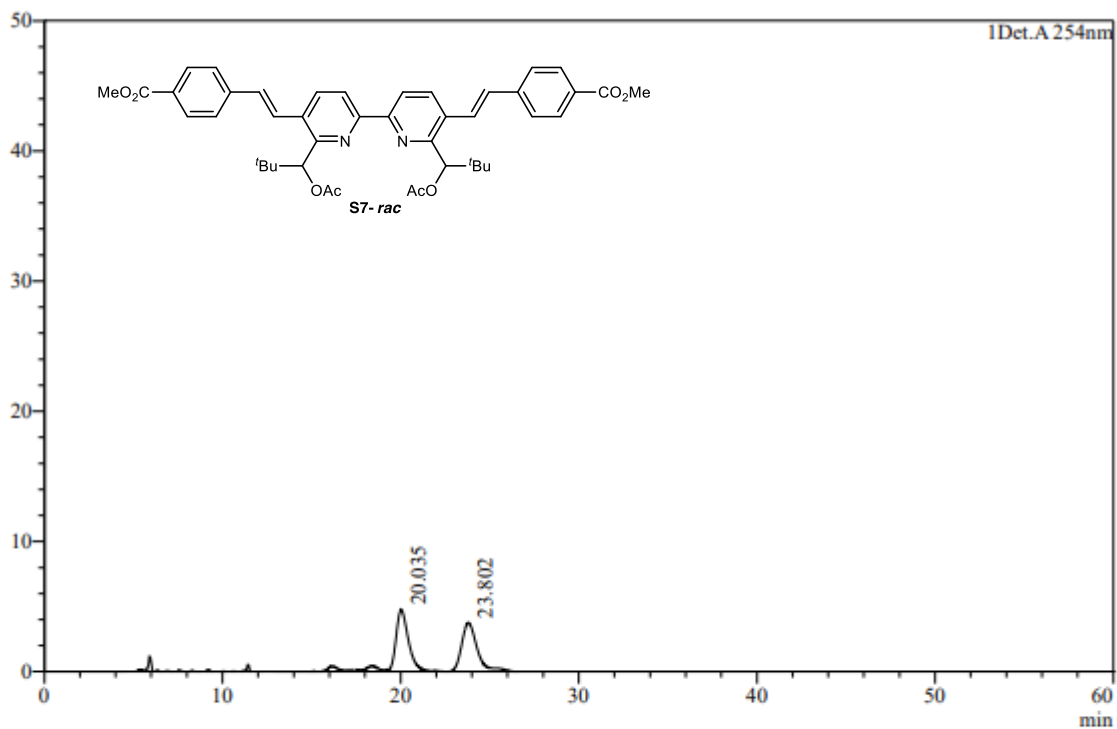
Peak#	Ret. Time	Area	Area%	Height	Conc.
1	30.550	494087	100.000	18549	100.000
Total		494087	100.000	18549	



WS0922-13C

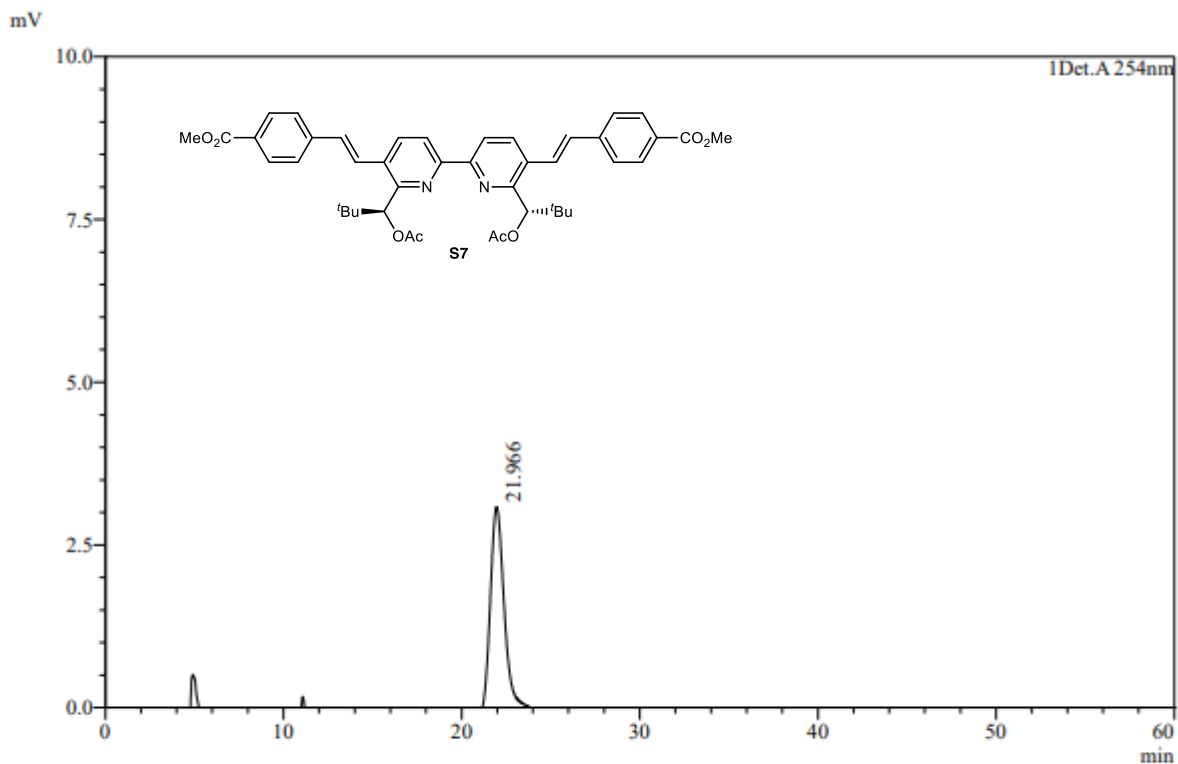


mV



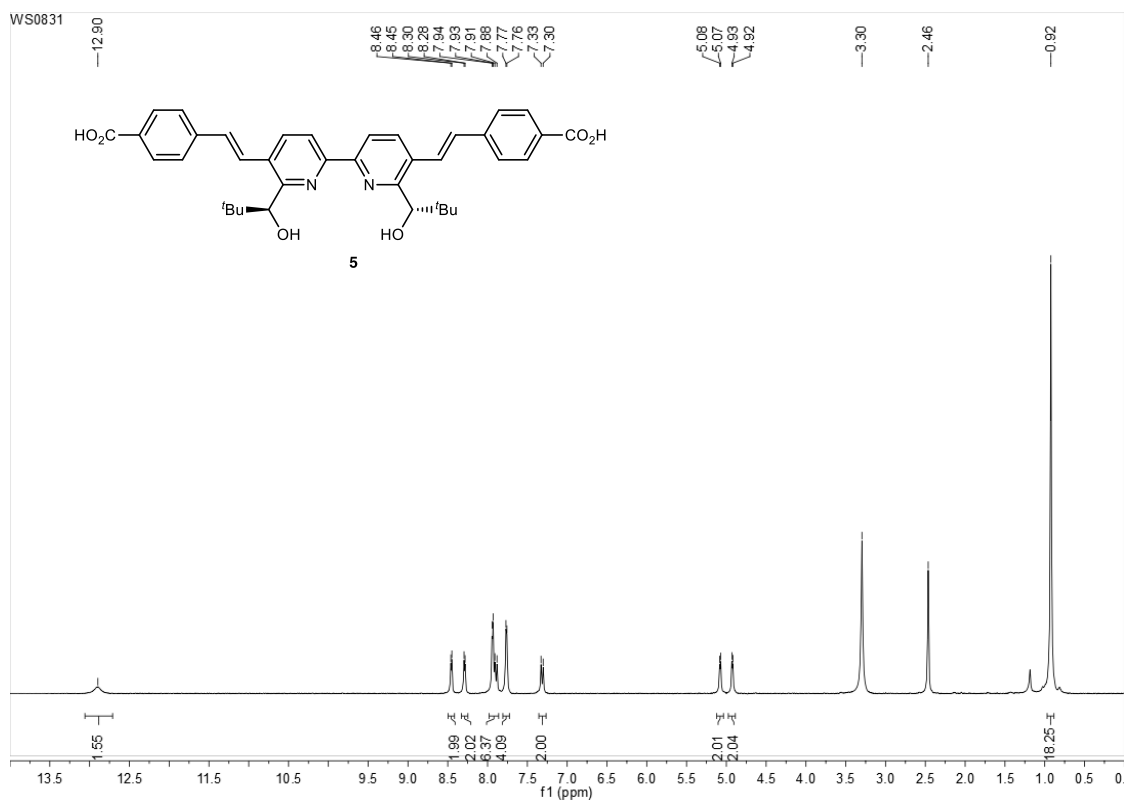
Peak Table

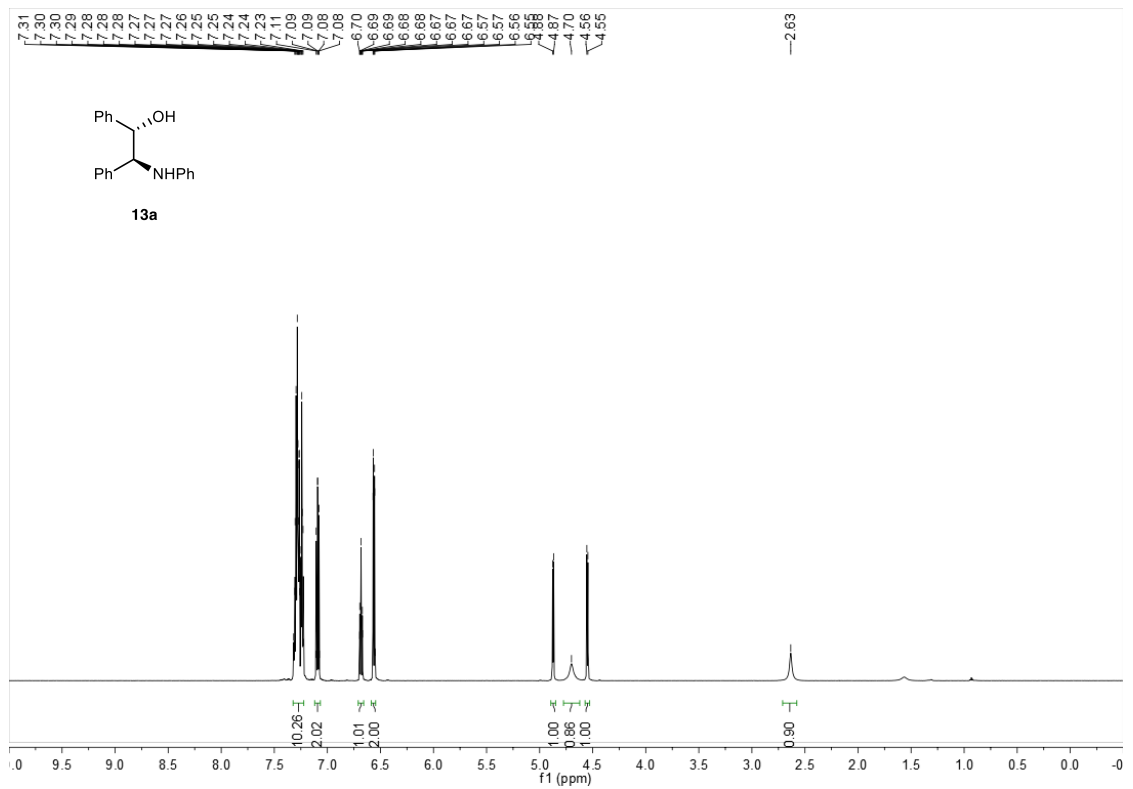
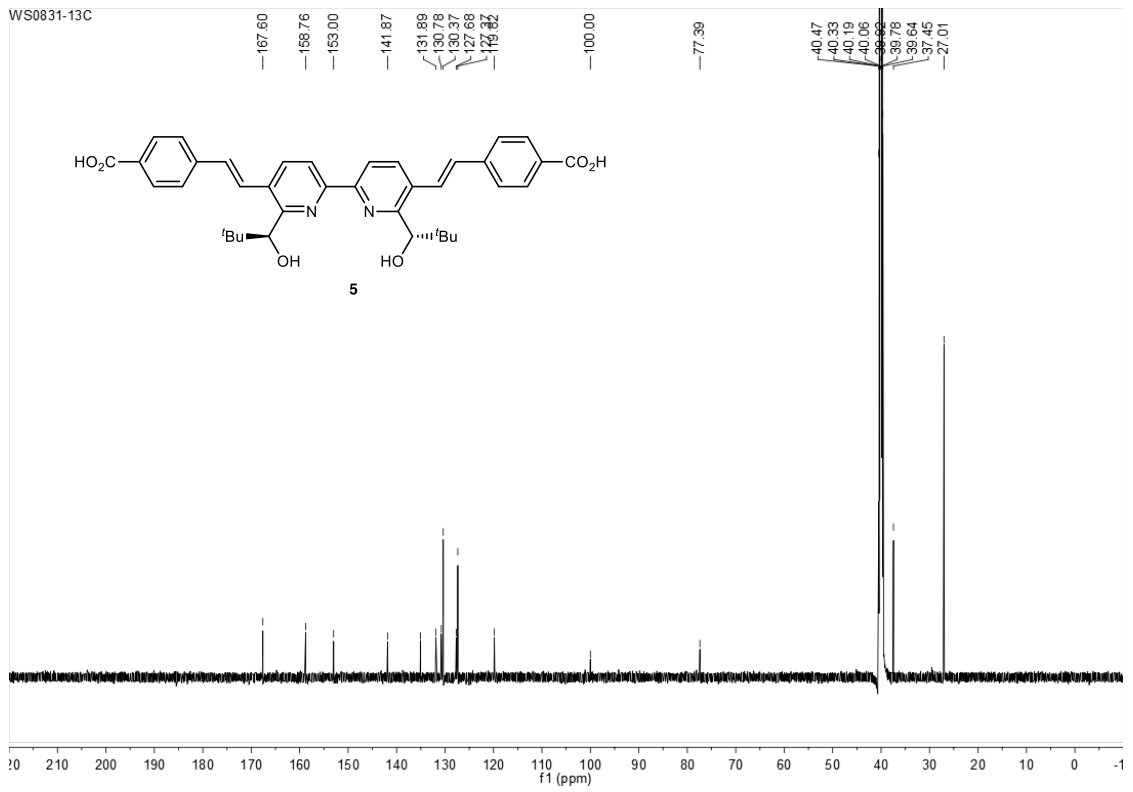
Peak#	Ret. Time	Area	Area%	Height	Conc.
1	20.035	197057	50.177	4465	50.177
2	23.802	195664	49.823	3602	49.823
Total		392721	100.000	8067	

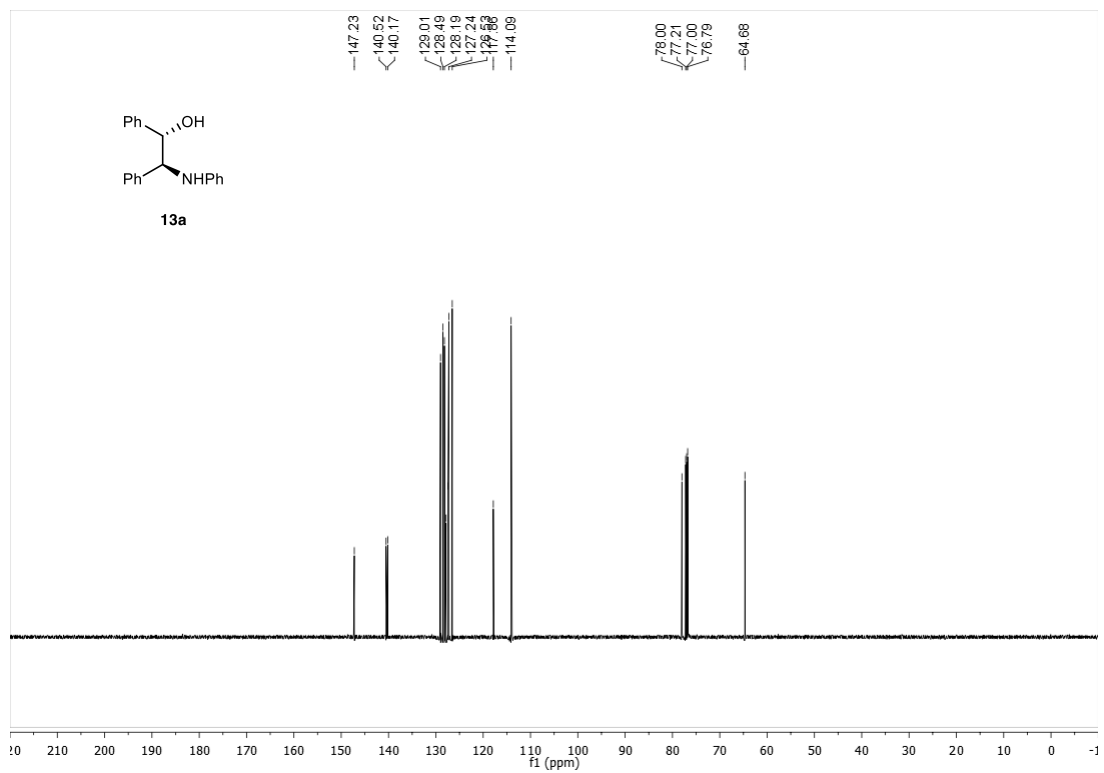


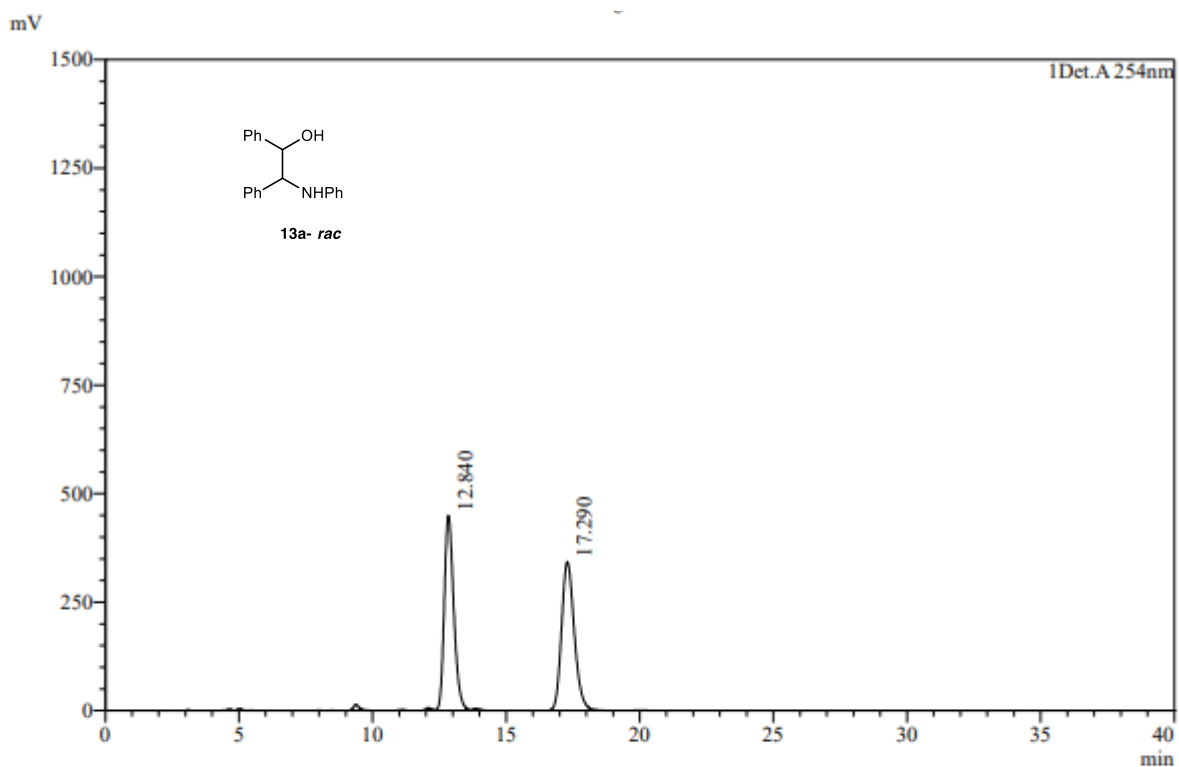
Peak Table

Peak#	Ret. Time	Area	Area%	Height	Conc.
1	21.966	181904	100.000	3199	100.000
Total		181904	100.000	3199	



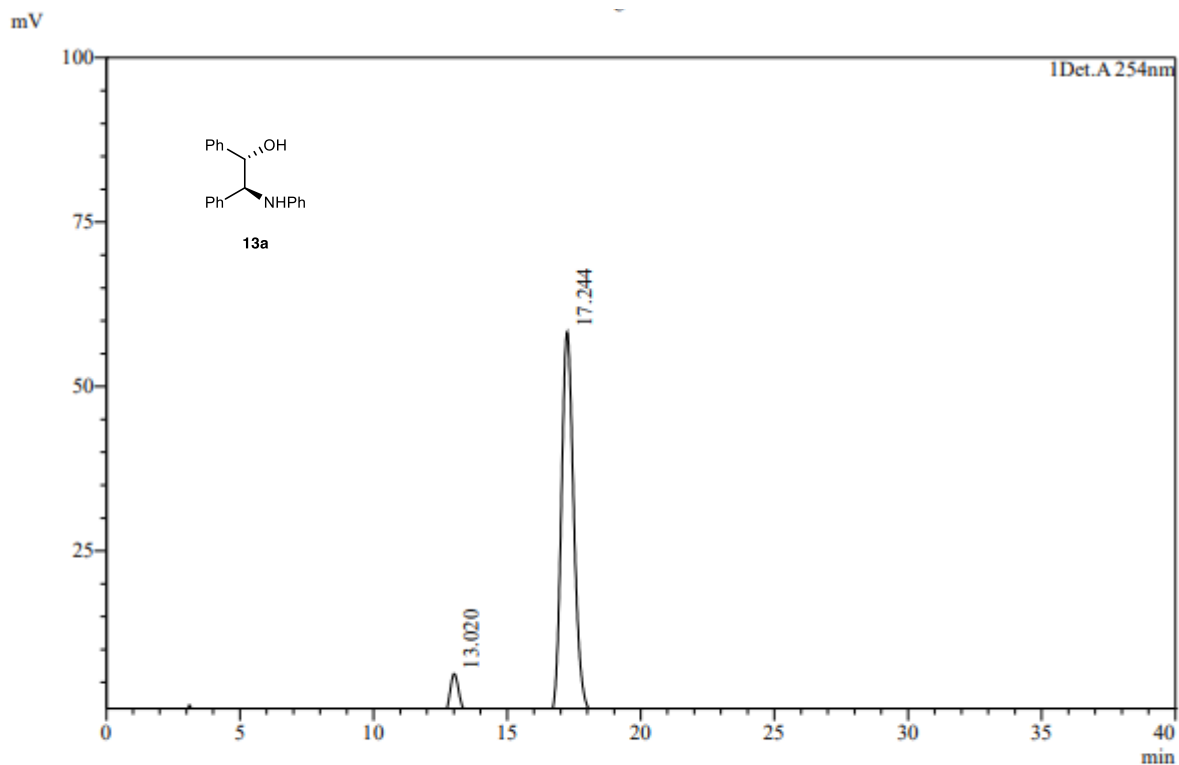






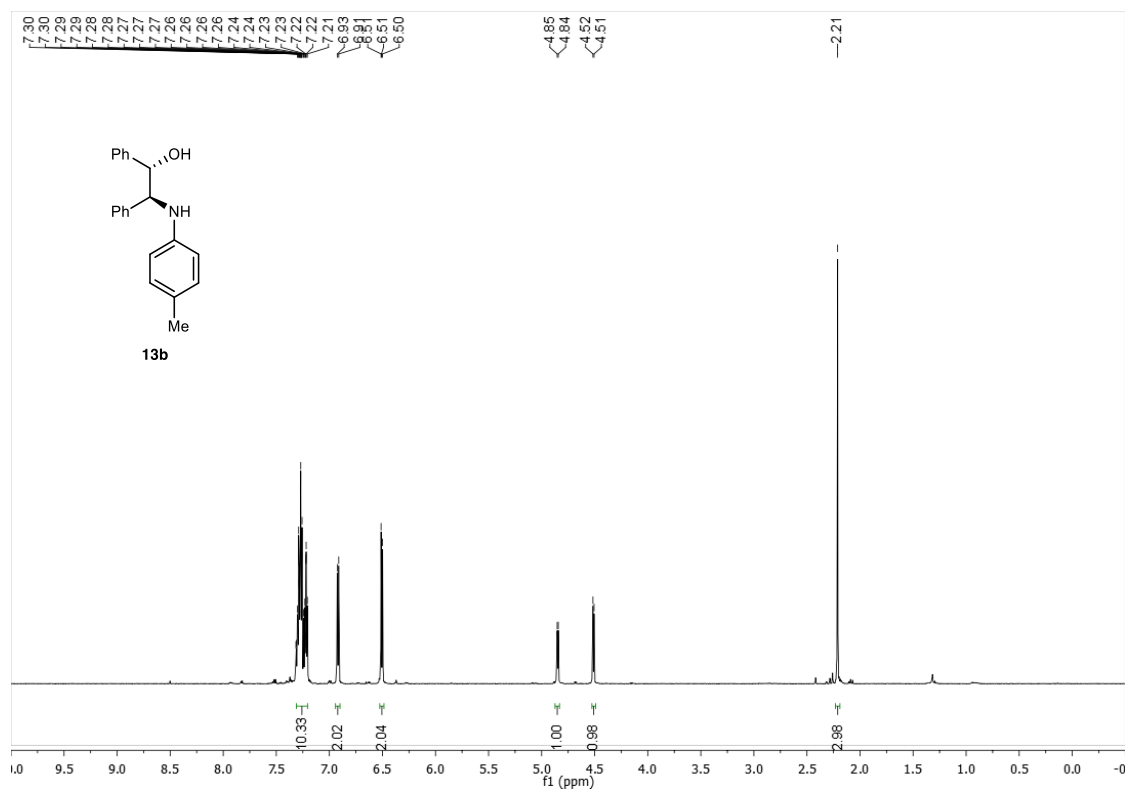
Peak Table

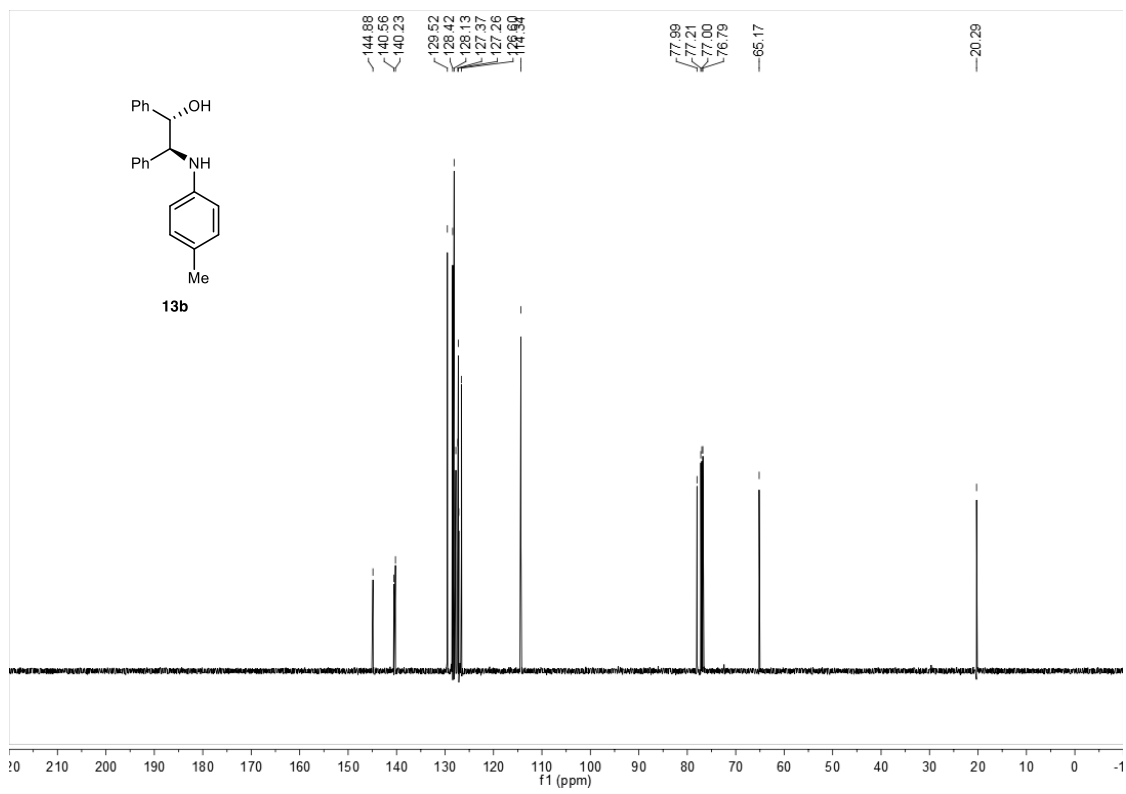
Peak#	Ret. Time	Area	Area%	Height	Conc.
1	12.840	10910629	50.001	446897	50.001
2	17.290	10910142	49.999	338205	49.999
Total		21820771	100.000	785102	

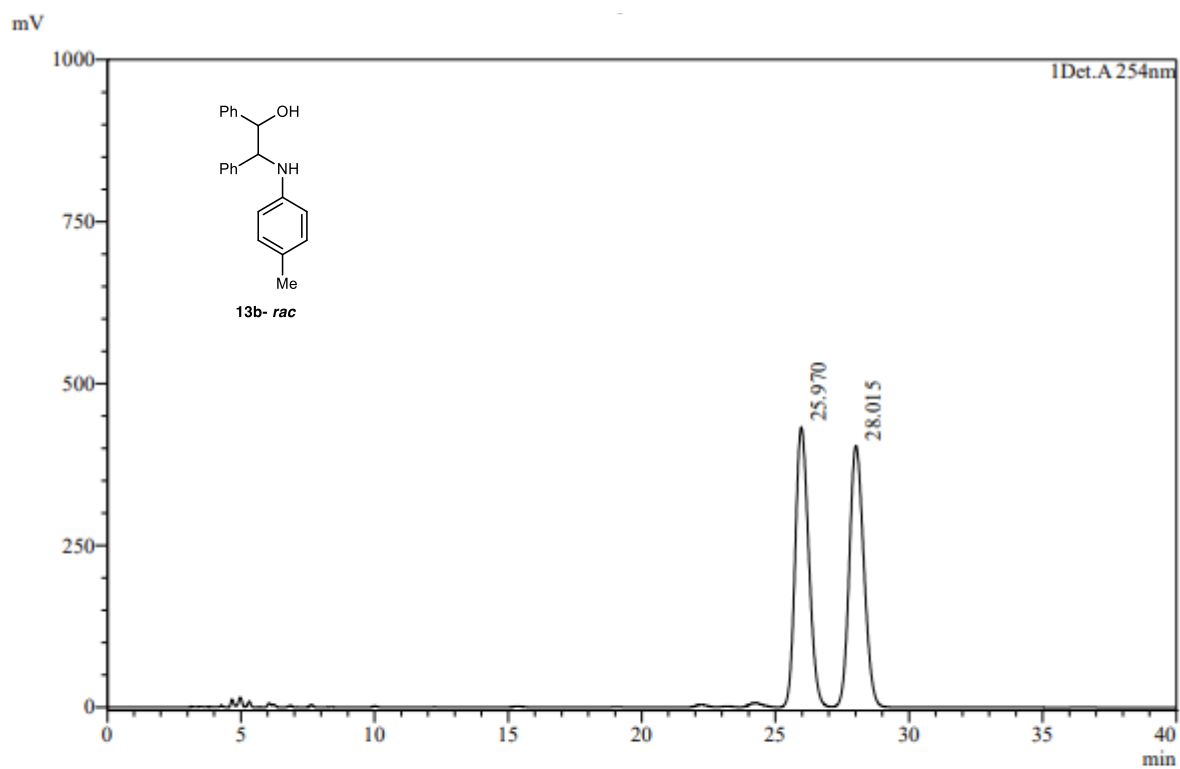


Peak Table

Peak#	Ret. Time	Area	Area%	Height	Conc.
1	13.020	134305	6.618	6012	6.618
2	17.244	1895046	93.382	58204	93.382
Total		2029351	100.000	64216	



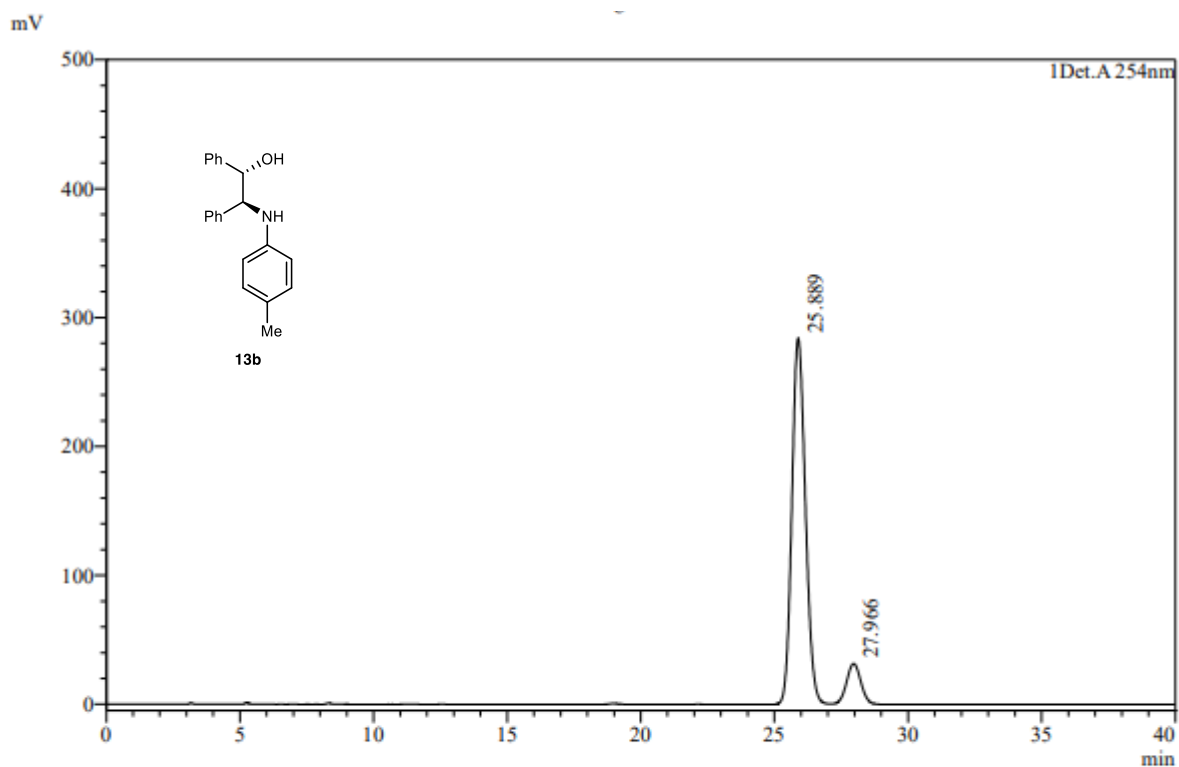




Peak Table

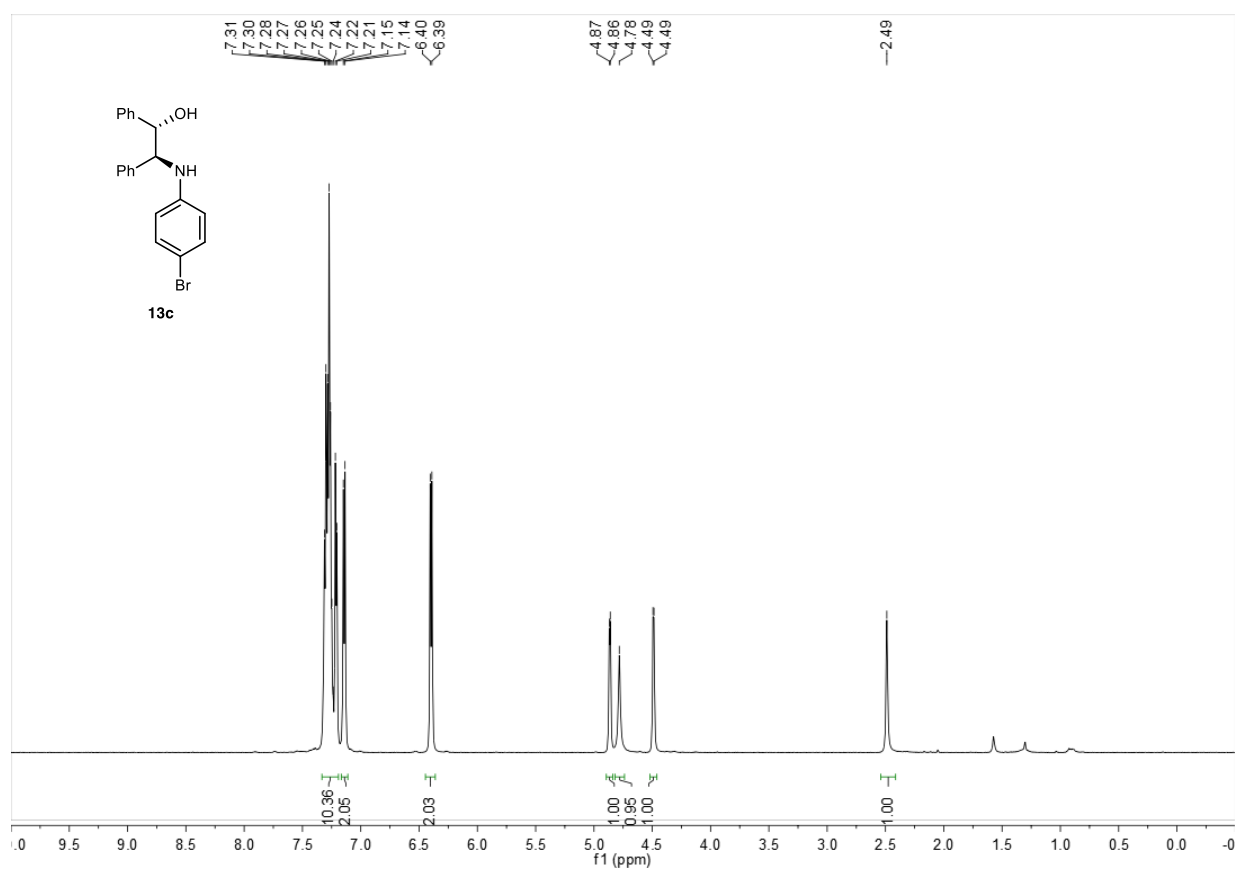
Det.A 254nm

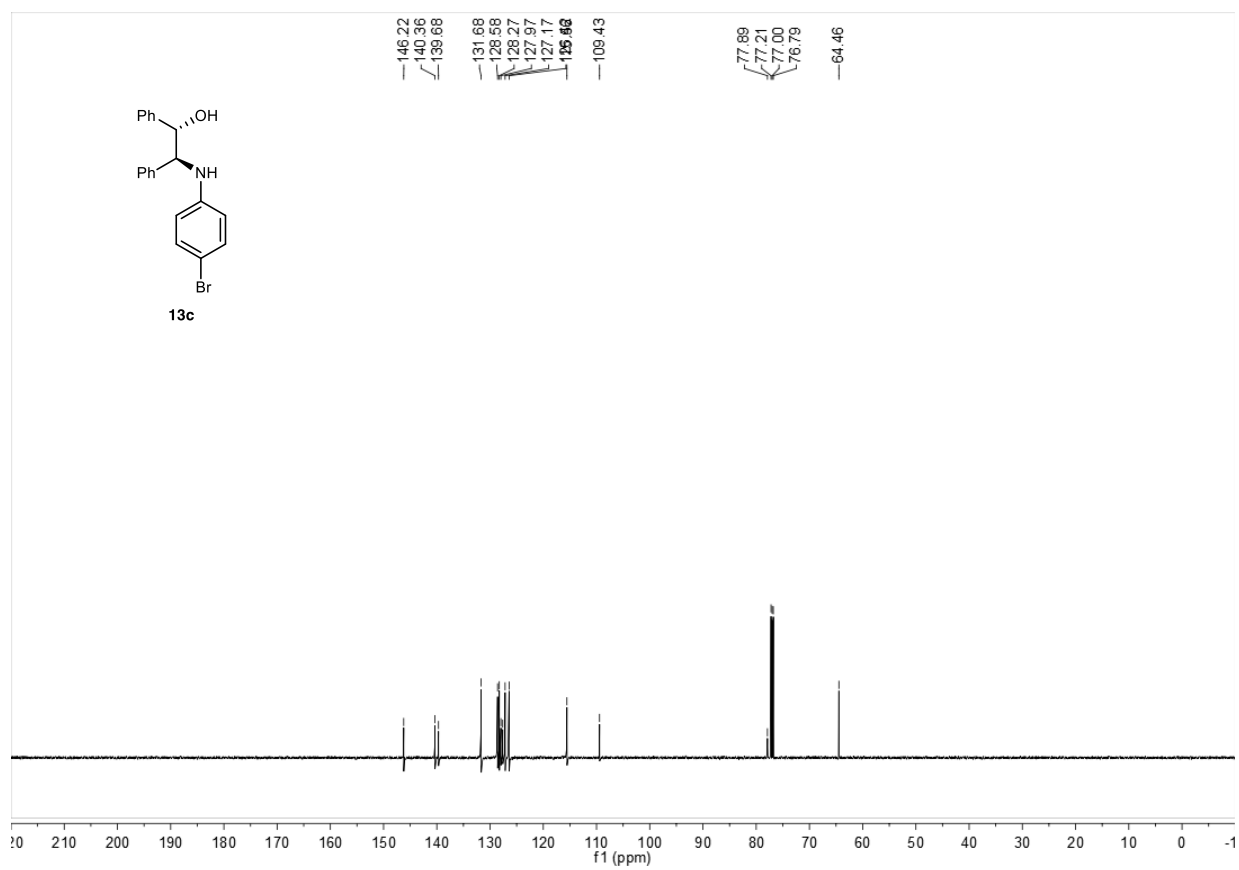
Peak#	Ret. Time	Area	Area%	Height	Conc.
1	25.970	15087690	49.819	431086	49.819
2	28.015	15197150	50.181	403049	50.181
Total		30284840	100.000	834134	

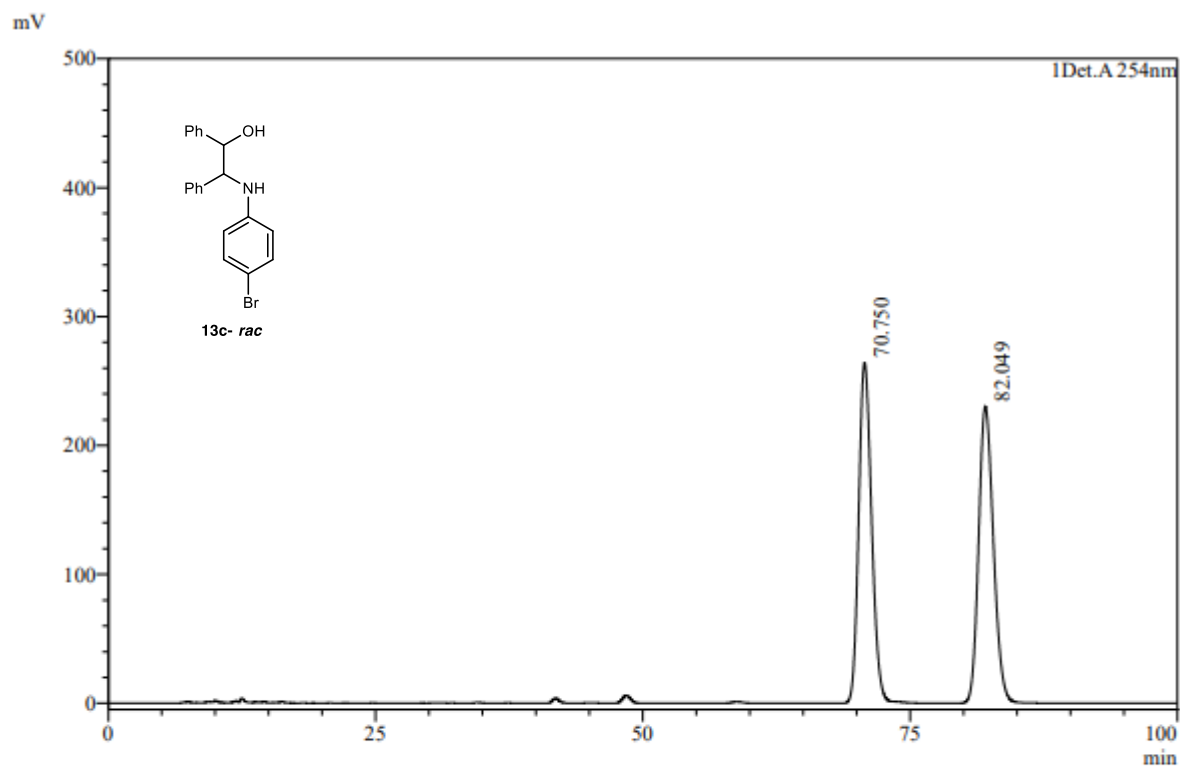


Peak Table

Peak#	Ret. Time	Area	Area%	Height	Conc.
1	25.889	9848182	91.690	282695	91.690
2	27.966	892545	8.310	27809	8.310
Total		10740727	100.000	310504	



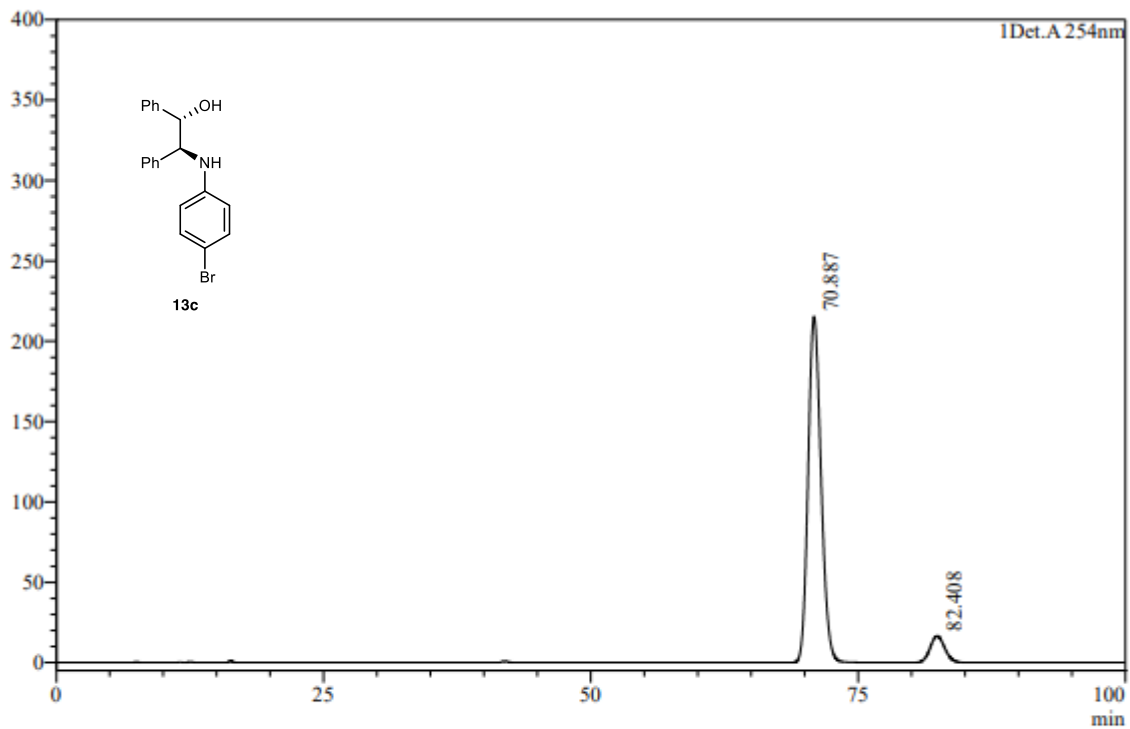




Peak Table

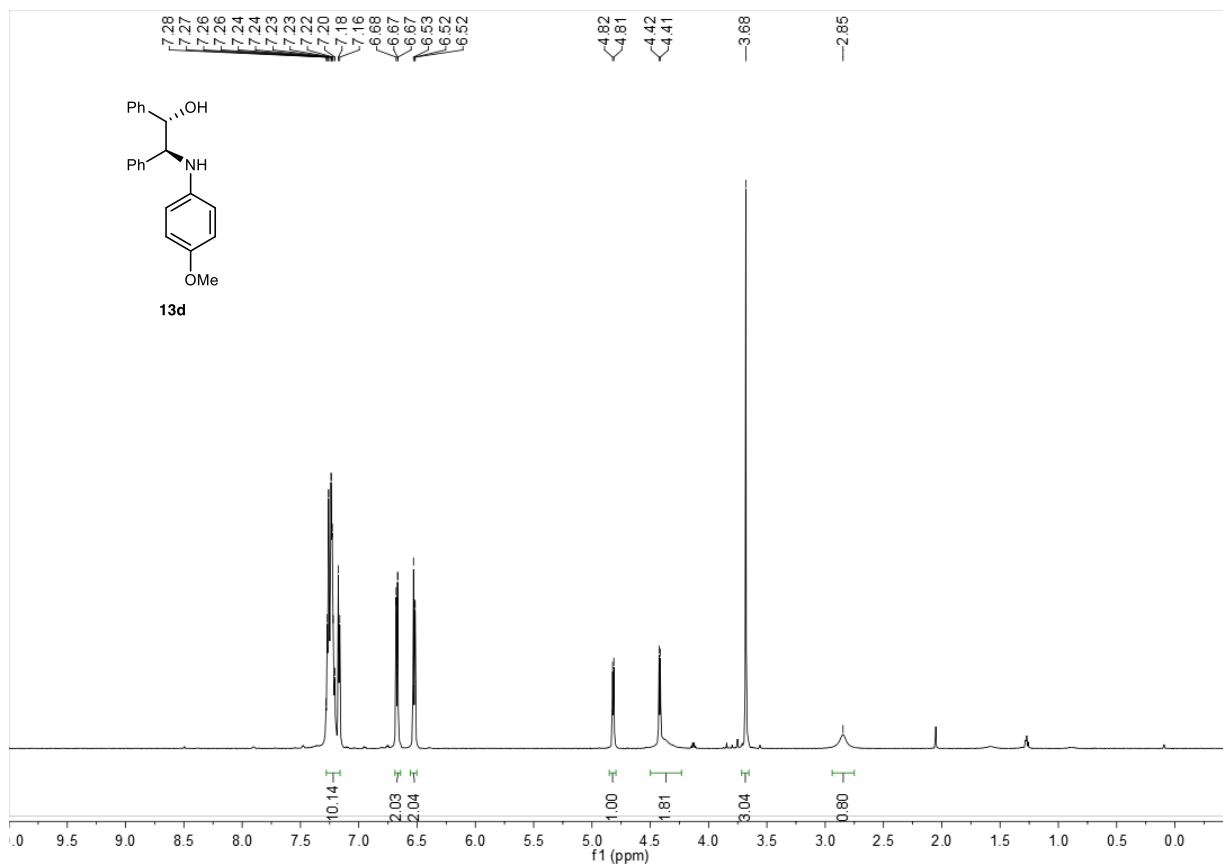
Peak#	Ret. Time	Area	Area%	Height	Conc.
1	70.750	22225974	50.087	264085	50.087
2	82.049	22148604	49.913	229850	49.913
Total		44374578	100.000	493935	

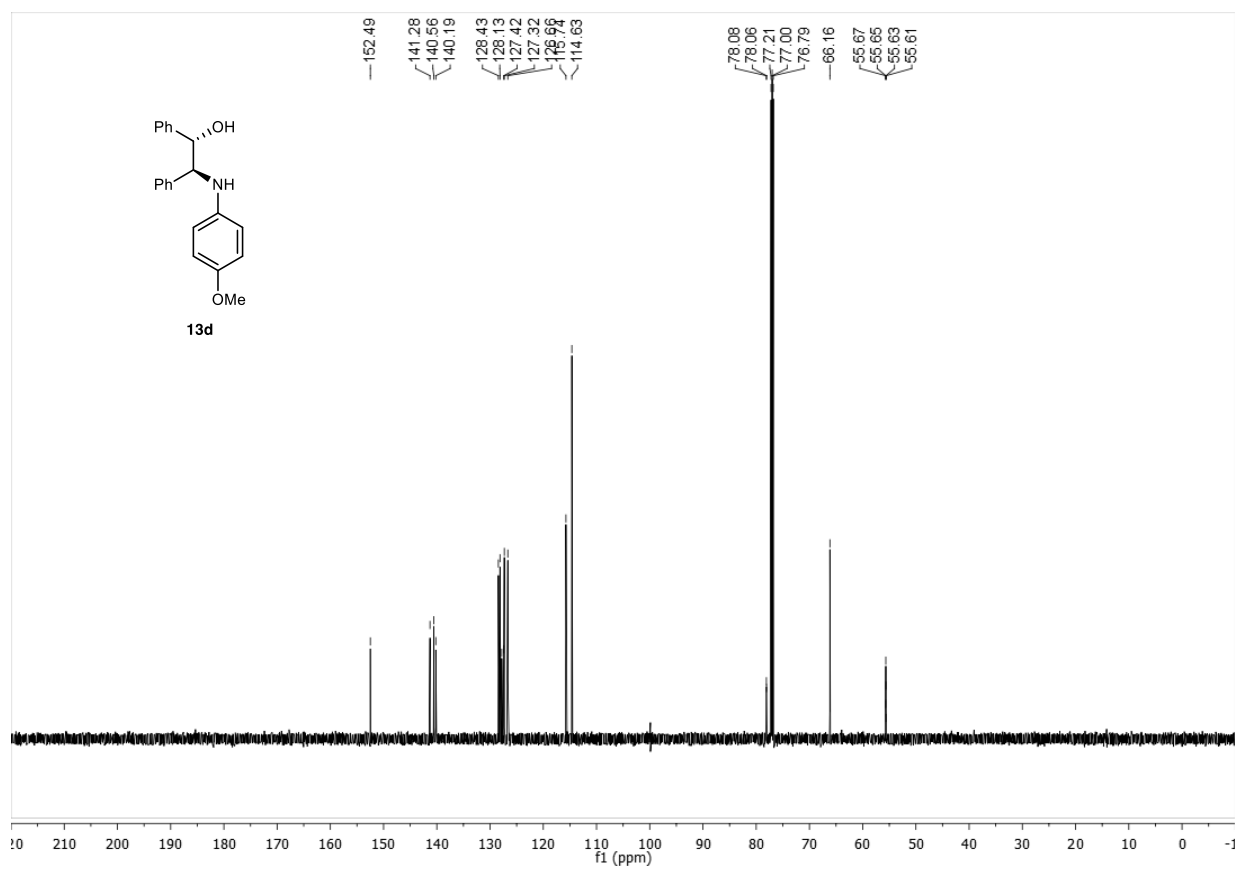
mV

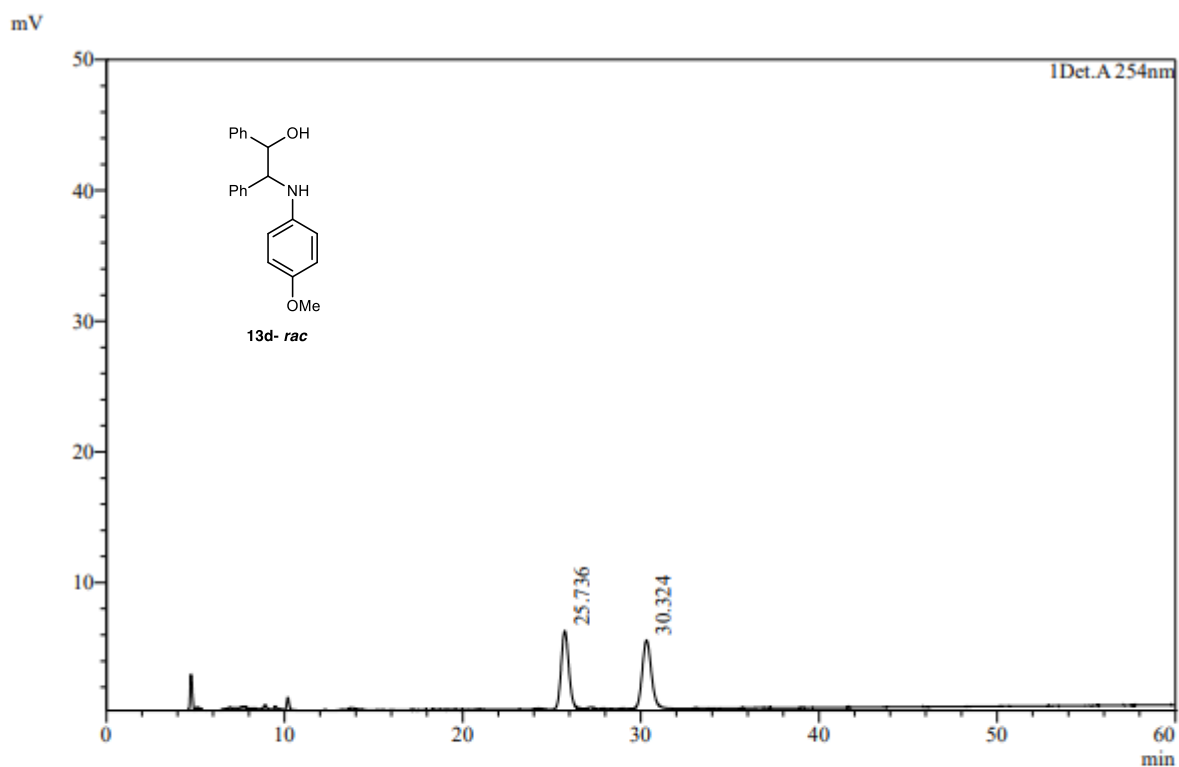


Peak Table

Peak#	Ret. Time	Area	Area%	Height	Conc.
1	70.887	18026472	92.472	214916	92.472
2	82.408	1467458	7.528	16048	7.528
Total		19493930	100.000	230964	

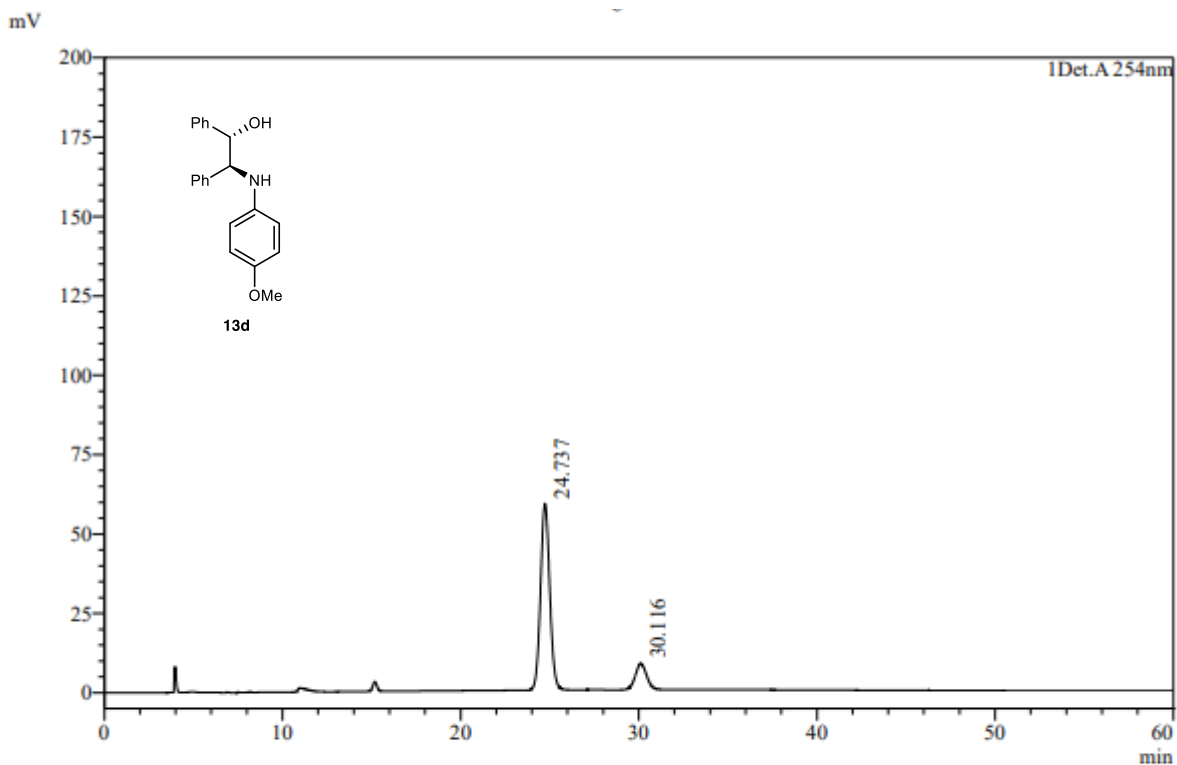






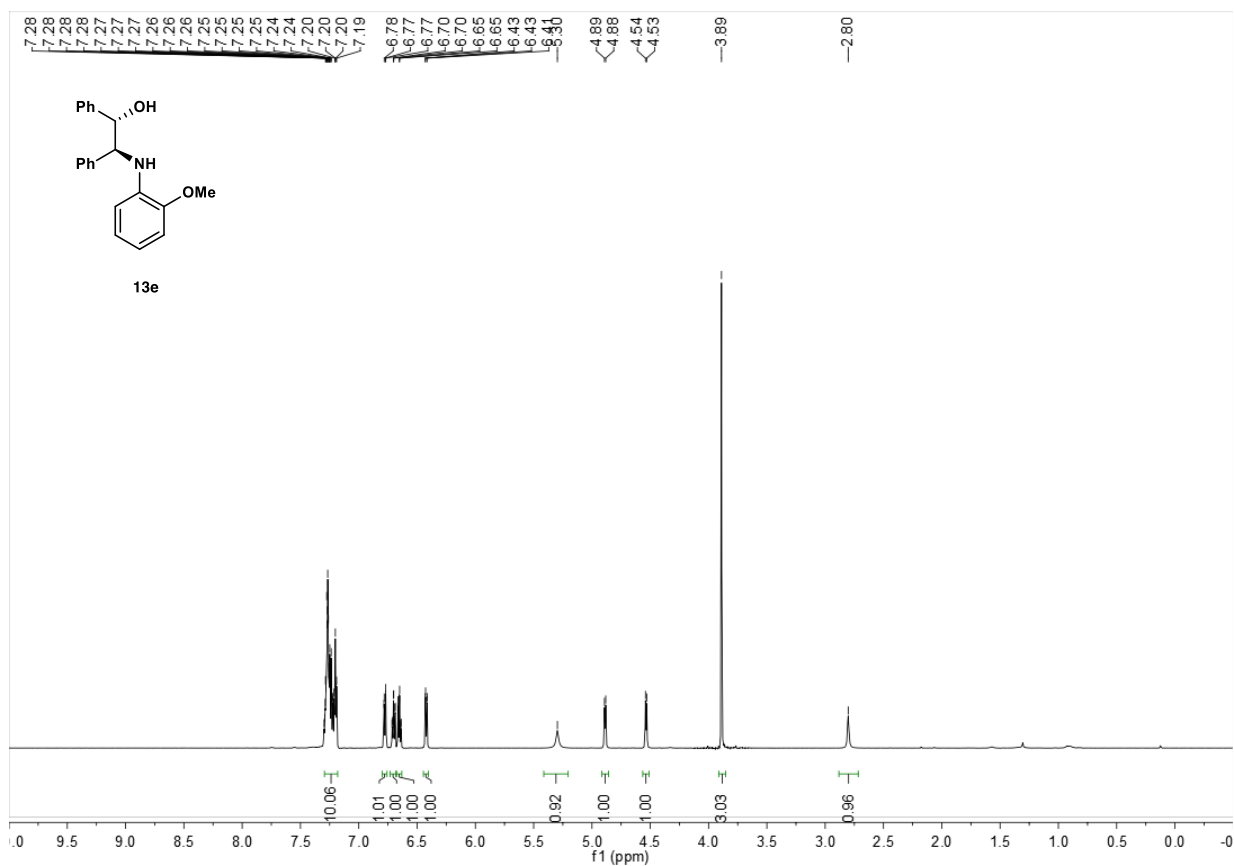
Peak Table

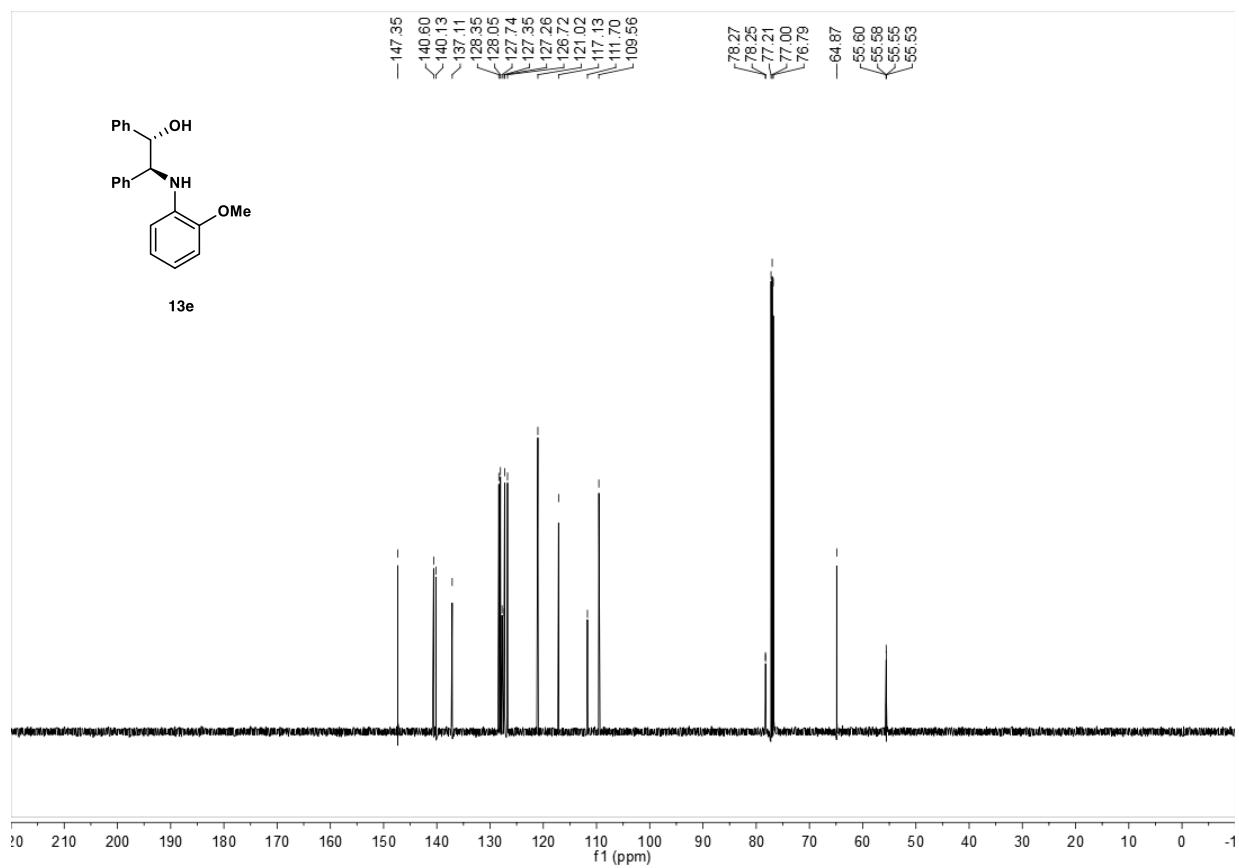
Peak#	Ret. Time	Area	Area%	Height	Conc.
1	25.736	178979	49.273	5986	49.273
2	30.324	184262	50.727	5199	50.727
Total		363241	100.000	11184	

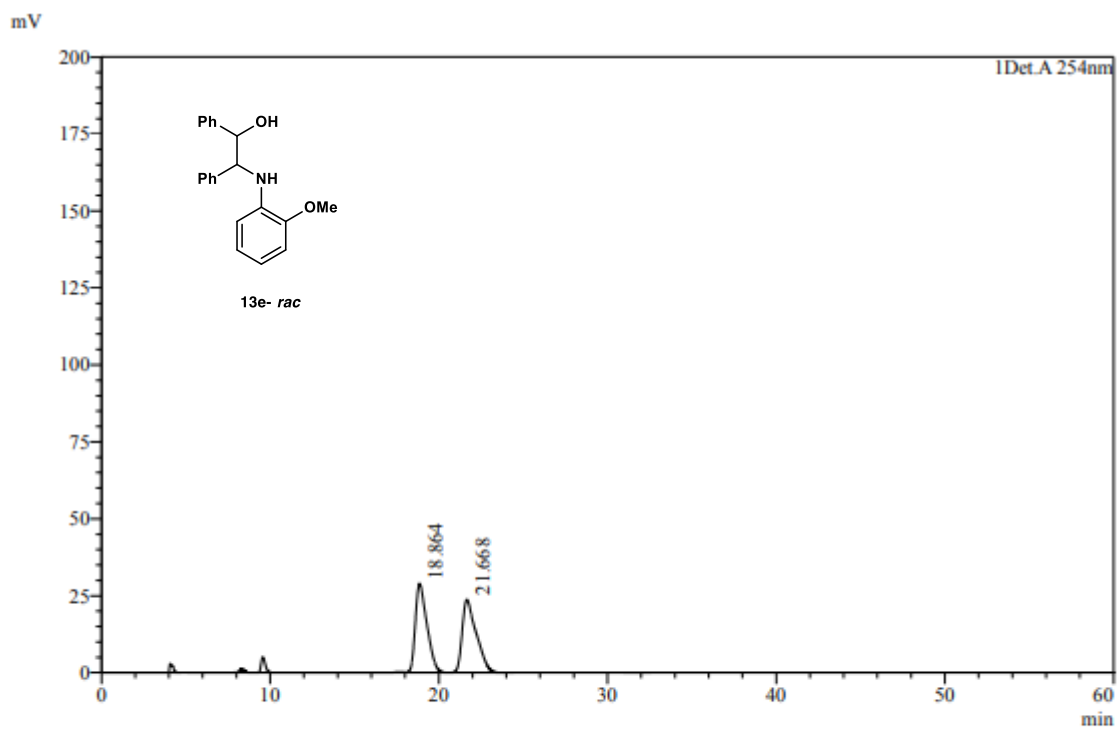


Peak Table

Peak#	Ret. Time	Area	Area%	Height	Conc.
1	24.737	2107024	86.768	58687	86.768
2	30.116	321314	13.232	7770	13.232
Total		2428338	100.000	66457	



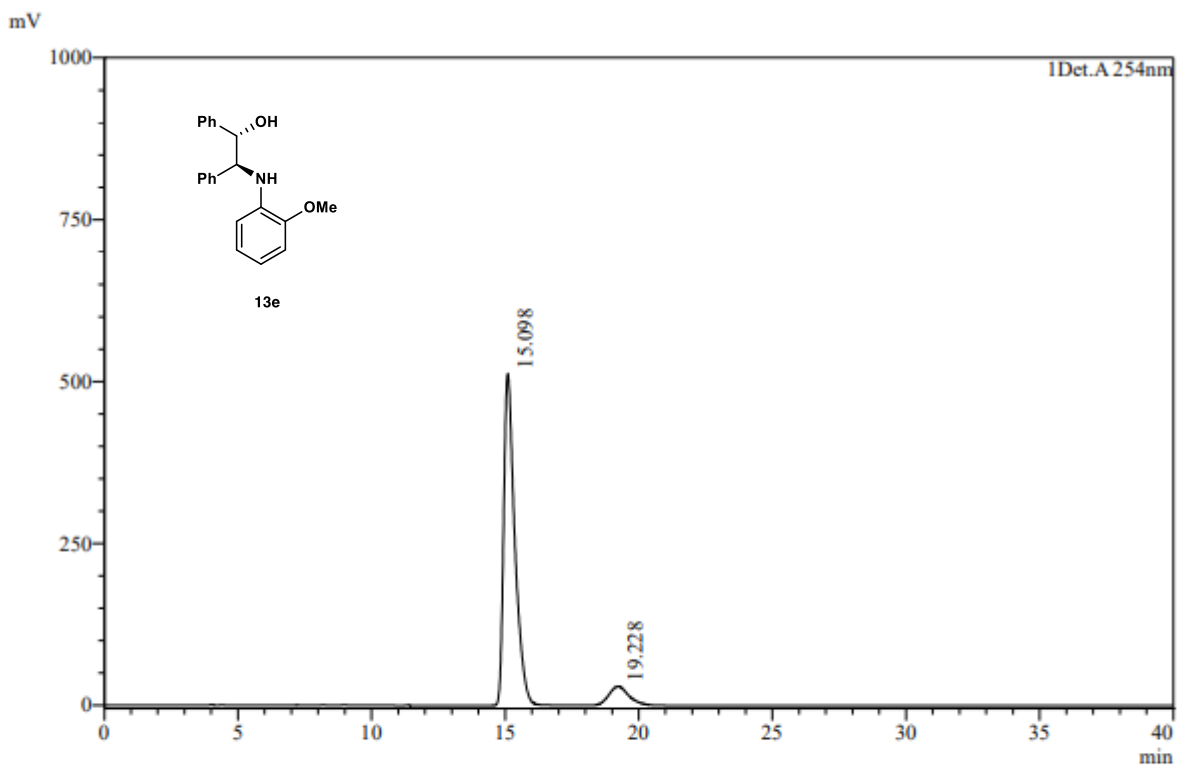




Peak Table

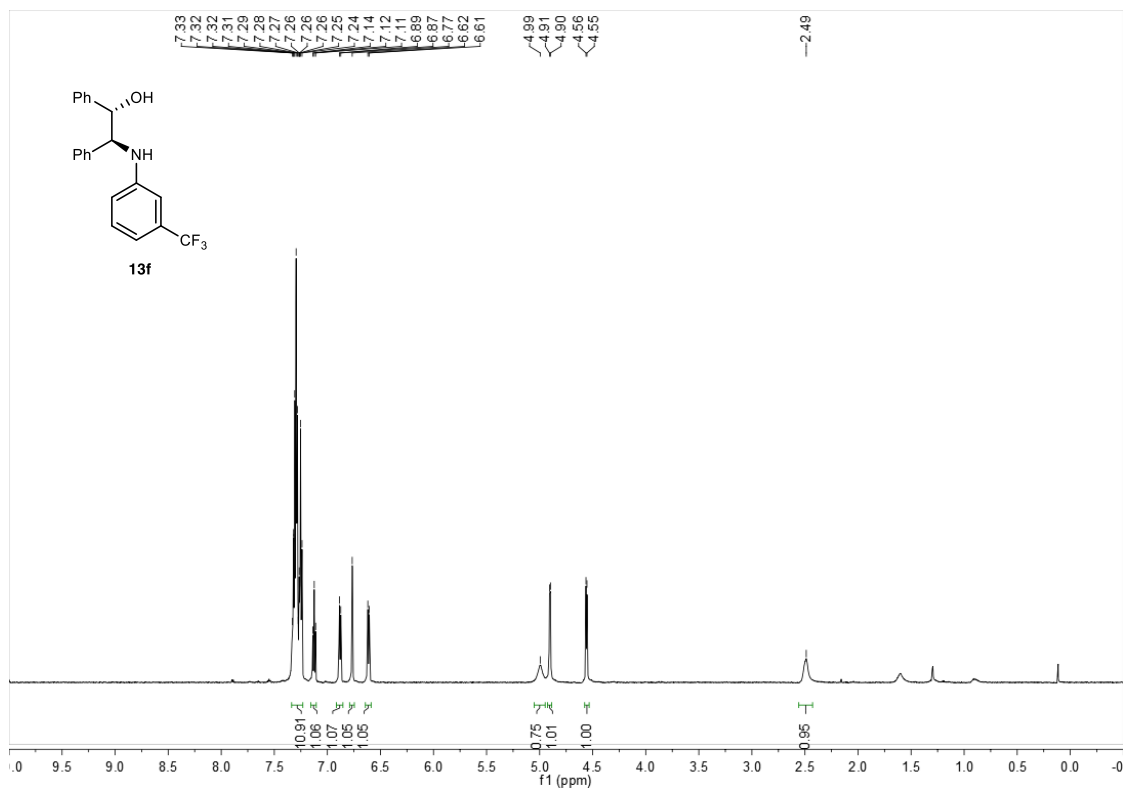
Det.A 254nm

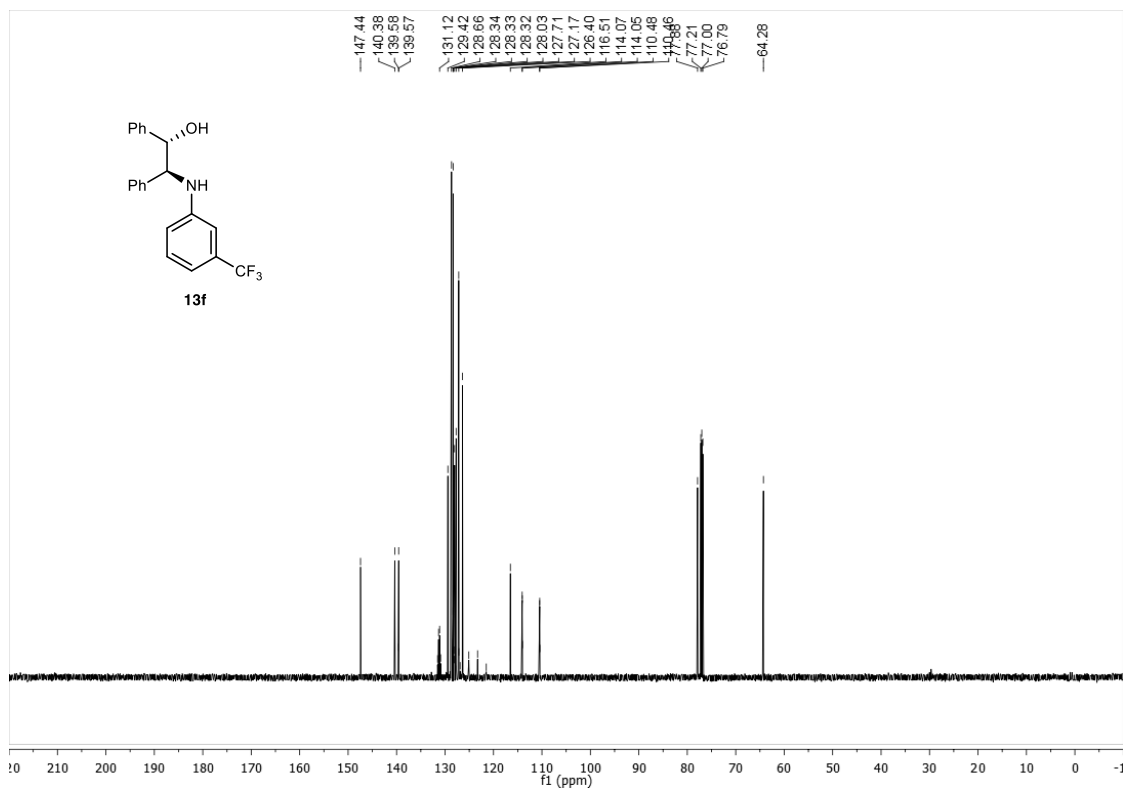
Peak#	Ret. Time	Area	Area%	Height	Conc.
1	18.864	1375099	49.841	28756	49.841
2	21.668	1383894	50.159	23734	50.159
Total		2758993	100.000	52491	

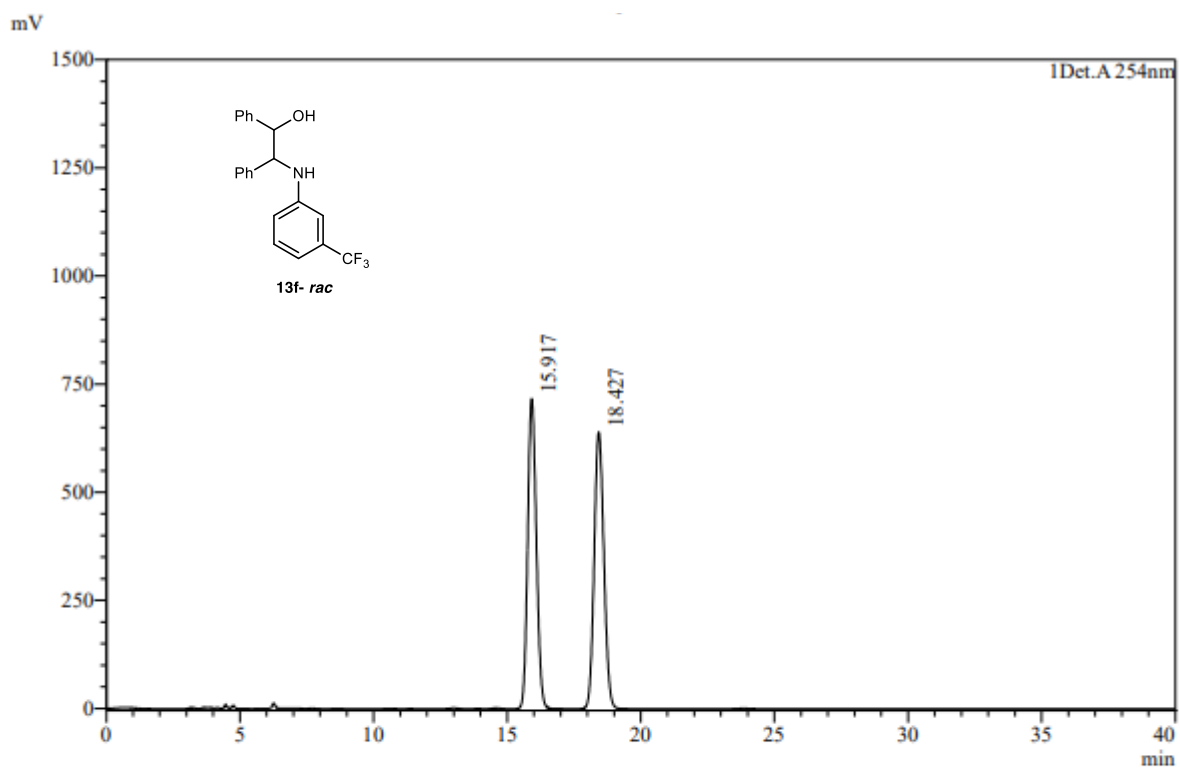


Peak Table

Peak#	Ret. Time	Area	Area%	Height	Conc.
1	15.098	14821632	91.387	511862	91.387
2	19.228	1396955	8.613	28287	8.613
Total		16218587	100.000	540148	



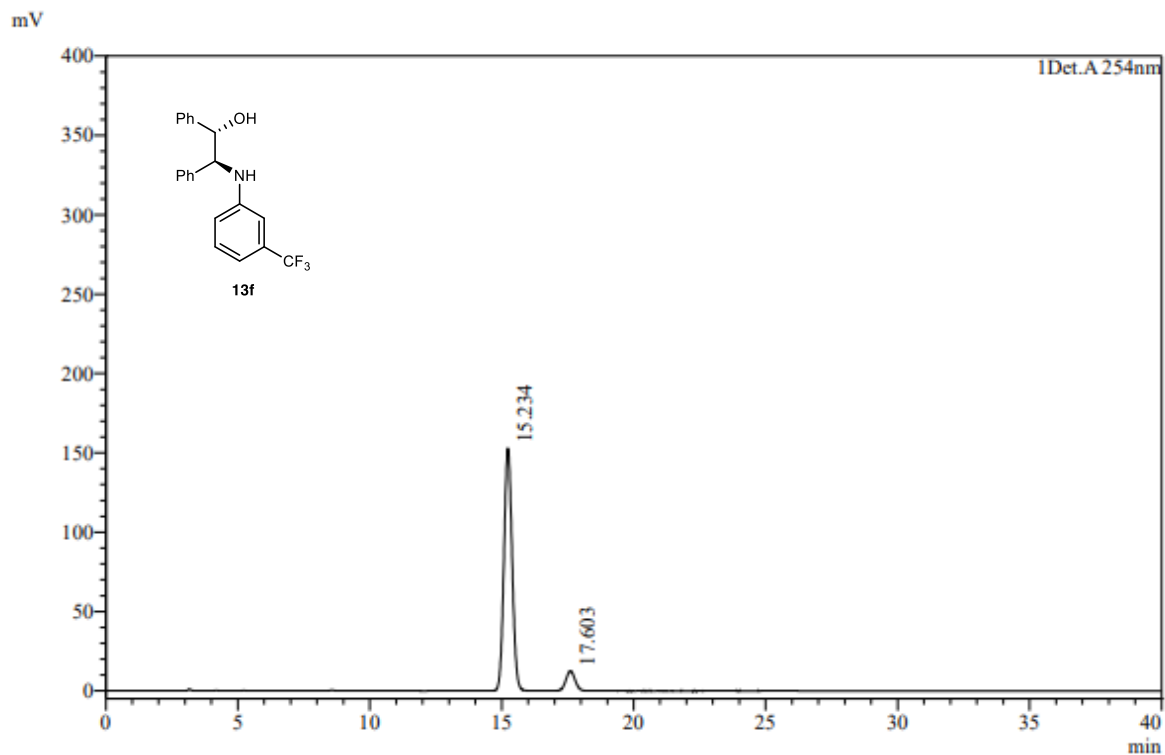




Peak Table

Det.A 254nm

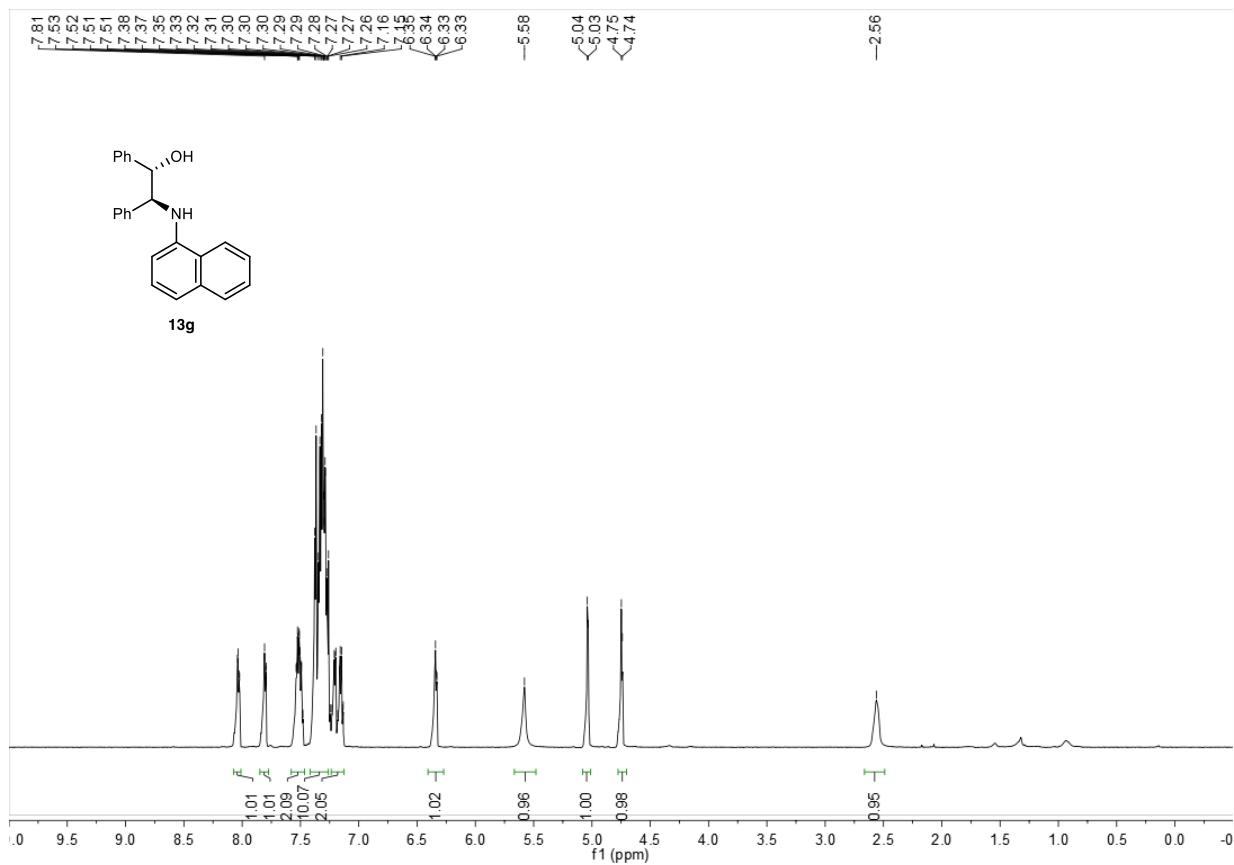
Peak#	Ret. Time	Area	Area%	Height	Conc.
1	15.917	16150709	49.935	716324	49.935
2	18.427	16192635	50.065	639652	50.065
Total		32343344	100.000	1355977	

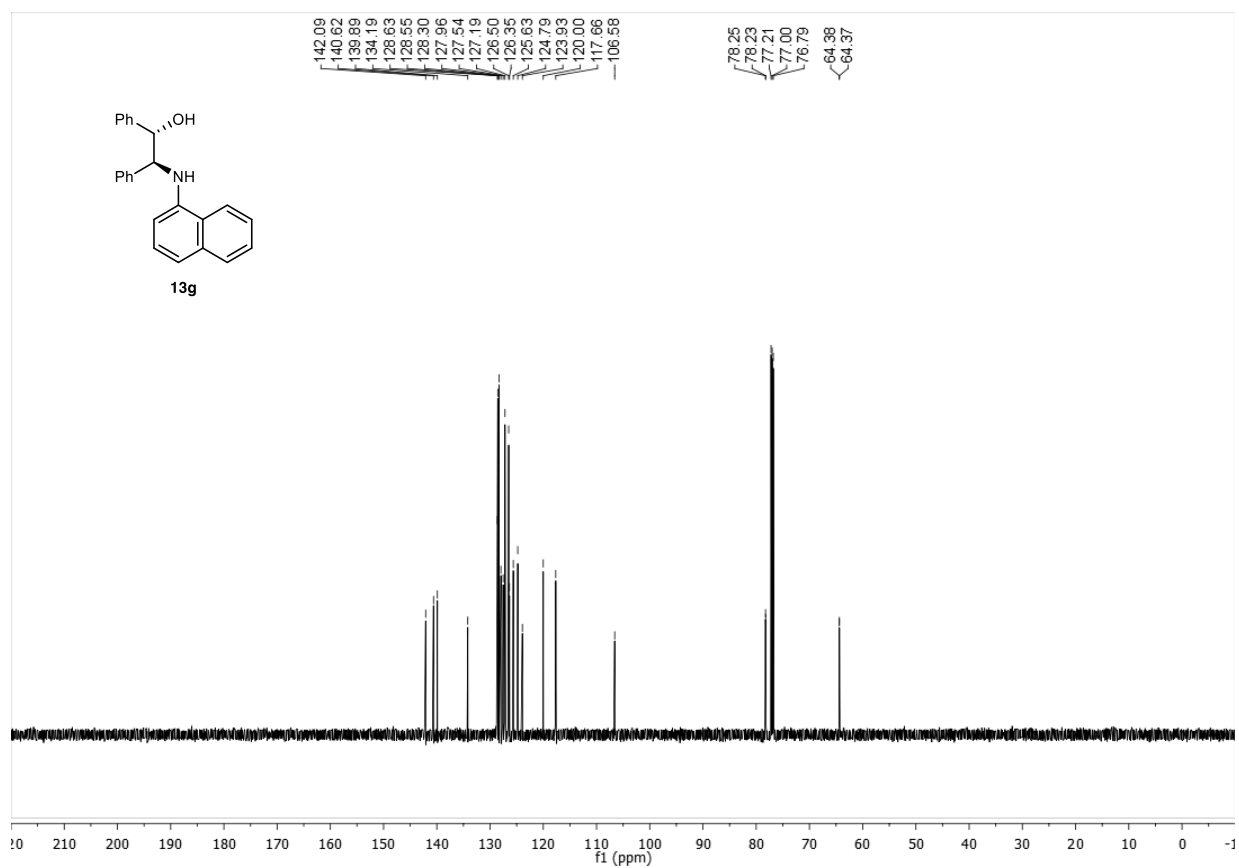


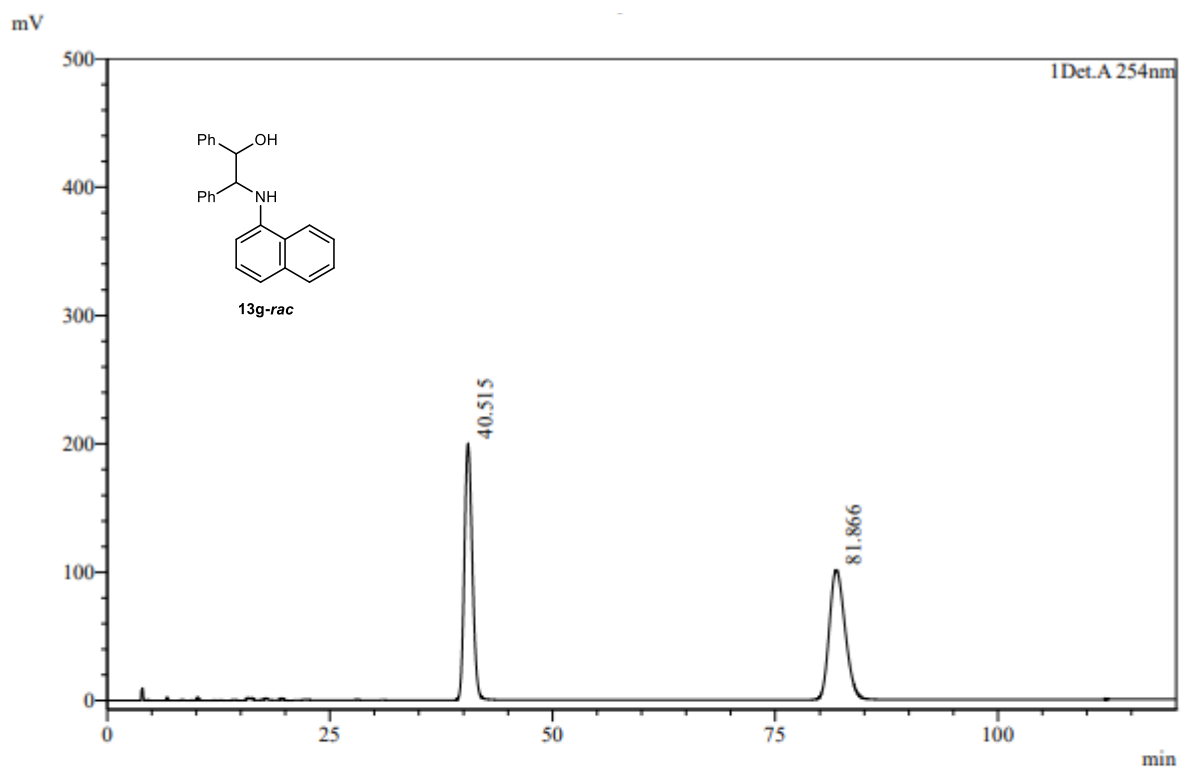
Det.A 254nm

Peak Table

Peak#	Ret. Time	Area	Area%	Height	Conc.
1	15.234	3288419	92.832	152805	92.832
2	17.603	253902	7.168	11537	7.168
Total		3542321	100.000	164342	



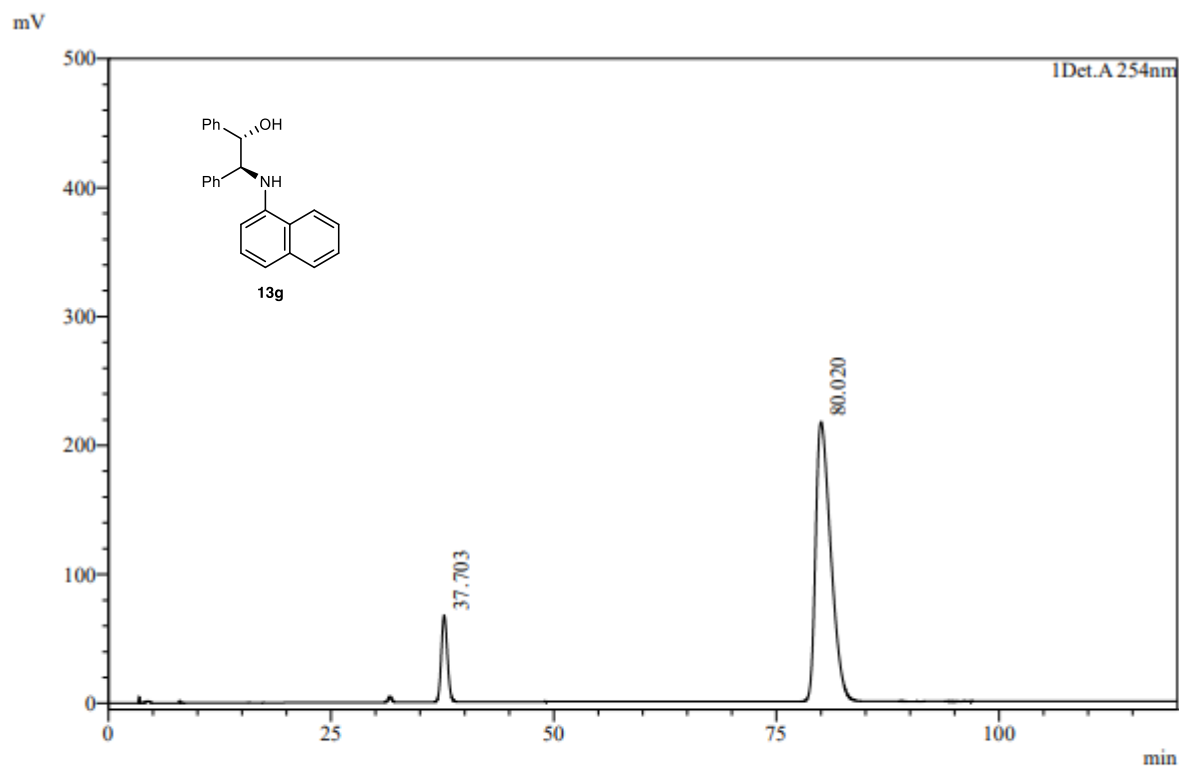




Det.A 254nm

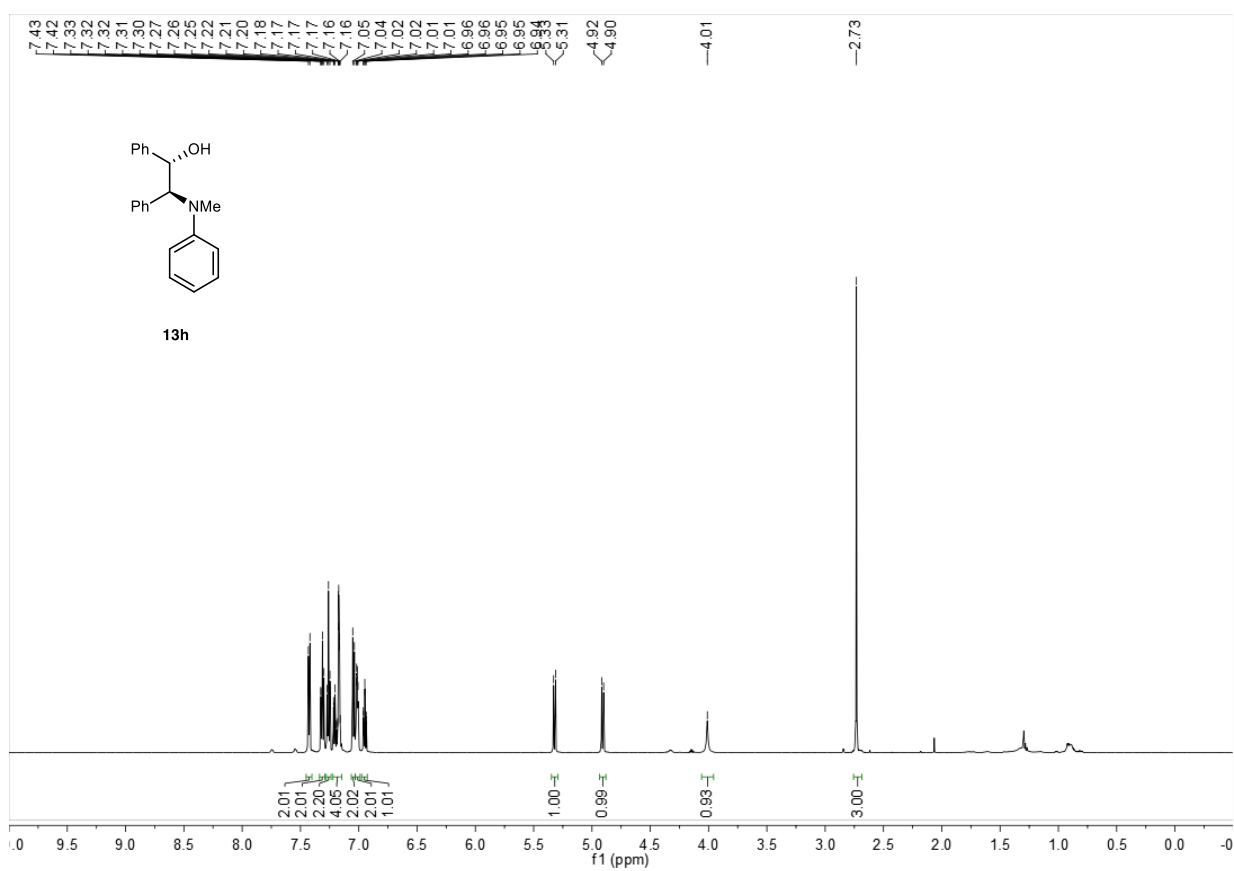
Peak Table

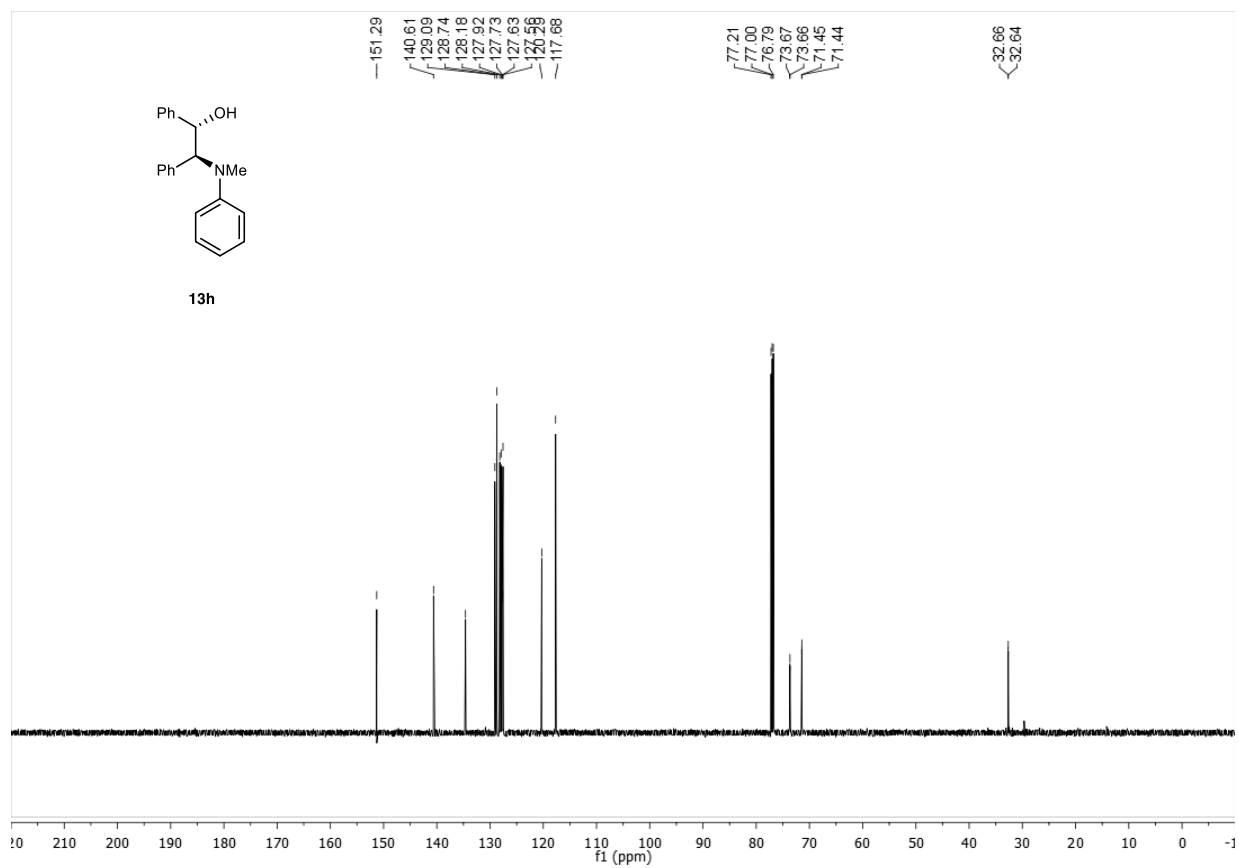
Peak#	Ret. Time	Area	Area%	Height	Conc.
1	40.515	12256747	50.006	198916	50.006
2	81.866	12253623	49.994	100531	49.994
Total		24510370	100.000	299447	

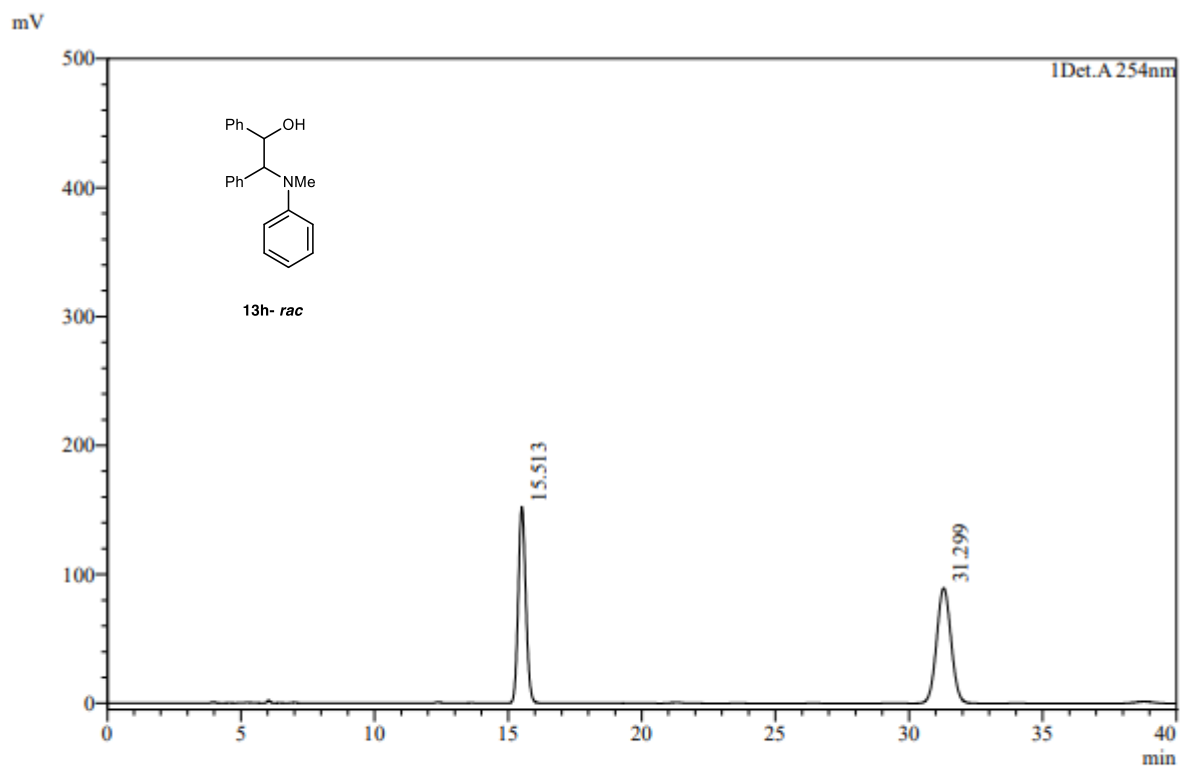


Peak Table

Peak#	Ret. Time	Area	Area%	Height	Conc.
1	37.703	2993650	10.478	65562	10.478
2	80.020	25577915	89.522	216746	89.522
Total		28571566	100.000	282308	

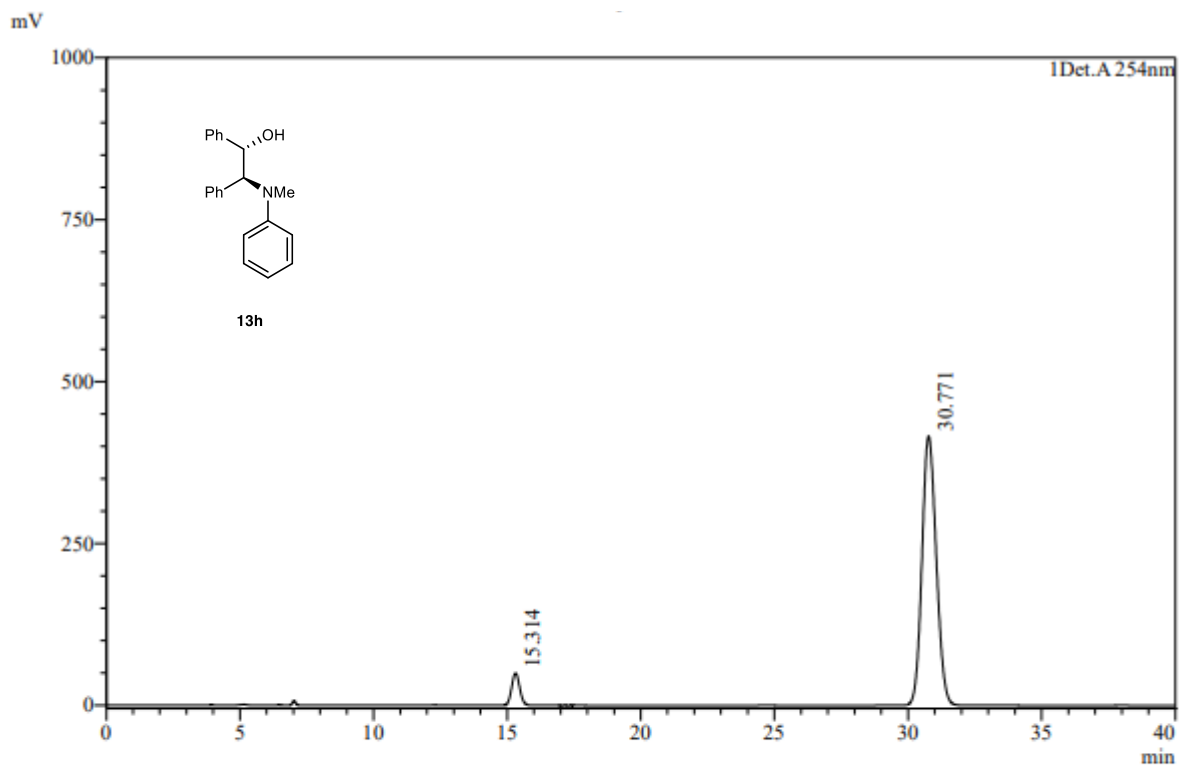






Peak Table

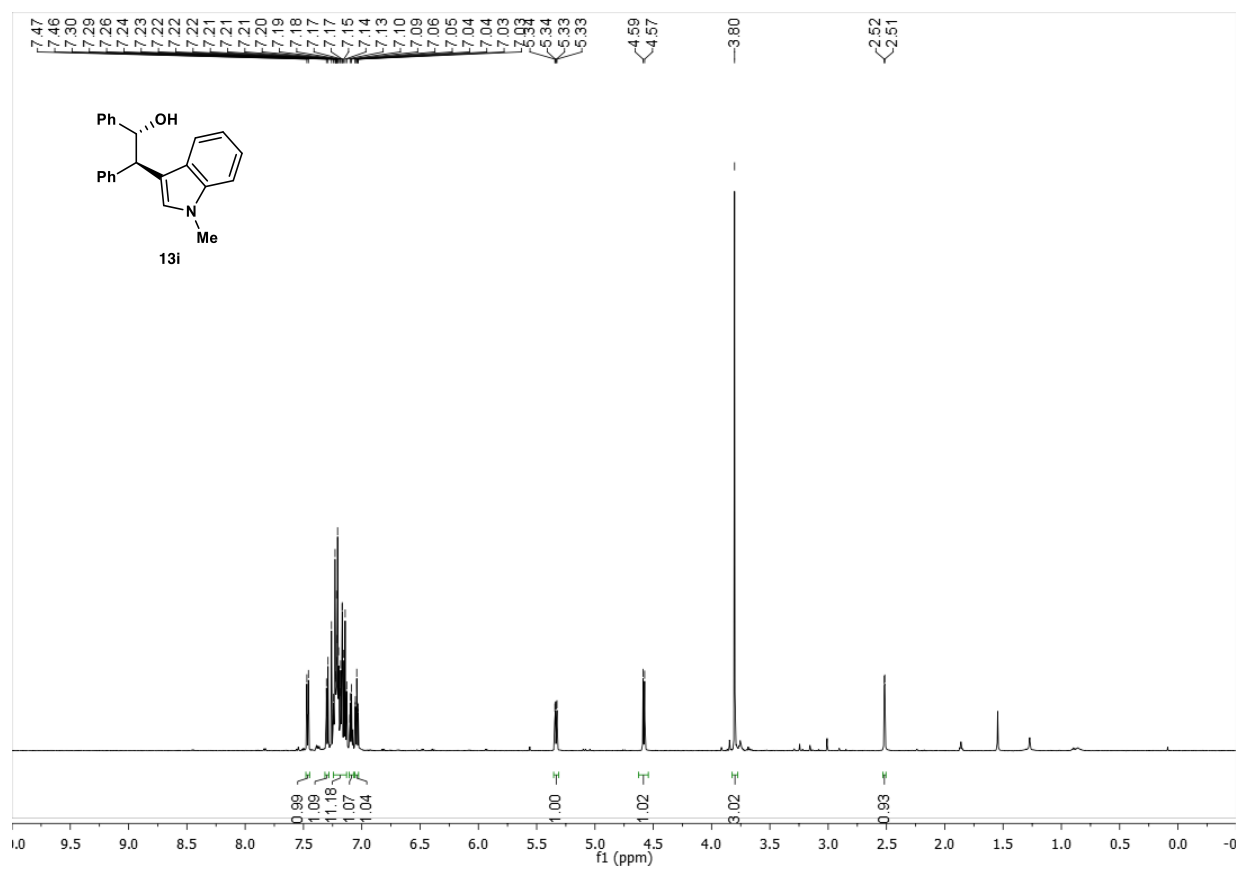
Peak#	Ret. Time	Area	Area%	Height	Conc.
1	15.513	2996178	49.867	152236	49.867
2	31.299	3012158	50.133	85557	50.133
Total		6008337	100.000	237792	

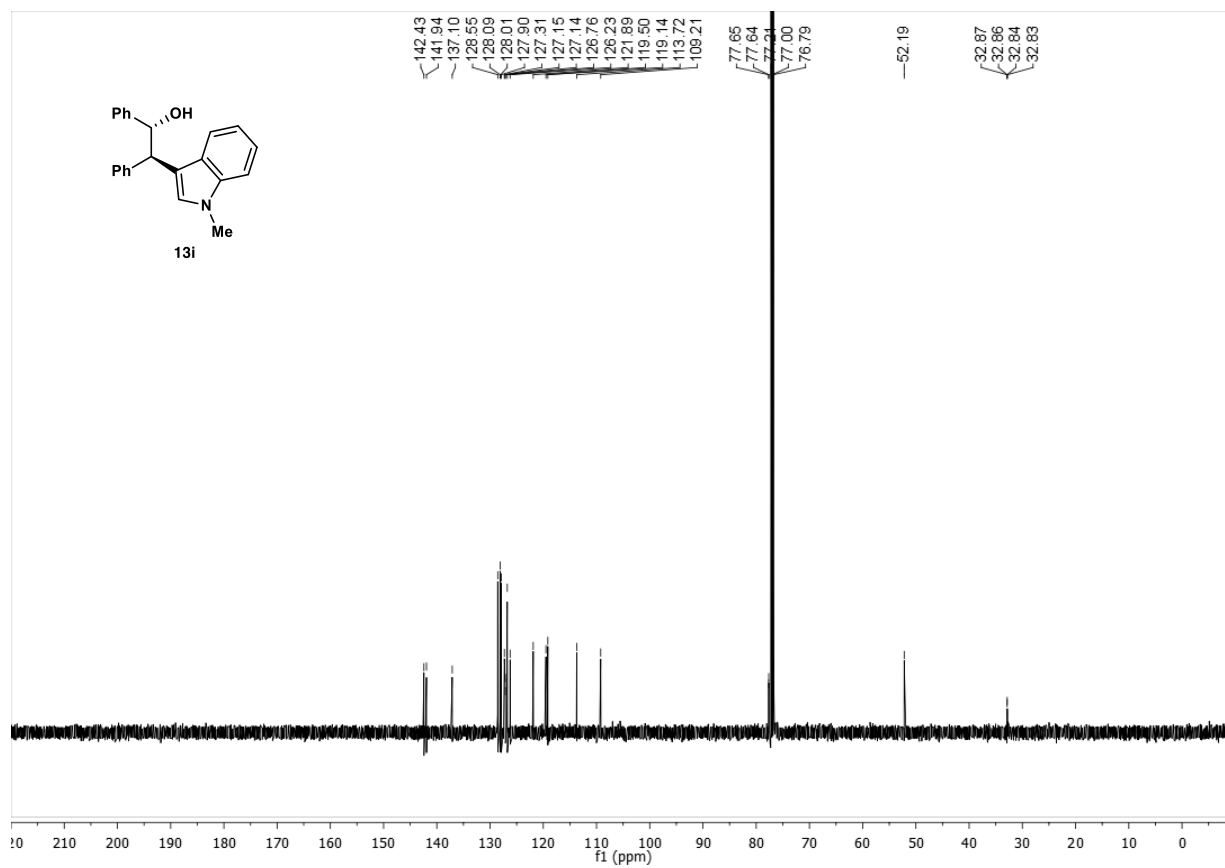


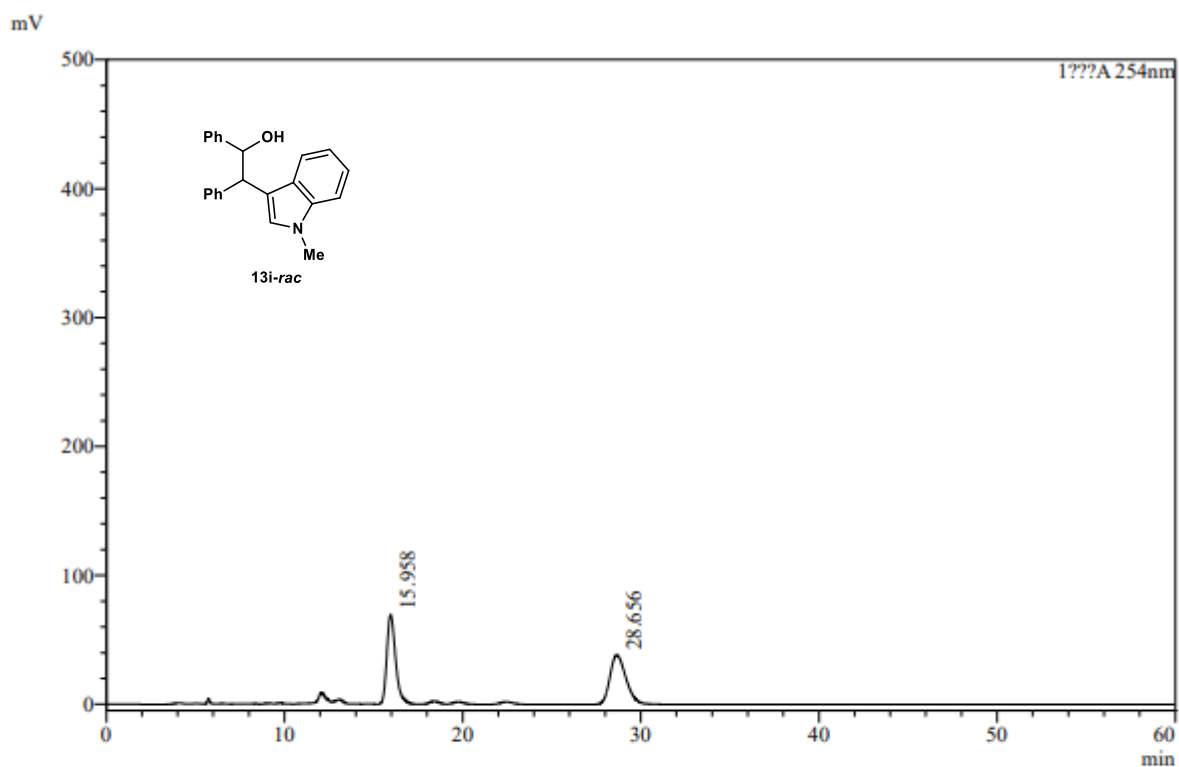
Det.A 254nm

Peak Table

Peak#	Ret. Time	Area	Area%	Height	Conc.
1	15.314	988606	6.020	48740	6.020
2	30.771	15432469	93.980	415638	93.980
Total		16421076	100.000	464378	

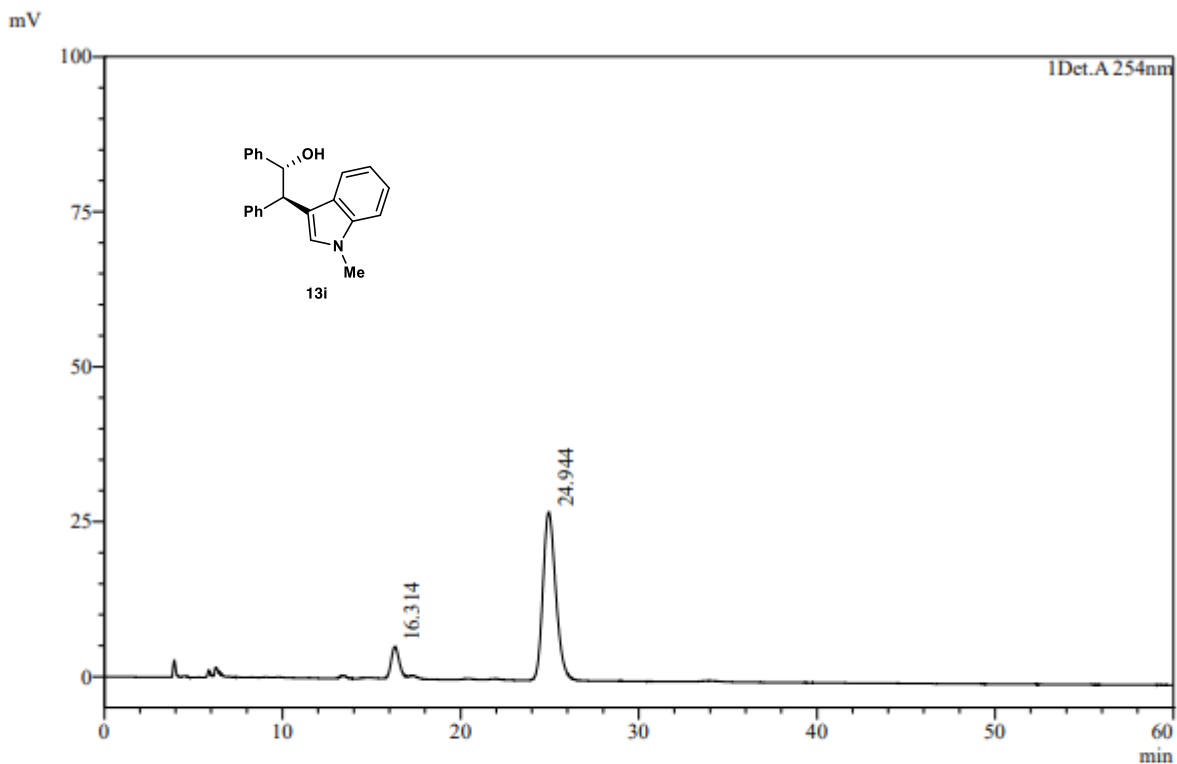






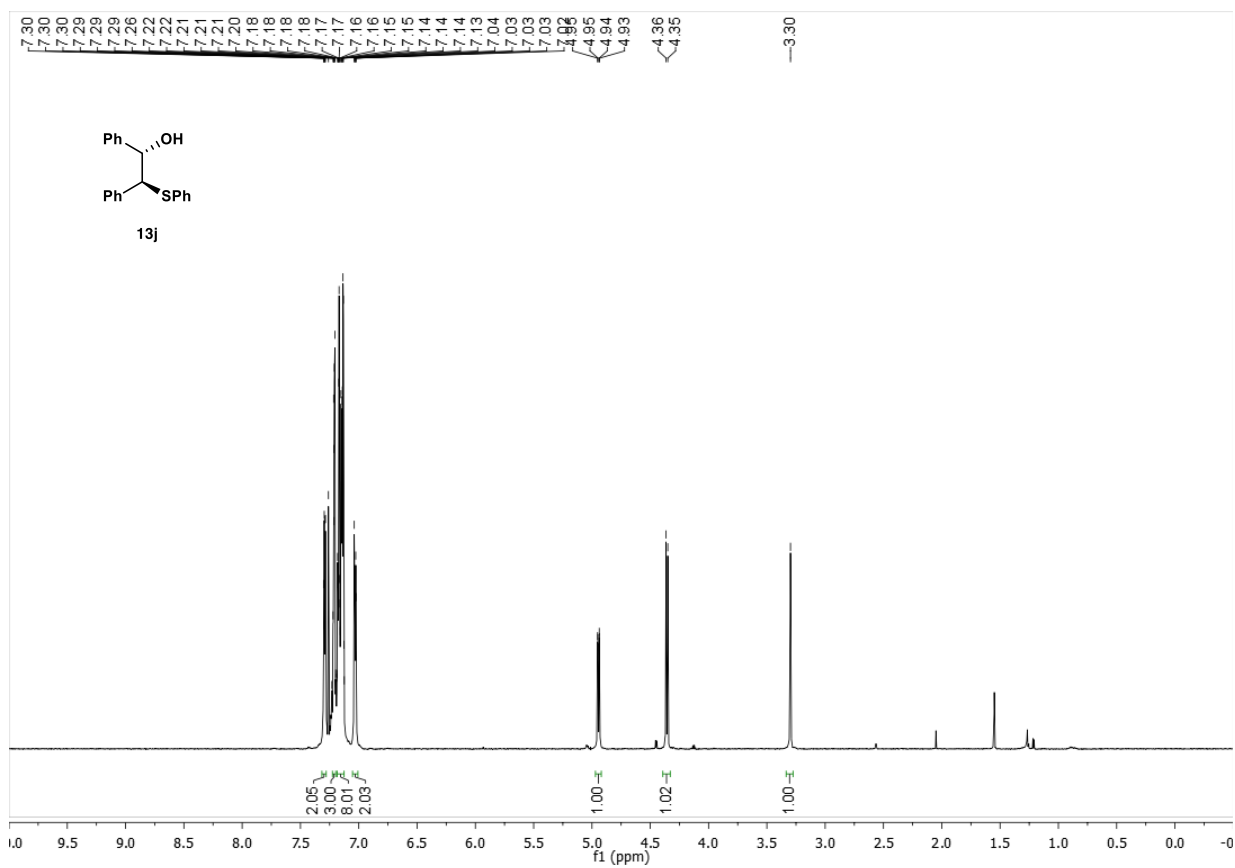
Peak Table

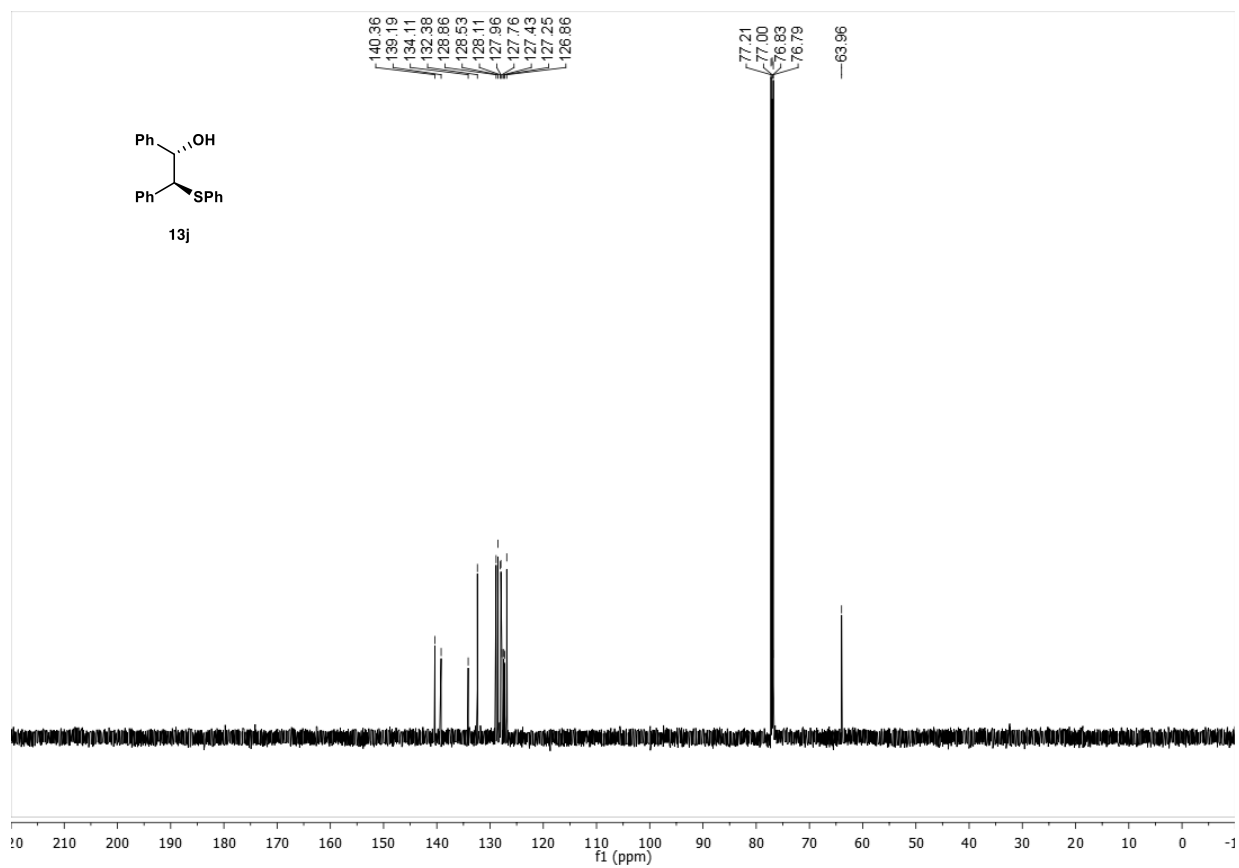
Peak#	Ret. Time	Area	Area%	Height	Conc.
1	15.958	2311099	50.110	68842	50.110
2	28.656	2300926	49.890	37832	49.890
Total		4612024	100.000	106674	

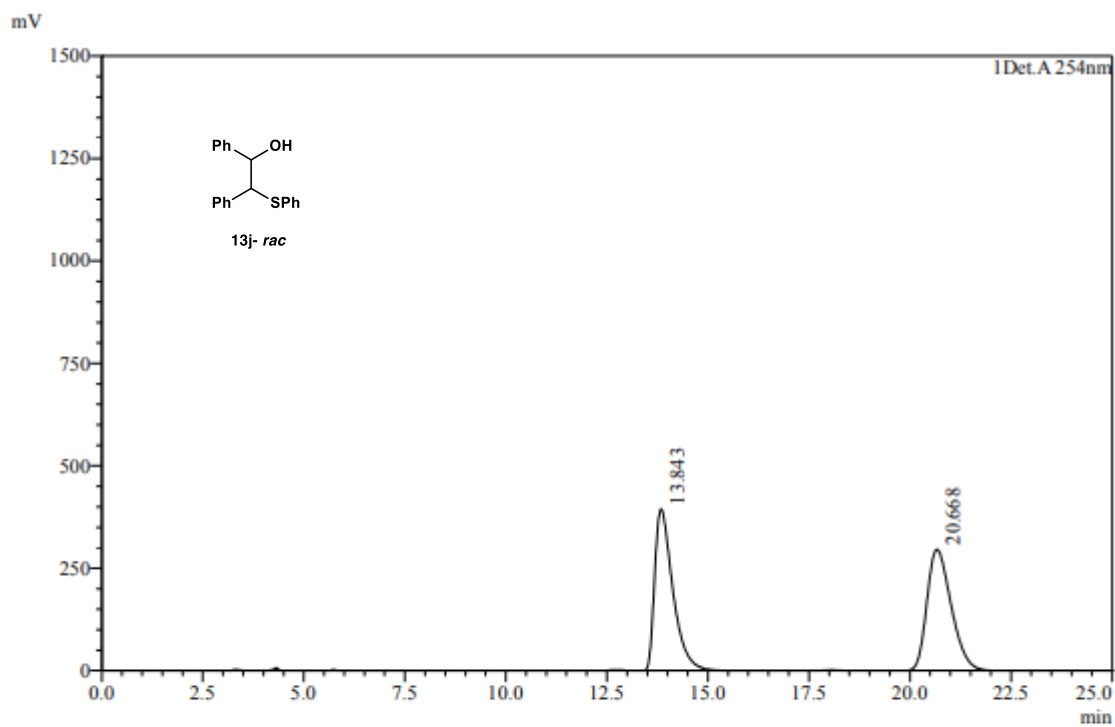


Peak Table

Peak#	Ret. Time	Area	Area%	Height	Conc.
1	16.314	150008	10.006	4988	10.006
2	24.944	1349143	89.994	27029	89.994
Total		1499151	100.000	32018	



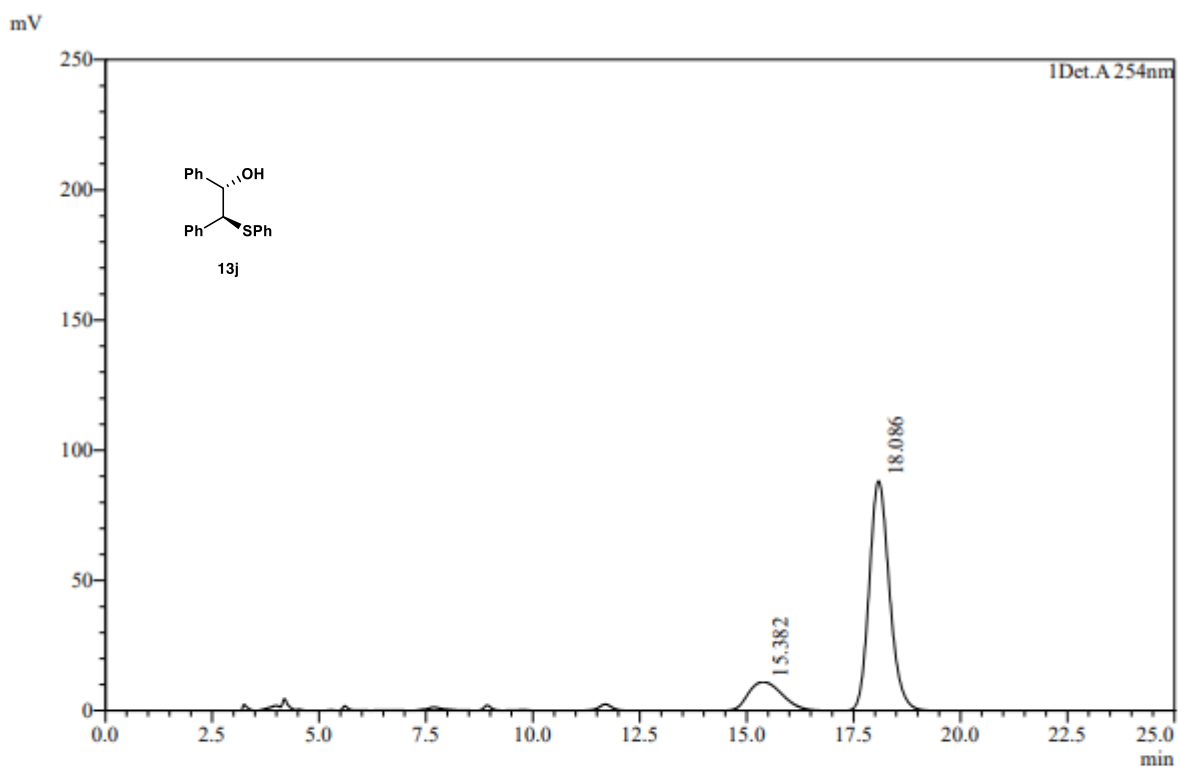




Peak Table

Det A 254nm

Peak#	Ret. Time	Area	Area%	Height	Conc.
1	13.843	12450290	50.006	394715	50.006
2	20.668	12447336	49.994	296333	49.994
Total		24897626	100.000	691048	



Peak Table

Peak#	Ret. Time	Area	Area%	Height	Conc.
1	15.382	558858	16.182	10668	16.182
2	18.086	2894724	83.818	88160	83.818
Total		3453582	100.000	98828	